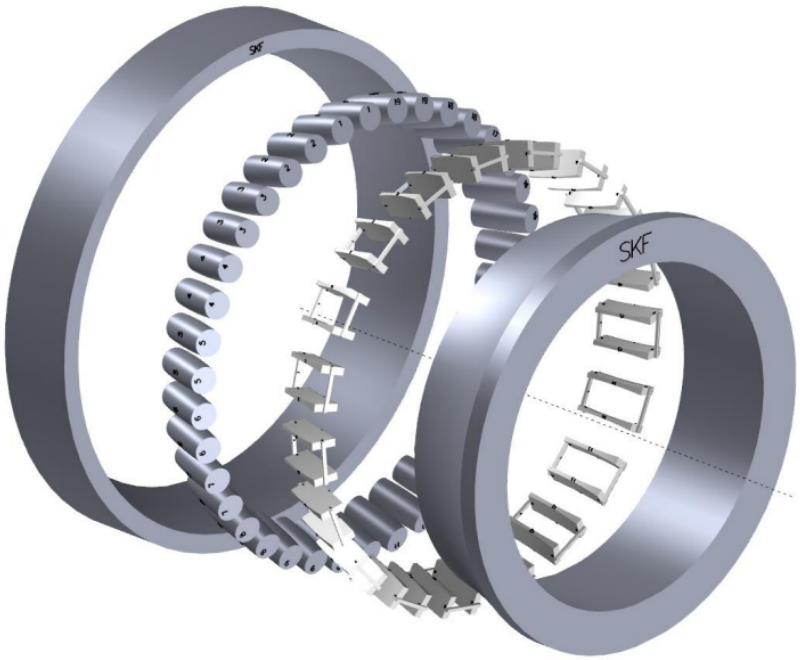

Design and Development of Cages for the Next Generation Self-Aligning Bearings

Master's Thesis in Product Development

DAVID KUHALAMPI
NIKI SADEGHI
DEPARTMENT OF INDUSTRIAL AND MATERIALS SCIENCE
CHALMERS UNIVERSITY OF TECHNOLOGY
Gothenburg, Sweden 2023
www.chalmers.se

Master's thesis 2023

Design and Development of Cages for the Next Generation Self-Aligning Bearings

In collaboration with AB SKF

DAVID KUHALAMPI
NIKI SADEGHI

CHALMERS
UNIVERSITY OF TECHNOLOGY

Department of Industrial and Materials Science
Division of Product Development
Chalmers University of Technology
Gothenburg, Sweden 2023

Design and Development of Cages for the
Next Generation Self-Aligning Bearings

Supervisor: Luke Dickens, SKF, Department of Product Development and Engineering
Academic Supervisor and Examiner: Magnus Evertsson, Chalmers, Department of Industrial and Materials Science

Master's Thesis 2023
Department of Industrial and Materials Science
Chalmers University of Technology
SE-412 96 Gothenburg
Telephone +46 31 772 1000

Cover: An exploded view of the SAT-bearing with the concept *every other pocket* assembled in it.

Typeset in LaTeX
Printed by Chalmers Digitaltryck
Gothenburg, Sweden 2023

Abstract

Roller bearings can provide a self-aligning quality when the rollers have a toroidal shape. The bearing can also take up both axial and radial forces when the rollers are inclined. By implementing a new bearing cage with lower cost and an excellent dynamic function, the SAT-bearing by SKF could become a strong competitor and the primary alternative for turbine shafts in wind power applications. By investigating polymer as a material for the bearing cage, factors such as design freedom, carbon footprint and price could be optimised.

The scope was limited to the wind power application for a reference for application-specific parameters such as service temperature, rpm and lifespan. During this project, a traditional product development approach was used to design and develop concepts for new bearing cages for the SAT bearing. The information retrieval consisted of interviews with experts on the topic, as well as studying internal and external literature and resources.

Three unique concepts were generated and screened using traditional product development methods and were tested and simulated before being developed further. During this process, a selection of polymer materials was also studied and compared. The cage designs were driven by their CAD models which were continuously improved throughout the process.

It was proved that using a polymer material instead of steel could offer benefits such as lower costs, more design freedom and a reduced carbon footprint. Out of the three concepts, two of the concepts performed best. One of these concepts, together with a polymer material, could utilize the elasticity of the material in order to absorb load.

Keywords: *bearing cage, polymer cage, roller bearing, self-aligning bearing*

Acknowledgements

We would like to express our deepest and most sincere gratitude to Luke Dickens, our supervisor at SKF, and Johan Sahlgren, manager at SKF, for their extensive contribution and inspiration throughout this project. Secondly, we would like to thank our supervisor and examiner Magnus Evertsson, professor at Chalmers University of Technology, for his feedback and excellent guidance during this time. Thank you to A[redacted] L[redacted], M[redacted] P[redacted], D[redacted] F[redacted], V[redacted] F[redacted], M[redacted], K[redacted] and M[redacted] B[redacted] for being available and answering our many questions on the technical and theoretical aspects of the project, and to and D[redacted] N[redacted] J[redacted] for helping with the 3D-printing. We also want to thank the PD&E department at SKF in Gothenburg for their encouragement and inspiring spirit, it has been a lovely time working with you.

David Kuhalampi & Niki Sadeghi
Gothenburg, June, 2023

Nomenclature

$Ax\ CLR$ Axial Clearance

BAR Individual Bar Segment

CAD Computer Aided Design

$CARB$ Toroidal Roller Bearing

EOP Every Other Pocket

EP Every Pocket

F Force

FEA Finite Element Analysis

FEM Finite Element Method

$G90$ Steel [redacted]

g Earth's Gravitational Acceleration

m_{roller} Roller Mass

$PD\&E$ Product Development and Engineering

$RKL01$ Roller Length

rpm Revolutions Per Minute

SAT Angular Contact Self-Aligning Toroidal Rolling Element Bearing

SRB Spherical Roller Bearing

$SRTB$ Spherical Roller Thrust Bearing

TRB Tapered Roller Bearing

Contents

1 Introduction

The following chapter introduces the project and presents the background of the purpose and the research questions. The delimitations and the focal areas of the project were also described.

1.1 Project Background

A bearing is a machine element used to reduce friction between moving parts and to guide motion. The bearing contains rolling elements which can be rollers or balls. These two kinds can be seen in figure 1. This project will focus on a bearing model which is using rollers as rolling elements. The rollers are often supported by a bearing cage and the primary purpose of the bearing cage is to guide the rollers and separate the rollers in order to obtain equal spacing around the circumference.

(a) An example of a roller bearing

(b) An example of a ball bearing

Figure 1: The cage is the grey material surrounding the roller elements, *www.skf.com*

Bearing cages help introduce the rollers to the loaded zones which is the zonal area of the circumference where rollers are induced by the load. They also restrict roller movement by separating the rollers, limiting angular movement of the rollers, i.e. skew, retaining rollers in the bearing to hinder them from swivelling out and helping limit axial displacement of the unloaded rollers. The bearing cage should also allow roller movement by letting the rollers roll at their preferred speed, letting rollers find skew equilibrium, and letting rollers contact the inner and outer rings. Furthermore, the job of the bearing cage is also to transport lubrication in the bearing so that there is sufficient lubrication in the most crucial areas at all times. Cages can also help ease the assembly process. When designing a bearing cage, different aspects have to be taken into consideration. These are aspects such as application, dynamics, strength, cost, mass, lubrication, manufacturability, assembly and transportation.

SKF is one of the world's largest bearing manufacturers and is one of the leading companies in terms of bearing development. Moreover, in addition to bearings, the company develops and manufactures seals, lubrication and lubrication systems, maintenance products, mechatronics products, power transmission products, conditioning monitoring systems, and related services globally (SKF, 2016). The company was founded in 1907 in Gothenburg

and has since then become one of the largest companies in Sweden and among the largest public companies in the world (Forbes, 2022). The company has a wide product catalogue with different bearings for various purposes. These bearings can be used in many different machines and products and are used in almost every industry. One example is wind turbines where rotation is the key factor to their function. The wind energy sector is bound to expand due to the global need for renewable energy, which means that the need for bearings suitable for the application will increase (International Energy Agency, 2022). Figure 2 is an illustration of the wind-bearing shaft with two different bearings mounted on it.

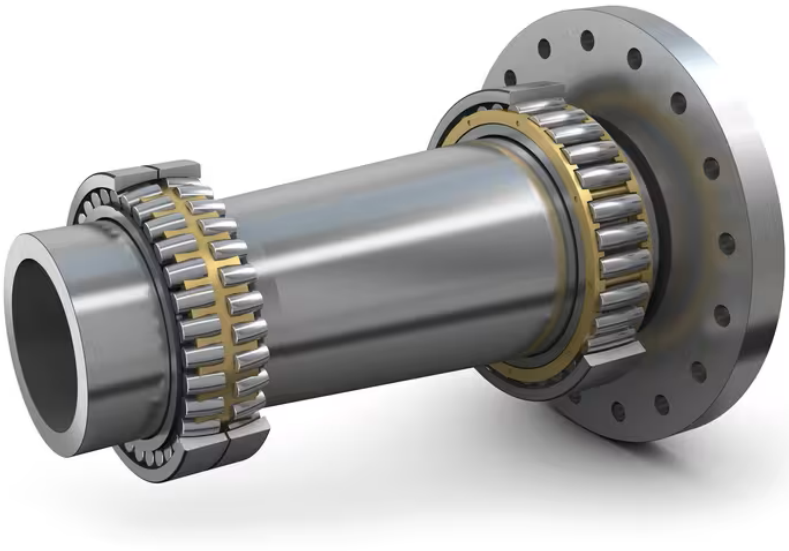

Figure 2: *A wind turbine shaft with roller bearings mounted on it, www.skf.com*

The project has been carried out at the Product Development and Engineering department at the SKF headquarters in Gothenburg. This department is mainly working on roller bearings. Roller bearings, in comparison to ball bearings, have a larger contact area and therefore a higher load-carrying capacity. For this reason, the bearings developed there are of particular interest to the wind energy industry for instance, where the bearings need to withstand high loads. The different roller bearings developed in Gothenburg are SRB (Spherical Roller Bearing), SRTB (Spherical Roller Thrust Bearing) and CARB (Toroidal Roller Bearing). An additional bearing called SAT (Angular Contact Self-Aligning Toroidal Rolling Element Bearing) is currently under development. The goal with this bearing is to be able to reap the benefits of the angular rollers which allow for the bearing to withstand axial load, as well as its self-aligning properties. The self-aligning properties will allow for more deflection and deformation in the wind turbines' horizontal shaft, without damaging the bearing. The bearings developed by the PD&E department in Gothenburg can be seen in figure 3.

(a) CARB, *www.skf.com*

(b) SRTB, *www.skf.com*

(c) SRB, *www.skf.com*

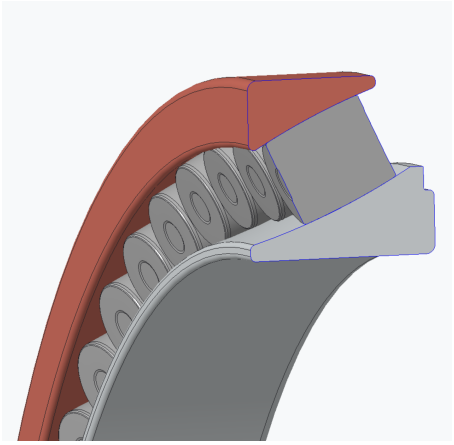

(d) SAT, *SKF CAD model*

Figure 3: Bearings developed in Gothenburg

A polymer cage for the SAT bearing could open up many possibilities with the design thanks to the design freedom that comes with the process of manufacturing polymer components compared to metal components. Another benefit of a polymer-bearing cage is its weight, which is lower compared to a metal one. When it comes to cost, polymer cages can also be cheaper than metal cages, depending on the volume and manufacturing process. These benefits make polymer cages interesting and this project has thus emphasised the investigation of the possibilities to design a bearing cage for the SAT bearing using polymer materials.

1.2 Purpose

The purpose of the project was to develop one or several concepts for a bearing cage for the new self-aligning bearing, SAT, which is deemed to be a competitive alternative for wind turbine applications. During the project, the possibility of a polymer cage was investigated in order to obtain the benefits of a lower cost, lighter weight, and an increase in design freedom. With the help of various methods and tools, the concepts were to be developed and later analyzed using digital simulation and physical testing. The goal was to motivate the different design choices with relevant theory by studying the topic and obtaining new information throughout the project.

Previously, a major part of the design and evaluation process has been done using pure mathematics outside of CAD and visual simulation software. Another goal of the project was to develop a model which was more visual in terms of the design and that could visually simulate certain stresses, deformations and dynamic behaviour.

1.3 Delimitations

Time was a limiting factor to this project which affected the process and the final results. The time frame of the project was 20 weeks and this led to narrowing down the areas of development. By recognizing and understanding the different areas of development, the focus areas could be defined and prioritised.

During this project, it was decided to focus on bearings for wind turbine applications. It could be possible to study other applications as well, but the wind turbine application is the most interesting for the SAT bearing, and because of the time frame of the project, other applications were not prioritised. Cage development involves analysis of how the lubrication should be distributed evenly to all contact points. This was regarded during the design process but was not tested in simulations. The lubrication fluids are difficult fluids to simulate due to them being non-newtonian. Testing of these would require computational fluid dynamic simulations and was not prioritized during the project due to time constraints.

1.4 Research Questions

The following research questions were formulated for this project:

- What is the most optimal design for a SAT bearing cage, and is it suitable for wind turbine applications?
- Is polymer a suitable material for the cage and if so, is there a polymer material most suitable?
- How can factors such as cost, weight, design freedom, manufacturability and assembly be improved with the new design?

2 Method and Application

This chapter goes into detail on the plans and actions that were gone through to create a valid and feasible concept and thereby answer the research questions thoroughly. The actions are described in detail as well as how the processes were iterated and analyzed. The timeline of the methodological approach is illustrated in figure 4.

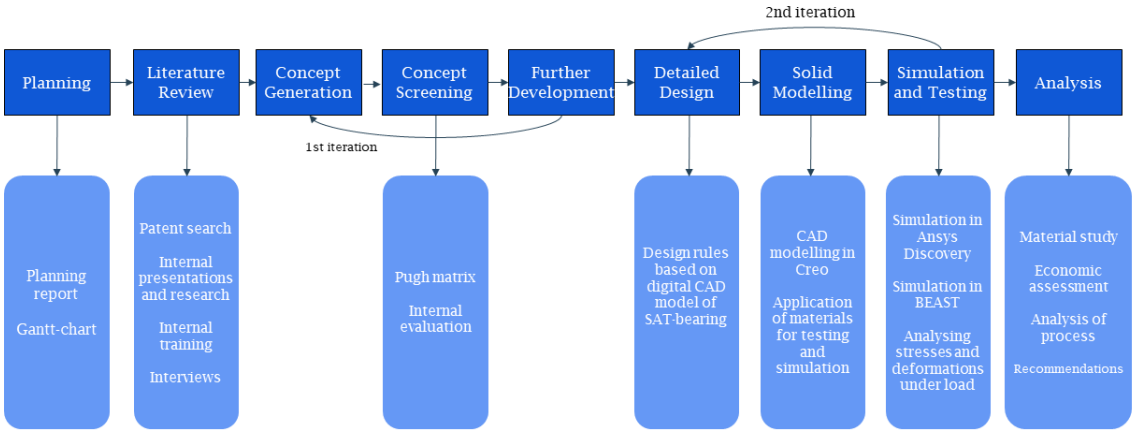

Figure 4: Timeline of the methodological approach, *inspired by "Product Design and Development" by Ulrich et al.*

2.1 Project Planning

Before planning the project in detail, the subject matter which in this case was bearing theory and cage theory, was studied using internal material from SKF. This provided an understanding of knowledge gaps and what expertise needed to be obtained to properly execute the product development project.

An estimation was achieved of how much time needed to be spent on literature studies and interviews to access product information and internal knowledge about the existing cages as well as the new SAT-bearing. In the early stages, a Gantt chart was set up to get a proper view of what tasks and deliverables were ahead and how to manage the time. This plan was updated continuously throughout the project and was updated as the project proceeded, since some tasks were more or less time-consuming than planned initially. This time plan gave a good overview of the project and its different phases, which also made the communication between all parties involved more effective. Two of the most involved contributors were the supervisors of the project. The supervisor at Chalmers gave feedback on the work throughout the whole project, and contributed with theoretical guidance. The supervisor at SKF was more involved in the day-to-day operations since the majority of the time was spent at the SKF headquarters. The supervisor at SKF contributed with expertise regarding technical aspects of the products, as well as relevant theory.

2.2 Information Retrieval

In order to learn more about the technical aspects of the bearing cage and to get a solid foundation for developing concepts, a literature review, a patent search and multiple interviews were conducted.

2.3 Literature Review

To obtain relevant information and knowledge for the project, internal resources at SKF were investigated and relevant sources were studied. The studies consisted of internal training courses, internal presentations and reports.

By studying these internal sources, a good base knowledge about the different bearing models was obtained. Furthermore, the different cage variants and their applications, benefits and drawbacks were studied. The courses also gave a good presentation of the different materials normally used for cages and when the different materials are used. The internal resources contained information based on years of knowledge that is specific to the products of SKF. In comparison to external information, the internal information was exceptionally relevant due to this. The discussions between attendees during the recorded meetings where different topics were presented gave additional depth to the information studied. By studying theory from internal sources at SKF, an understanding was obtained of how the PD&E department designs and develops their own bearing products, with which mathematical methods, and how they document the process.

Most of the literature studied was available digitally. The search also involved searching for relevant information in different books that are available internally at SKF, but the information available digitally was more up-to-date and the digital resources were therefore the main source of information. The product catalogue for rolling bearings was used throughout the project and helped with understanding certain technical concepts regarding bearings thanks to its descriptions (SKF, 2018).

External literature was also studied. This involved studies of articles and reports published online, and books regarding certain topics. These studies resulted in relevant information for the more theoretical parts of the project.

2.4 Patent Search

A patent is an intellectual property containing a detailed and accessible source of technical information including drawings and descriptions of products and how they function. A patent search has an advantage as it shows what concepts already exist and it can be useful in order to learn which inventions and ideas that need to be avoided. One can also use patents as an inspiration for the next development as long as it is stated clearly in the new patent (Karl T. Ulrich, 2011). A patent search is also a good method for learning more about a certain technology, how it works and what differences there are between different inventions.

A patent for the new SAT bearing is granted by SKF and this patent was primarily studied in order to obtain a good understanding of the design. The patent can be found in Appendix A.

To learn more about cage design and how the design differs between different bearings and manufacturers, a keyword patent search was conducted on external and internal databases. This was done by searching for relevant patents for bearing cages and analyzing these. By searching for patents covering cage designs used in relevant applications, a handful of relevant patents were discovered. The following databases were used for the patent search:

- **Espacenet (EPO)**
  An external database which provides searches and examinations on European patent applications as well as international applications filed under the Patent Cooperation Treaty (Espacenet, 2022).

- **Unycom**
  An internal database which provides patents licensed only by SKF (Clarivate, 2021).

The publishing years of the patents were also of relevance. The ones found before the 1980s were screened out as novelty was an important aspect of the patents searched for. The keywords used were iterated and consisted of text strings coded to obtain different results each time. Some examples were the following:

- ”Bearing” AND ”cage”
- ”Bearing cage” AND ”wind turbine”
- ”Bearing cage” AND ”segmented”
- ”Bearing cage” AND ”pocket”

When a relevant patent is found, it is possible to track which other patents the invention has been inspired by. In that way, it is possible to find similar inventions. The result of the search was patents of both designs developed by SKF, as well as designs from other bearing manufacturers from different countries globally. This provided insight into how the cage design can vary, and gave knowledge about different design choices that had been made for various designs. The knowledge obtained about the different technical aspects of the cage, as well as information about the different design choices, was useful in the next steps of the project.

Many relevant and interesting designs were found and analysed during the patent search. Some of these are presented in figures 5 - 8.

One-piece Cage for a Tapered Roller Bearing

- Applicant: NTN TOYO BEARING CO LTD [JP]
- Patent Code: WO2008056562A1
- Published: 2008-05-15

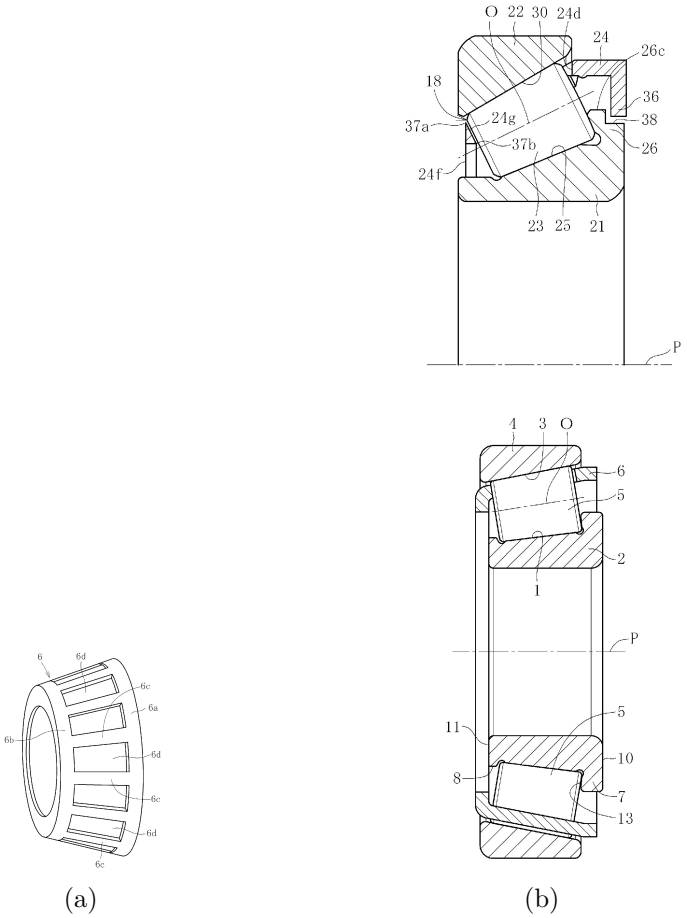

(a) (b)

Figure 5: One-piece cage, *WO2008056562A1*

This patent involves a one-piece cage suitable for rollers tilted at an angle. This is similar to the design of the SAT bearing, where the rollers are also inclined.

Segmented Cage for Multiple Rollers in a Tapered Roller Bearing

- Applicant: NTN TOYO BEARING CO LTD [JP]
- Patent Code: WO2022244872A1
- Published: 2022-11-24

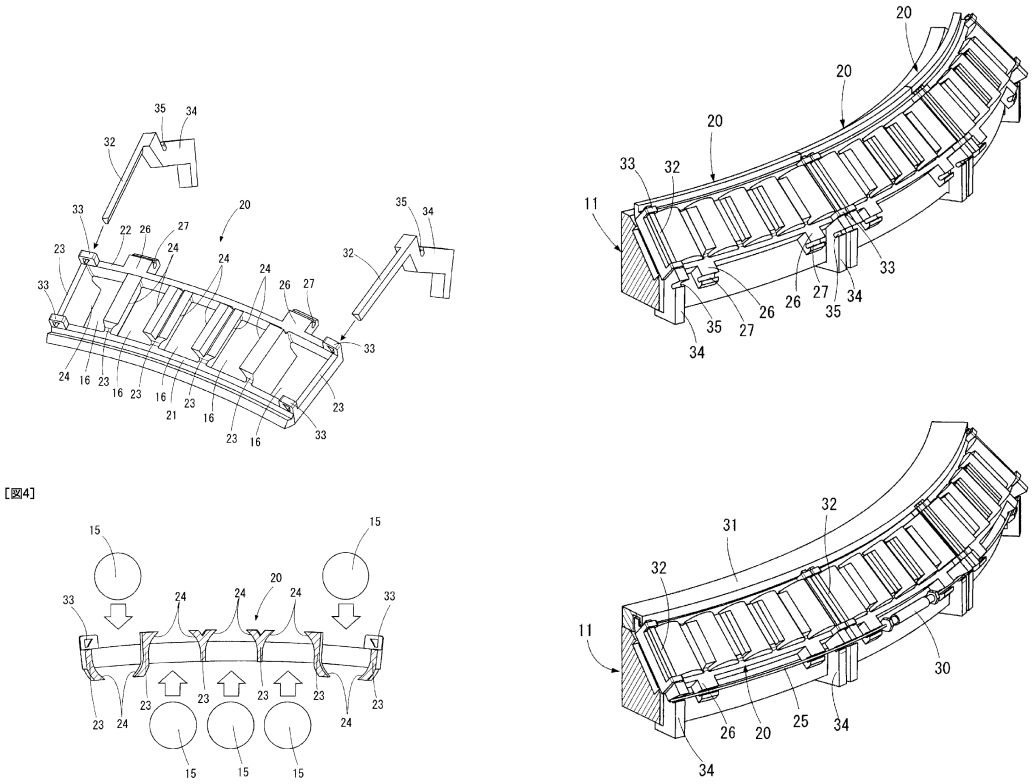

(a) (b)

Figure 6: Cage segment containing several rollers, *WO2022244872A1*

This patent involves a cage segment, where the segment holds five rollers. The drawings show how the segments are assembled. It can also be seen that the design allows for roller retention thanks to its features.

Cage Segment for a Tapered Roller Bearing

- Applicant: SKF AB [SE]
- Original Patent Code: WO2012076583A2
- Published: 2012-06-14

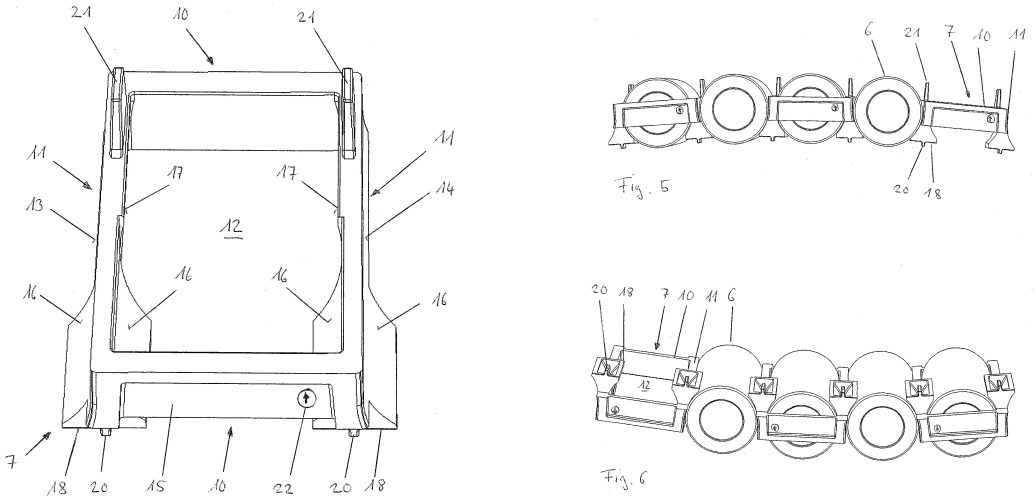

(a) (b)

Figure 7: Cage segment with a roller between each segment, *WO2012076583A2*

This patent involves a cage segment containing one roller and has another roller between itself and the next segment. The cage segment has a pocket shape.

Roller Bearing Separator Cage

- Applicant: NSK LTD
- Patent Code: JP2007100909A
- Published: 2007-04-19

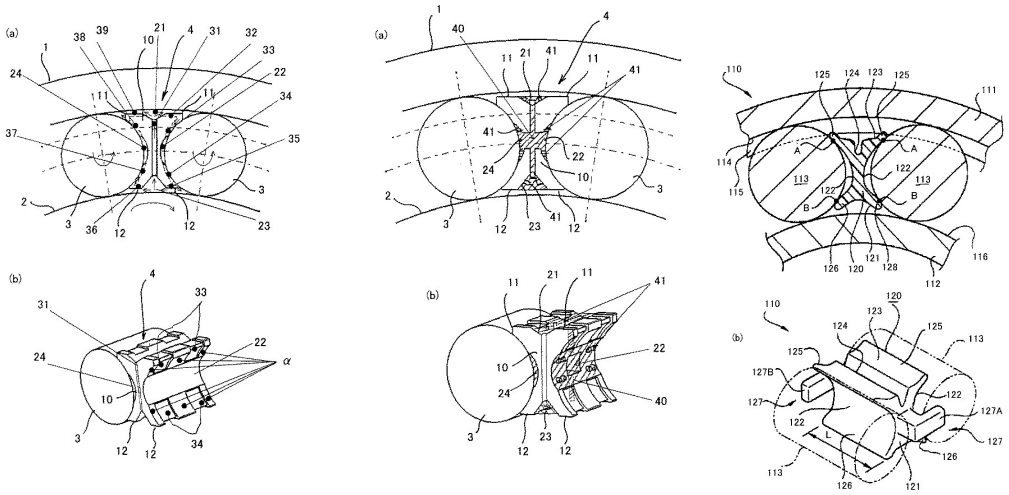

Figure 8: Individual cage segments between each roller, *JP2007100909A*

This cage segment functions as an individual separator between each one of the rollers in the bearing. As can be seen in the illustrations, the segment also has a feature functioning as an axial stop for the rollers.

2.5 Hands-on Study

To obtain a better understanding of the designs of the different bearings and cages existing, a more hands-on study was conducted. This involved looking at the different bearings displayed at the SKF headquarters, as well as different prototypes of bearings and cages in the prototype lab at the site.

A hands-on study gave additional information about the bearings and the different cage designs. Various features in the different bearings, as well as in the different cage designs had been difficult to grasp fully without studying the physical products and prototypes. The study therefore led to a better understanding of the existing products, and information about other projects conducted at SKF was obtained which was useful in the concept generation phase of the project.

2.6 Interviews with Experts

Information about the different requirements and wishes of the company had to be obtained in order to decide which routes to take during the project and to make appropriate decisions. More detailed and technical information about the different components, design choices and applications also needed to be gathered. More information about the different attributes of the cage design was needed in order to make the most suitable design choices when developing the concepts. This information retrieval was performed by interviewing multiple experts with different areas of expertise and experiences. Every expert interviewed is working in the SKF organization.

The interviews were conducted in person or in an online meeting. The interviews consisted of multiple open-ended questions, and the interviews lasted for approximately one hour. The information obtained from the interviews was written down throughout the meetings, and relevant photos were taken on certain sketches presented.

L[redacted] D[redacted], who is the supervisor for the project at SKF, and experienced with the bearings being developed in Gothenburg, was able to answer a lot of questions regarding the various bearing types, the attributes of the bearings and cages, as well as the different applications for the different bearings.

A[redacted] L[redacted], who is also based in Gothenburg and has been working with the SAT bearing, was able to explain specific technical details about the bearing dynamics and the application-specific conditions that the bearing should be able to operate in. He was also able to answer questions regarding the different attributes of the bearing cage and how these affect the bearing dynamics.

M[redacted] P[redacted], who is working with wind turbine applications in Amsterdam, was able to answer questions regarding the application-specific conditions that were relevant to the project. He was also able to elaborate on the different attributes of the bearing cage.

D[redacted] F[redacted], who is working with the TRB bearing in Schweinfurt explained how their different bearing cages are designed. This is of great interest since the SAT bearing has similarities with the TRB bearing. He also explained the benefits of the chosen attributes in the designs.

2.7 Description of Customer Needs

Before proceeding with the creative work of the cage design, the customer needs were established and summarized in table 1 below. Roughly, the needs were goals which were to be fulfilled by the end of the development process. The importance of the different needs in the customer needs list is a combination of what the primary stakeholders at SKF found to be the most important and also what was emphasised during internal expert interviews. The customer needs were later used when creating a requirement specification, where the needs are formulated as measurable requirements and desires.

Table 1: Customer Needs List

No	Needs	Importance
1	Good Bearing Dynamics	High
2	Low Cost	High
3	Long Life Span	High
4	Low Carbon Footprint	High
5	Design Optimised for Light Weight	High
6	Scalable Design	High
7	Adapted to Wind Turbine Applications	High
8	Design for Good Lubrication Flow	High
9	No Maintenance	High
10	Ease of Assembly and Mounting	Medium
11	Transportation-friendly Design	Medium

In order for the SAT bearing to be a competitive alternative on the market, all these factors need to be taken into account and optimised when designing the bearing cage.

- The most important need is to have a bearing which works well. The dynamics of the bearing is therefore the most crucial factor to be optimised.

- An important need for the SAT cage communicated by the stakeholders at SKF, was keeping the cost down throughout all aspects of the development, manufacturing, assembly and transportation. Manpower is expensive and not needing it for maintenance during the long lifespan of the cage will also help keep the cost down.

- A low carbon footprint for the cage is also a need of high importance for the stakeholders at SKF. SKF as a company is on a path to net zero emissions by the year 2050 and therefore the environmental aspect is important throughout all operations (Axelson et al., 2022).

- Optimising the design for lighter weight will also lead to lower emissions from trans-

portation. Moreover, a lighter weight would be beneficial for the bearing dynamics. Optimising the design for lighter weight will also lead to lower emissions from transportation. Moreover, a lighter weight would be beneficial for the bearing dynamics.

- The design must also be optimised for efficient lubrication in the bearing.
- A need of high importance is to have a design that can be scaled depending on the bearing size.
- The properties of the SAT bearing are particularly advantageous in the wind power application which was prioritised by the stakeholders to be a focus area.
- It is important that the bearing cage is easy to assemble and mount onto the bearing. This should be straightforward and safe.
- When the bearing is being shipped to the customers, it is important that all components are designed so that they do not get damaged during the transportation. This includes the bearing cage.

2.8 Requirement Specification

A requirement specification is set up during a product development process in order to communicate to the developing team what capabilities and functions must be included in the product by the time it is ready for production. The requirements become goals that are measurable and worked towards in an agile product development process (ProductPlan, 2021). Presented in table 2 are the requirements for this product development project.

Table 2: Requirement Specification

Criteria	R/D	Requirement	Justification	Evaluation/verification
Material Cost	R	Low	SKF	Economic Assessment
Material Cost	D	Very Low	SKF	Economic Assessment
Manufacturing Cost	R	Low	SKF	Economic Assessment
Manufacturing Cost	D	Very Low	SKF	Economic Assessment
Transportation Cost	R	Low	SKF	Economic Assessment
Transportation Cost	D	Very Low	SKF	Economic Assessment
Service Temperature [°C]	R	-10 - 40	Customer	Testing and Simulation
Mass	R	Low	Customer/SKF	CAD
Climate impact	R	Low	Product Developers	Environmental Analysis
Rotational Speed [rpm]	R	3-10	Customer	Testing and Simulation
Material	D	Polymer	SKF	Testing and Simulation
Maintentance	R	None	Customer/SKF	Testing and Simulation
Maximum Skew [rad]	R	[redacted]	SKF	Testing and Simulation
Lifespan [years]	R	20-30	Customer/SKF	Testing and Simulation
Assembly	D	Simple procedure	Customer/SKF	Testing and Simulation
Lubrication	R	Good lubrication flow	Product Developers/SKF	Testing and Simulation
Friction	R	Low friction	Product Developers/SKF	Testing and Simulation

The table is set up with a number of criteria. The criteria are either graded with an R or a D with the R representing *requirement* and the D representing *desire*. The justification column is a list of the stakeholders expressing that criteria and the evaluation/verification column lists how these criteria will be evaluated and verified.

The customer needs and their importance was summarized in chapter 2.7 but they were not measurable yet. What was added as measurable parameters in the requirement specification were criteria such as service temperature, rpm, lifespan and maximum skew. The service temperature, rpm and lifespan were chosen with respect to wind turbine applications. The locations for wind parks can provide harsh conditions and extreme temperatures. Therefore, the cage must be built to withstand these conditions. The requirement specification was more detailed than the customer needs list, and included some additional criteria which were of importance for the product.

These requirements affected the technical aspects of the design process of the cage, including the geometry and materials investigated. The requirements also served as inspiration for what needed to be tested later during the simulation. What was also added here as a desire, was the use of polymer materials which was expressed by stakeholders at SKF early on.

3 Technology Assessment

This chapter describes bearing and cage theory and goes into depth on the functionality of the SAT-bearing which is the application of the cage concept. Before developing concepts, there needs to be clarity in what functional attributes can be chosen and combined.

3.1 Basic Attributes

The design of a bearing cage was chosen to be divided into four different product attributes. The product attributes occur in every cage design but what differs is the design choices made for these attributes. The product attributes were used throughout the project in order to understand the differences between varying cage designs and to generate concepts. By dividing the bearing cage into its product attributes, it was easier to identify differences between different designs since it was possible to look at the differences for the product attributes and not only the whole products which have complex designs. It was beneficial to split the product into different attributes when developing concepts. By doing this, it was possible to combine different designs for each attribute in order to generate concepts that resemble the whole product.

3.1.1 Geometry of Cage

The most common types of bearing cages are one-piece cages and segmented cages. One-piece cages consist of a single piece that reaches around the whole bearing and supports all the rollers. The design of the cage can vary in terms of other attributes in order to allow for certain features.

Segmented cages consist of individual parts which act as separators between the rollers. These segments can have different designs depending on the different features the cage is gonna have. Some bearings have segments between every roller while others have segmented pockets that the rollers are sitting in. These segmented pockets can house one or several rollers and can be designed in a way so that every other roller is sitting inside the pocket and every other roller is sitting between two segments.

3.1.2 Cage Centering

The centering of the cage is how the cage is resting radially in relation to the rest of the bearing elements during operation. The cage can either be centered on the rollers, on the inner ring, or on the outer ring. Some designs allow for the centering of the cage to vary during bearing operation, where the centering can shift in different positions around the circumference, due to gravity. The different centerings are illustrated with simple sketches in figure 9.

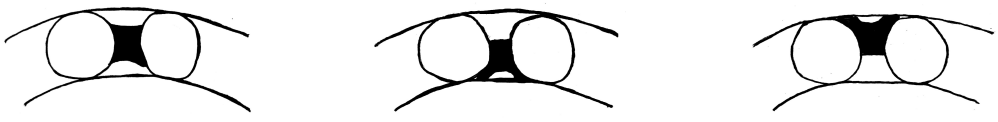

(a) Roller centering (b) Inner ring centering (c) Outer ring centering

Figure 9: Roller retaining features

3.1.3 Pitch

The pitch of the cage is how the contact with the rollers is designed. If the contact points are located in the middle of the roller diameter, the cage is so-called *on pitch*. On the other hand, if the contact points are located over or under the middle section of the rollers, the cage is called *over pitched* or *under pitched*. For some designs, it is also possible for the pitch to alternate during operation, depending on the positions around the circumference, due to gravity. For example, if the cage segment is centered on the inner ring and between two rollers, then the pitch can alternate between on pitch and under pitch. When the cage segment is outer ring centered and between two rollers, it can alternate between on pitch and over pitch. The different variants of the pitch are illustrated with simple sketches in figure 10.

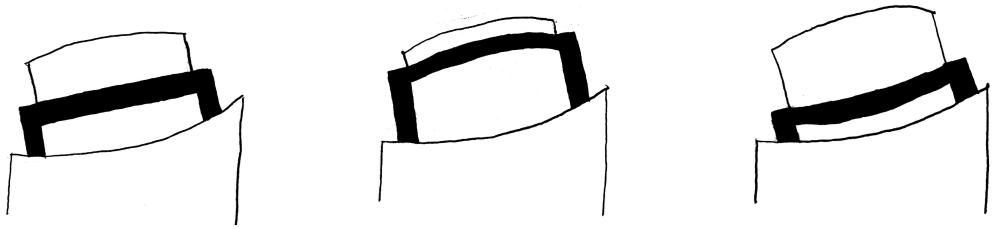

(a) On pitch (b) Over pitch (c) Under pitch

Figure 10: Roller retaining features

3.1.4 Roller Retention During Assembly

There are different solutions when it comes to keeping the rollers and the cage in place during the assembly of the bearing. Bearings can both be assembled horizontally and vertically, but due to the large size of the bearing which was in focus during this project, methods for horizontal assembly were deemed to be the most reasonable option.

3.2 Function-Means-Tree

One crucial step before the generation of concepts with various functions was to analyse the cage's functional structure. As part of describing what functions the cage must fulfil and what means are necessary for them to be achieved, a function-means tree was set up. A function-means tree is a systematic method of modelling a product or main function upon the idea that there are causal relations between the means and functions (Robotham, 2002). The function-means-tree for this project can be seen under Appendix B. The top function is the purpose function which in this case is to *Aid Bearing Function*.

The way the tree has been implemented in this project is by illustrating various solutions to a function. The function-means tree is a hierarchical structure which illustrates all the functions and means from the purpose function, down to the sub-functions and in this case, the sub-sub-functions.

Each means has sub-functions which is a result of breaking the means down into its constituents. The cage supports the bearing during operation when the bearing is in a dynamic state, as well as if the bearing is in a static condition. The function-means-tree resulted in four sub-functions below the purpose function. The sub-functions were the following:

1. Aid Bearing Dynamics

This sub-function is an umbrella which covers means and sub-sub-functions related to the cage during operation. The cage can be designed to benefit the bearing dynamics by controlling hammering, which is when rollers drop from a distance, causing damage to other rollers or to the cage. Hammering damage is prevented by minimizing the clearance in the cage design, as well as having the cage segment absorb the load. Another sub-function is skew control which means that the roller has its angular position controlled on the raceway. There needs to be room for the roller to skew at a certain angle to obtain the self-aligning qualities and to reduce friction and high contact forces. This is fulfilled by designing with clearance as well as designing for higher friction between the rollers and the ends of the raceways. The raceway is the surface on the inner ring and outer ring on which the roller is positioned.

An additional sub-function related to dynamics is the loaded zone introduction. The cage helps the rollers enter the loaded zone in a beneficial way by having a design which helps guide the rollers. Lastly, the cage helps separate the rollers which minimizes wear over time. The cage thickness is the means to this function.

2. Preserve Roller

In their static and dynamic conditions, the rollers must be supported by the cage. This is achieved with a load-bearing structure which is the cage itself. It needs to be able to carry the load induced from multiple rollers and segments stacked on top of each other, if a segmented design is used. The means for achieving these functions is a robust design, as well as a proper material choice.

3. Enhance Lubrication

Another sub-sub-function which aids the main function is enhancing lubrication. As mentioned previously, the bearing will not be maintained during its lifespan, however, it will have to be re-lubricated during that time. For the lubrication to flow in the cage structure, there need to be pathways for it to do so, such as grooves and cavities. It is of high importance that lubrication can reach all contact points at all times.

4. Ease Assembly

The cage can ease assembly by having roller retention features. The rollers need to be positioned and secured to not fall out of the bearing during assembly, which applies to the cage or cage segments as well. The position of the cage and the rollers can be controlled and secured with different assembly-aiding tools, such as a strap used to prevent the rollers from falling out during assembly. The bearing itself can also have assembly-aiding features such as a flange, which acts as a stop for the rollers and prevents them from sliding down the raceway during assembly. An additional solution for controlling and securing the position of the rollers is to machine dimples on the rollers, which are small indentations in the geometry, which the cage geometry then goes into to lock the rollers. The dimples can be seen in figure 11a. To prevent the rollers from falling out of the cage structure, another solution could be that the cage has material overlapping the radius of the roller as a securing mechanism, also known as lugs which can be seen in figure 11b which is from patent WO2022244872A1.

(a) Dimple on the side of the SAT-roller, *SKF CAD model*

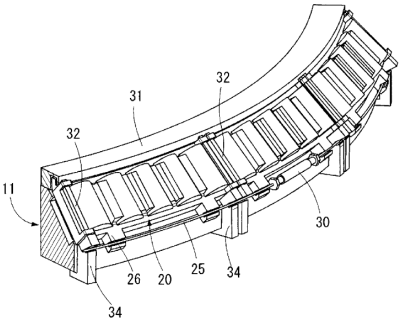

(b) Lugs, *WO2022244872A1*

Figure 11: Roller retaining features

4 Concept Development

The following chapter goes into depth into the process of generating base concepts, evaluating them and screening them using traditional product development methods. The methodology used in this phase of the project was inspired by the book *Product Design and Development* by Karl T. Ulrich and Steven D. Eppinger (2011). The benefits of using a structured approach early were that there were incentives for every decision made further in the process.

The development of concepts was divided into two parts. The primary part consisted of generating base concepts where the concepts only had the three base attributes mentioned in chapter 3.1 to distinguish them from each other. The second part consisted of further development of the remaining concepts after the screening.

4.1 Concept Generation by Combining Attributes

The concepts were generated by combining the three attributes described in chapter 3.1. Three geometries, three pitch levels and three centering types generated $5 * 3 * 3 = 45$ unique concepts which created a concept catalogue consisting of all possible combinations. Figure 12 illustrates a snippet of the concept catalogue. Normally in a traditional product development process, some sort of brainstorming is included, but using the combination of the different design choices for the three attributes to generate concepts was deemed to be a better method due to the complex nature of the product. With a more traditional brainstorming method, the risk of generating unfeasible concepts would be too high. Materials were not considered during this phase of the process.

Attributes	1	2	3
Geometry	One-piece	Individual Bar Segment	Segment (N r in segme
Centering	Outer ring and roller centering	Inner ring and roller centering	Inner ring a center
Pitch	Over pitch	On pitch	On pitc

Figure 12: A snippet of the combinations in the concept catalogue

4.2 Concept Evaluation and Screening

Since all generated concepts seemed feasible, it was decided to go ahead with a Pugh matrix in order to evaluate and screen the concepts. This was iterated twice for an equitable result.

The Pugh matrix is a method which was employed as a just way of comparing concepts with one another. The method is that it holds one concept as a reference, i.e. a *datum* and then all the other concepts are compared to this (Karl T. Ulrich, 2011). The concepts were

compared to the datum based on the following criteria:

- Low manufacturing cost
- Good bearing dynamics
- Low storage/transportation cost
- Ease of assembly and mounting
- Roller retention during assembly

The criteria are not weighted in the Pugh matrix but consist of +, -, and 0. A plus indicates that a concept performs *better* than the datum at a certain criterion, a minus means that it performs *worse* and a zero means that the concept performs *just as well* as the datum. The criteria were chosen so that engineering assumptions would be enough to assign fair weightings. However, assumptions had to be made based on information from the literature search and interviews.

Generally, the more parts one had during assembly, the harder it would be to assemble the bearing. Roller retention was based on the pitch of the cage and the bearing dynamics had a lot to do with the guidance of the cage and its size. If a concept had an inner ring-centered cage versus a roller-centered or outer ring centered, then this would mean there was lower friction and less wear in the individual parts over time. This is due to the lower relative velocity of the inner ring compared to the outer ring. The datums chosen during the grading were different in each iteration for a fair result. After iterating the matrix twice, the concepts had gone from 45 to 12. These concepts are presented in figure 13.

The geometry called Individual Bar Segment is a segment that looks like a bar, which acts as a separator in between each roller. The geometry called Individual Pocket is a segment that looks like a pocket that the rollers are positioned in. This concept can vary between having a pocket around every roller, and having a roller in between each pocket, so that every other roller is in a pocket. The geometry called Segment (N rollers in segment) is a segment containing several rollers.

Concepts	Geometry	Centering	Pitch
Alternative #11	Individual Bar Segment	Inner ring and roller centering alternating	Alternating
Alternative #12	Individual Bar Segment	Outer ring and roller centering alternating	Alternating
Alternative #22	Individual Pocket	Roller centering	Alternating
Alternative #19	Segment (N rollers in segment)	Outer ring and roller centering alternating	Over pitch
Alternative #20	Segment (N rollers in segment)	Between rollers	Over pitch
Alternative #21	Segment (N rollers in segment)	Inner ring and roller centering alternating	Over pitch
Alternative #23	Individual Pocket	Inner ring and roller centering alternating	Alternating
Alternative #24	Individual Pocket	Outer ring and roller centering alternating	Alternating
Alternative #18	Segment (N rollers in segment)	Inner ring and roller centering alternating	On pitch
Alternative #25	Individual Pocket (every other)	Between rollers	Alternating
Alternative #26	Individual Pocket (every other)	Inner ring and roller centering alternating	Alternating
Alternative #27	Individual Pocket (every other)	Outer ring and roller centering alternating	Alternating

Figure 13: Remaining concepts after two iterations

As can be seen in the figure, the one-piece cage concept did not make it far during the concept screening. This was due to the problems that can occur with large one-piece cages in polymer. In large size bearings, a one-piece cage is induced by strong forces which can cause ovalization of the cage. Since polymer was supposed to be investigated as a cage material during the project, this concept did not seem feasible and was eliminated during the screening process.

The concepts in the figure all have different colours which represent the last two screenings. These were done based on engineering assessments. The concepts in red are the ones which were screened out first. Segments containing several rollers have a risk of causing heavy hammering. Due to the weight of several rollers being held together in a segment, a lot of impact force would occur if the segment was to drop a distance and collide with another segment. This concept was therefore eliminated. Even though the concept would contain fewer parts, which would ease assembly, the dynamics of the cage was considered more

important. Since the bearing is expected to operate for many years, the assembly process could not be prioritised over the dynamics.

The yellow and green colours represent the concepts that made it through the first screening. The three alternatives in green were deemed to be the most feasible concepts. These concepts had different geometries, but were all inner ring centered and roller centered, alternating. This centering was deemed to lead to the least amount of friction in wind turbine application, due to inner ring rotation often being chosen there. The reason for three different concepts making it through all screenings is that it was of interest to compare three different concepts further using simulations and testing. Therefore, the concepts with the centering leading to the lowest friction were chosen, and these three concepts were taken on to further development.

4.3 Solid Modelling and Further Development

When three concepts were selected, these were further developed. In order to get more information about how these would be optimally designed, the rest of the SAT-bearing was studied. By studying the CAD models and drawings of the inner ring, outer ring, and rollers of the SAT bearing, it was possible to see how the design of the segments should depend on the design of the rest of the bearing. In the SAT bearing, the raceways and rollers are inclined. This in combination with the rings being round leads to the segments having to be designed in a way so that they ensure optimal distances between the rollers at the same time as the contact between all rollers and segments are optimal. When having an inclined design like SAT, the radius of the raceways will vary along the rollers. How the raceway on the inner ring is inclined and curved, as well as how the rollers are positioned can be seen in figure 14.

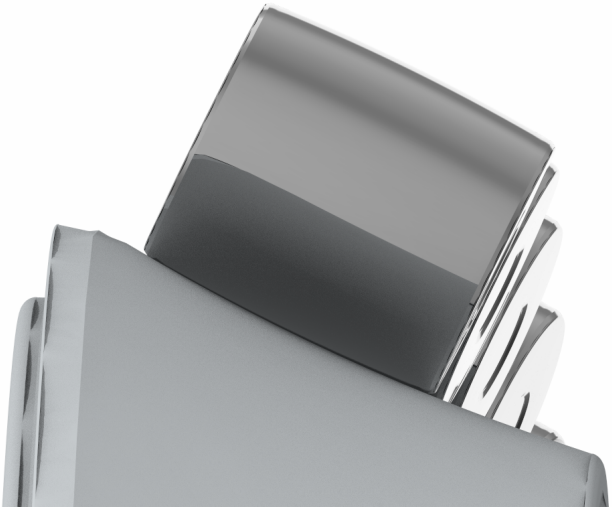

Figure 14: SAT inner ring raceway incline and curvature, as well as roller positioning, *SKF CAD model*

Due to these design choices in the SAT bearing, the spacings between each roller will vary axially along the rollers. This can be seen in figure 15.

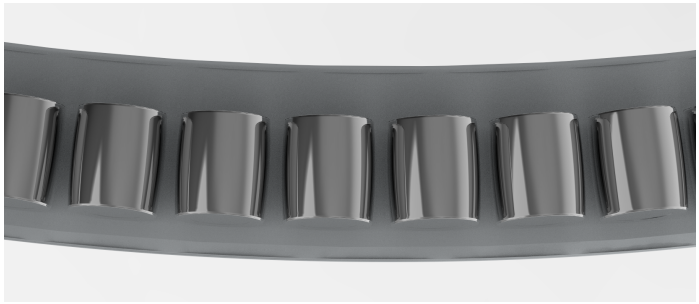

Figure 15: Varying roller spacings in the SAT bearing, *SKF CAD model*

In order to get an idea of what needed to be done and how this should be carried out in order to create solid models of the three concepts in Creo Parametric, quick and dirty prototyping took place. Creo Parametric is a 3D-modelling software. It is frequently used in product development processes due to its advanced features (PTC, n.d.). The quick and dirty prototyping in Creo consisted of trying different methods for creating certain features and trying out different designs for these. This led to design choices and methods that were considered most suitable for the task at hand (Gómez & Lopez-Leon, 2019).

Quick and dirty prototyping in Creo, in combination with different courses in the software, gave good know-how and provided a good foundation to create the desired solid models.

When further developing and designing the concepts, there were different parameters that had to be taken into account. The segments had to be designed in such a way that they allowed for some radial and axial clearance for the rollers. By having some clearances in the cage, the rollers can skew a bit. Since the rollers naturally want to skew a bit, the skew would cause the cage to break without any clearance. This clearance results in lower contact forces to the cage, as well as less friction between the rollers and the cage caused by skew. Since the SAT bearing is a self-aligning bearing, it is important to have some skew in order for the rollers to self-correct, i.e. self-align when angular misalignment between the shaft and the housing occurs. The axial and radial clearance can not be too big or too small and need to be optimal in order to achieve the desired dynamic performance in the bearing. Too much clearance can lead to sliding in the roller to raceway contact. It can also lead to excessively skewed rollers entering the loaded zone, where skew correction occurs really fast and energy is dissipated through the contact, leading to surface damage to the raceway and early bearing failure.

The clearances that the cage should allow for were estimated using trigonometric calculations on the bearing geometry. The axial clearance on each side of the rollers was estimated. Also, the tangential clearance on each side of the rollers was estimated and these clearances are presented in table 3. The tangential clearance is the space between the radial contact points on the rollers and the cage. The clearances were estimated for the wind turbine size, as well as a prototype bearing with a roller diameter of 24 millimetres. This was in order to be able to use both sizes during simulations and prototyping.

Table 3: Axial and Tangential Clearances

Roller Diameter [mm]	Axial Clearance One Side [mm]	Tangential Clearance One Side [mm]
90	[redacted]	[redacted]
24	[redacted]	[redacted]

The design choice to have point contact between the segments and the rollers, as well as between the segments and the inner ring and outer ring was made. The reason behind this design choice was that it would lead to less friction between the components. It was also assumed that this would lead to a more optimal flow of lubrication to the contact points. The point contact was obtained by having larger radii around the contact points on the segments in comparison with the radii of the rollers, by having larger radii on the bottom and top of the segments in comparison with the radii of the raceways, and by having larger radii on the bottom and top of the segments in comparison with the radii of the inner ring and outer ring at the different locations. This is called *osculation*. This gave two contact points between the rollers and the segments, and four contact points between the foundation of the segments and each raceway.

A design rule for the axial distance between the contact points on the rollers derived from analysis of the CARB bearing and its contact points. The CARB bearing uses the same rollers as the SAT bearing and has multiple similarities to the SAT bearing. This led to a design rule for the SAT bearing which states that the axial distance between the contact points on the rollers should be [redacted].

4.4 Design of Proposed Concepts

The three remaining concepts are all based on the same geometry before being built on further. The *individual bar segment* functions as a base which has been built on further to create *every other pocket* and *every pocket*. The concepts were modelled in Creo Parametric.

The details of the concepts are presented together with their calculations and input data. The reason why it was chosen to make solid models was to be able to use these in various simulations and physical prototyping. After learning more about the bearing dynamics and how the segments move when the bearing rotates, and learning more about the different contacts between the segments, rollers, and rings, it was decided to design the segments to alternate between inner ring centering and outer ring centering. The reason for this was that the concepts had an on pitch design, which was desirable. By letting the segments drop between inner ring centering and outer ring centering, it was possible to have only on pitch contact between the segments and the rollers.

4.4.1 Input Data

When designing the solid models, the data from the SAT bearing which had a size compatible with wind turbine bearing applications was used as a reference.

$$Roller\ \ diameter : \varnothing_{roller} = 90\ mm$$

$$Roller\ \ length : RKL01 = 100\ mm$$

$$Axial\ \ Clearance\ \ One\ \ Side : Ax\ CLR = [redacted]\ mm$$

$$Roller\ \ curvature\ \ radius : Radius_{roller} = [redacted]\ mm$$

$$osculation = [redacted]$$

4.4.2 Concept #1: Individual Bar Segment

The individual bar segment is located between each roller in the bearing. This is visualized in figure 16a and 16b. Figure 17 shows the segment from the bottom, and from the side. The individual bar segment functions as a separating cage segment and is both inner ring guided and outer ring guided. This segment will never be roller-centered no matter which position it is in during operation. During the design of the cage segment, continuous comparison with the digital solid model of the SAT bearing was done in order to make sure the segment would be a good fit. This meant that the measurements of the bearing had to be shown consideration when designing the details of the bar segment.

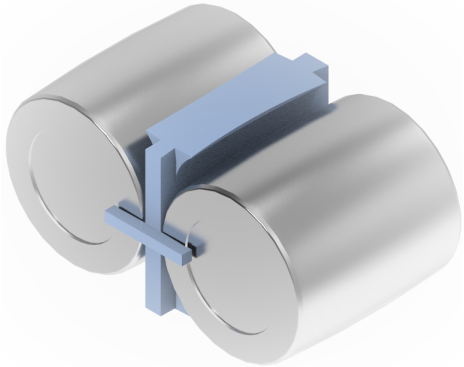

(a) Overview with rollers

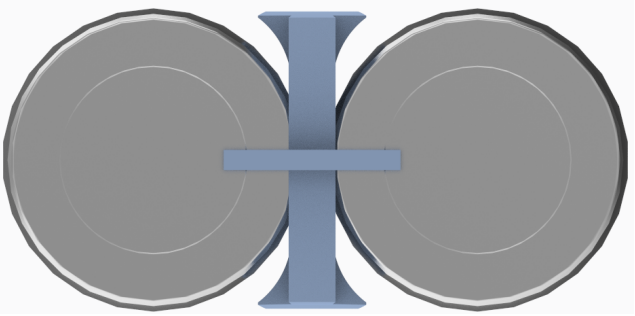

(b) Front view with rollers

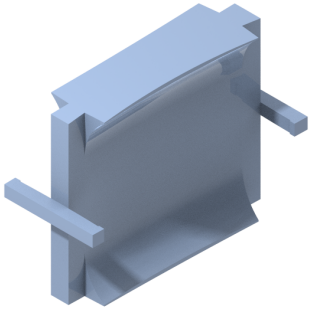

(c) Overview

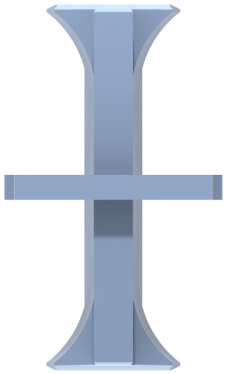

(d) Front view

Figure 16: Individual Bar Segment

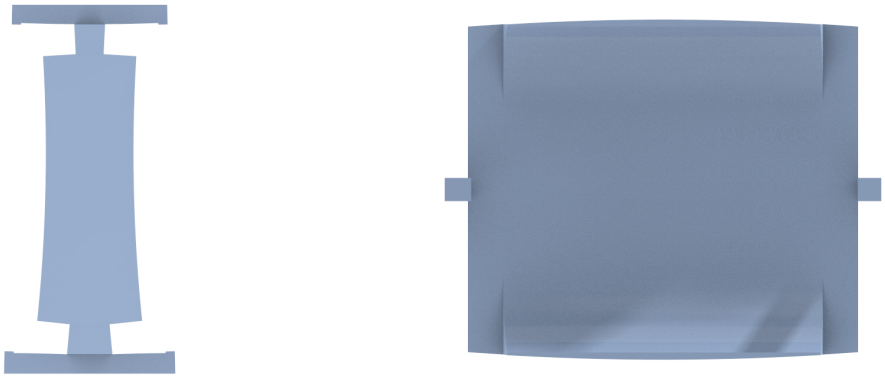

(a) Bottom view (b) Left view

Figure 17: Individual Bar Segment

Adapted Design
Since the bearing has an inclined design, the segments needed to be designed with respect to the nearby rollers where the distance between the rollers varied along the axial length of the rollers. This meant that the segment had to be designed in a way so that its contact points were adapted after this phenomenon. This phenomenon is presented in section 4.3 and can be seen in figure 15. The distances between the different parts of the rollers were measured in the solid model of the bearing, and the appropriate clearances were accounted for in the design.

Total Length Between Stops
For the roller to fit between the stops of the individual bar segment, the total axial length between the stops was set to be the axial length of the roller plus axial clearance on both sides.

$$Total\ Length\ Between\ Stops = RKL01 + Ax\ CLR * 2 = [redacted]\ mm \quad (1)$$

Contact Zones
The roller comes in contact with the bar segment via point contact. This reduces friction compared to having a larger surface with contact with the roller.

There is room for the segment to drop from one ring to another which means that the point of contact could vary radially. It is also possible for the rollers to move axially, which means that the contact points can vary in that direction as well. The axial distance between the contact points was [redacted] of the roller length. Radially, the geometry of the contact zones allowed for the segment to vary between inner ring centering and outer ring centering, due to the geometry just being extended in that direction. To let the rollers move axially without losing point contact, contact zones where the radius was increased with the osculation factor were designed. These zones extended from the axial ends, to the points which were [redacted] of the roller lengths in between them, plus a certain length in order to keep the point contact when the rollers were moving axially which can be seen in figure 18. This additional length was calculated by taking the total axial clearance multiplied by a factor

of 1,5. This assumption derived from studies of the geometry and seemed like a feasible safety factor.

$$Distance_{contactponts} = [redacted] * RKL01 = [redacted] \ mm \tag{2}$$

$$Area_{contact} = 1.5 * Pocket\ Ax\ CLR = 1,5 * [redacted] = [redacted] \ mm \tag{3}$$

$$Radius_{contact\ points} = Radius_{roller} * osculation = [redacted] * [redacted] = [redacted] \ mm \tag{4}$$

Figure 18: Contact zones of the individual bar segment marked in red

Radii of Bar Segment
Should the roller press down too hard on the segment and the segment was to deform, there would be a risk of losing point contact which had to be prevented. Therefore, the radius between the two contact zones was set to be much smaller than the roller curvature radius and was set to [redacted] millimetres. This was in order to avoid surface contact in this area if the segment was to deform.

Height
The individual bar segment has its centering varying between inner ring centering and outer ring centering. This was designed in a way so that the segment only has contact with the rollers in the contact zones or the stops. The height of the segment is decided so that it can drop between the inner ring and the outer ring. The distance for it to drop was [redacted] millimetres in order to allow for some clearance, but still preserve the desirable contacts in the contact zones.

Foundations
The individual bar segment is centered on one of the raceways which has a radius. The foundations are the parts of the geometry where the individual bar segment allows for point contact with one of the raceways. The geometry of the top and bottom foundations of the individual bar segment needed to match the surface radii of the raceways on the inner and outer rings. This was done by having curved surfaces for the foundations, where the radii matched the radii of the raceways, but with an osculation in order to allow for point contact. The curvature of the raceway can be seen in figure 14 in chapter 4.3. The curvatures on the individual bar segments can be seen in figure 17b. The foundation facing the inner ring was designed with a concave shape and the foundation facing the outer ring was designed with a convex shape. This was required because of the round geometry of the bearing. Due to the inclined and round design of the bearing, the different radii on the foundations varied along the raceway. The individual bar segment was designed with additional width for the foundations, in relation to the circumference of the bearing. This was in order to increase stability.

Stops
What is unique about this design is that it aids the assembly process by having axial stops with a design that allow them to connect with the dimples in the rollers. Since the SAT bearing lacks a flange that would normally stop the rollers from sliding down the raceway during assembly, a temporary snap ring is proposed to serve the same purpose. This could be a snap ring that is fastened around the circumference of the ring, acting as a stop for the rollers. This snap ring can then be removed when assembly is done. During the assembly process, the rollers and cage segments can be placed in the raceway, resting on the snap ring, and the segments and rollers can be connected so that they create a chain when all parts are connected around the circumference. The idea is that the fact that all parts are connected in a chain will allow for the snap ring to be removed after all segments and rollers are in place.

The roller comes in contact with the stops through point contact which is obtained by having a radius on the surface of the stops that is in contact with the roller of [redacted] millimetres which is derived from assumptions and calculations of the bearing geometry.

The radius of the dimple on the roller is set to 55 millimetres. The bulging geometry on the stops is therefore designed with a curvature with the same radius but with an osculation factor of [redacted] to allow for point contact. As the walls of the dimples are at an angle of 20 degrees, so is the slope of the bulging geometry on the stops. The design of the stops is illustrated in figure 19.

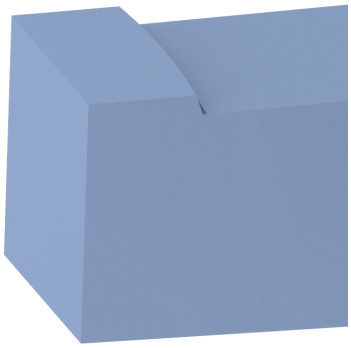

(a) Close-up of bulging geometry

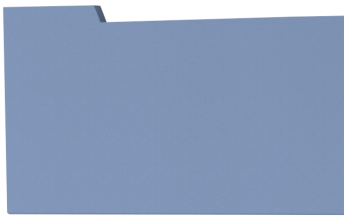

(b) Angle of bulging geometry and surface radius

(c) Curvature of bulging geometry

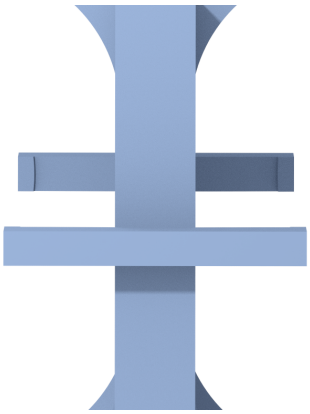

(d) Overview of axial stops

Figure 19: The stops on individual bar segment

4.4.3 Concept #2: Every Other Pocket

Every Other Pocket is a pocket segment which is placed between every other roller as can be seen in figures 20a and 20b. One benefit of placing a roller between each segment is that there it can allow the segments to absorb forces by flexing a bit if it is made with a polymer material. As one can see in figure 20c and 20d, this segment is built up of two individual bar segments which are connected and tilted at an angle to match the round geometry of the bearing, and at an angle to fit properly in the SAT bearing with its inclined design. Figure 21 shows the segment from the bottom, and from the side. The two bar segments are connected on two sides of the geometry.

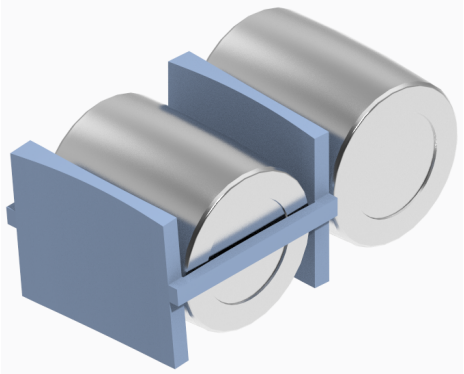

(a) Overview with rollers

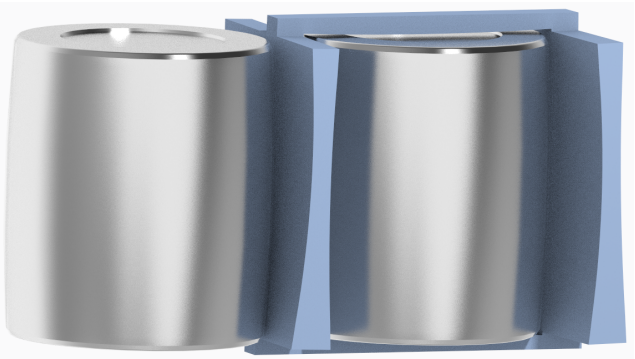

(b) Top view with rollers

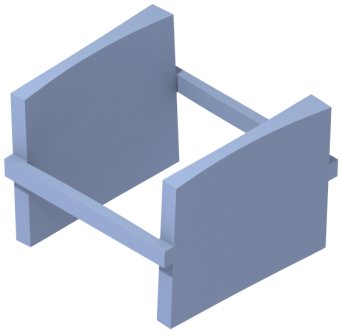

(c) Overview

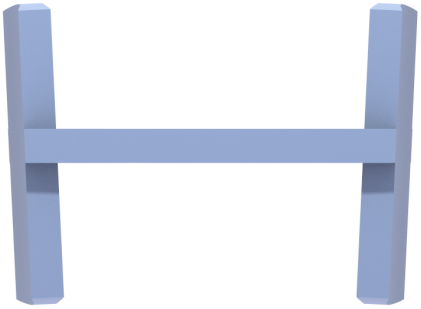

(d) Front View

Figure 20: Every Other Pocket

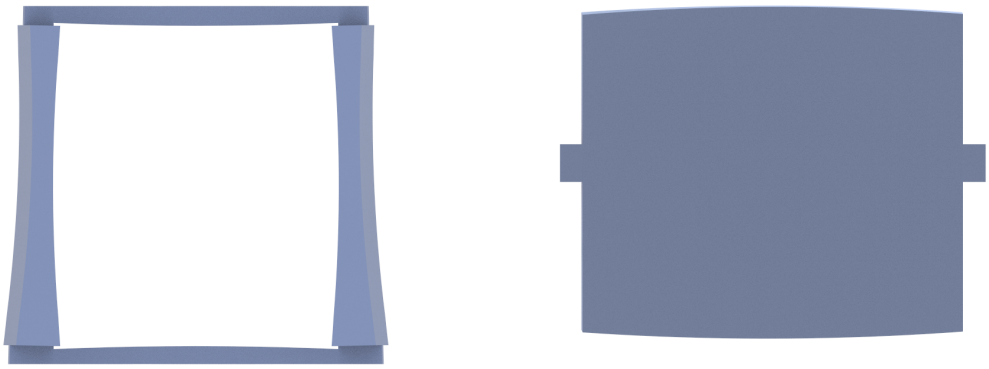

(a) Bottom View (b) Left View

Figure 21: Every Other Pocket

Foundation
Unlike the individual bar segment, the every other pocket segment does not have additional width on the foundations for extra stability since the segment is stabilised by having four foundations.

Connecting Beam
The two bar segments are connected with a connecting beam. The beam has a convex geometry to achieve point contact with the roller inside the pocket which can be seen in figure 22. The radius is set to be [redacted] millimetres and is based on engineering assumptions and studies of the bearing geometry. In order to allow for the desirable axial clearance for the roller in the pocket, the connecting beam is designed in a way so that the total pocket length with axial clearance is calculated from the contact point on one beam to the contact point on the other.

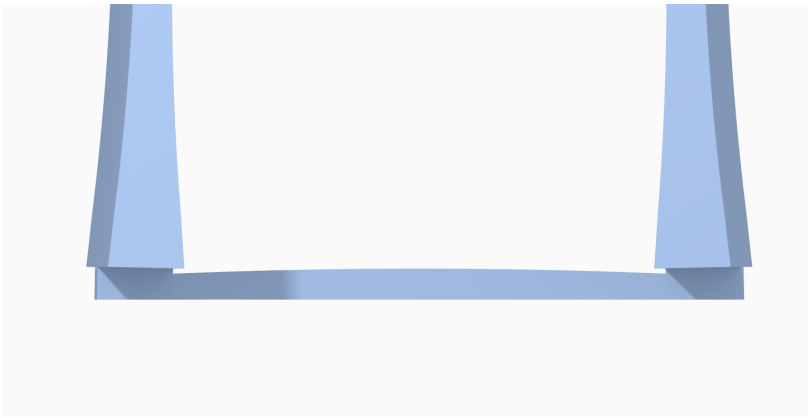

Figure 22: Connecting beam on *every other pocket*

4.4.4 Concept #3: Every Pocket

The third concept, *every pocket*, is an iteration of *every other pocket*. What has changed is that the bar segments on each side have been cut in the middle, leading the segments to be thinner in order to fit all segments in the bearing without having to lower the number of rollers. The number of segments when using this concept would be the same number as rollers in the bearing instead of half like in *every other pocket*. Two segments next to each other will create the same dimensions between the rollers as one individual bar segment, as can be seen in 23a. Figure 24 shows the segment from the bottom, and from the side. This lead to a large contact area, which can be beneficial in terms of the forces induced on the segment when two pockets are in contact. The forces induced will because of the design be distributed on a larger area. The benefit of having a pocket segment around each roller is that the risk of damage caused by hammering decreases since the clearances are more evenly spread out around the bearing. The pocket segments will have surface contact with each other around the bearing and do therefore not have the same curvature on the sides as *every other pocket*.

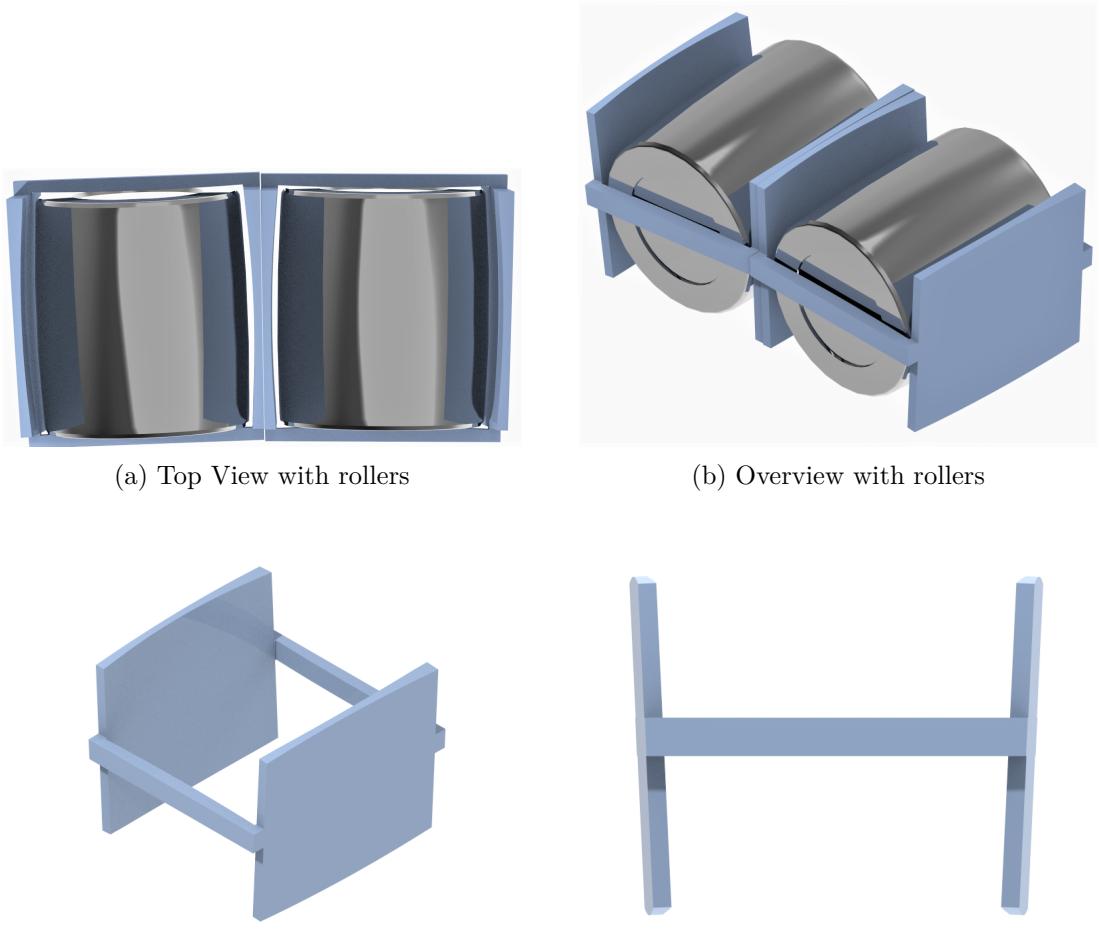

(a) Top View with rollers

(b) Overview with rollers

(c) Overview

(d) Front View

Figure 23: Every Pocket

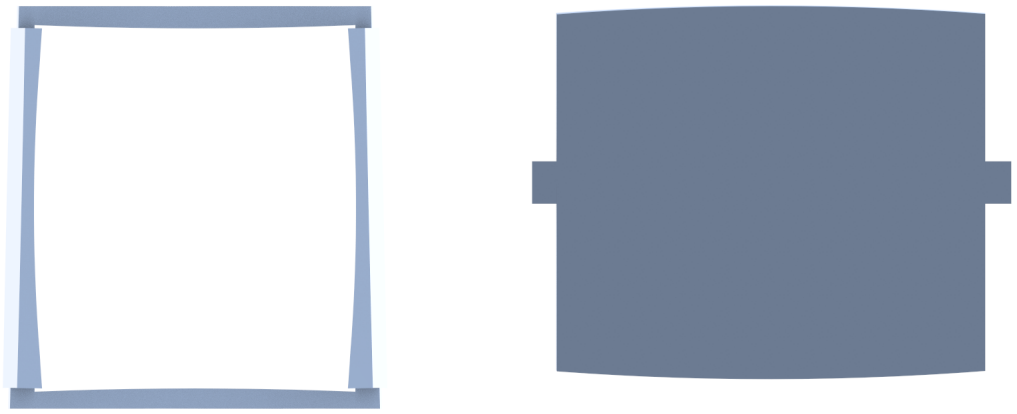

(a) Bottom View (b) Left View

Figure 24: Every Pocket

5 Material Study

For the bearing cage to have the most optimal properties for its application and to be able to last for 20-30 years, choosing the most suitable material is of great importance. Different materials have different strengths and weaknesses and can be dependent on application-specific factors such as load conditions, temperature, and humidity. Different materials also differ in terms of physical properties, mass, and price. These are all factors that play a big role when selecting materials for a bearing cage. SKF are world-famous for their high-quality products and services, but they also have competitors. Another crucial aspect, besides quality, is therefore the price that SKF can offer to their customers for their products and services. Polymer materials are becoming more common in bearing cage design thanks to improvements in engineering polymers and their mechanical properties, as well as the advantages of flexible production.

5.1 Benchmarking of SKF Materials

There are three different polymers that are approved for bearing cages at SKF and that are the most commonly used polymer materials for this purpose. To be able to compare the properties of the polymer materials with metal materials, a commonly used steel for bearing cages is used as a reference. The information about the exact materials used by SKF and their curing procedures for each material is confidential and can not be shared publicly. For this purpose, information about similar materials that is publicly available will be used to benchmark the different materials. The material data for these materials are found in the Ansys Granta material database. The data studied in the scope of this project is only enough for a first rough estimation regarding the different properties of the materials. It is also needed to take ageing effects caused by lubricants or other chemical media, in combination with different load conditions into account in order to make a definitive material choice. Load simulations were also performed using the different materials and are further presented in chapter 6 of the report.

The materials studied are PEEK, PA46, PA66 and a hot rolled bearing steel.

The PEEK material is a thermoplastic polymer called Polyetheretherketone that is reinforced with [redacted].

Table 4: Material data for PEEK

PEEK ([redacted])	
Price:	773 - 857 SEK/kg
Density:	1,38e3 - 1,41e3 kg/m^3
Maximum service temperature:	220 - 250 °C

The PA46 material is a thermoplastic polymer called Polyamide (Nylon) that is reinforced with [redacted].

Table 5: Material data for PA46

PA46 [redacted]	
Price:	93,6 - 97,8 SEK/kg
Density:	1,42e3 - 1,45e3 kg/m^3
Maximum service temperature:	73 - 87 °C

The PA66 material is a thermoplastic polymer that also is a Polyamide (Nylon) that is reinforced with [redacted] glass fiber.

Table 6: Material data for PA66

PA66 ([redacted])	
Price:	47,1 - 60,2 SEK/kg
Density:	1,35e3 - 1,38e3 kg/m^3
Maximum service temperature:	90 - 130 °C

The metal material studied is a hot rolled bearing steel. The steel is of drawing quality, which means that it is a low-carbon steel with lower yield strength for easy forming.

Table 7: Material data for steel

[redacted] ([redacted])	
Price:	11,6 - 14,4 SEK/kg
Density:	7,8e3 - 7,9e3 kg/m^3
Maximum service temperature:	495 - 509 °C

As can be seen in the tables, the PEEK material is a low-density material and can handle high service temperatures, but it is also the most expensive polymer material out of the three. When comparing the PA46 and PA66 materials, it can be seen that the PA66 material offers a lower price, lower density, and also a higher maximum service temperature. The properties of these polymer materials are temperature dependant and can change if reaching certain service temperatures, which is something that has to be carefully evaluated. When considering the wind turbine application, the temperature of the environment around the bearing is low compared to other applications, and therefore having a very high maximum service temperature of the materials is not something that is of great importance.

From this rough first estimation, the PEEK material, as well as the PA66 material, both seem like good candidates for use in bearing cages in wind turbine applications. The PEEK

material is considered a premium material and can offer great properties and performance for a higher price. Having a low price is of great importance and is discussed further in chapter 5.2. It is also of great importance to keep the mass of the bearing cage low in order to minimize internal forces in the bearing, as well as to allow for rotation as efficiently as possible since a higher mass of the cage means that more force is needed for all of the parts to move in the bearing.

As previously mentioned, many factors need to be studied further in order to choose a definitive material for the application, but after a brief overview of some of the material properties, the PA66 material is considered an interesting candidate thanks to its low price, low density and a good limit in terms of its maximum service temperature.

5.2 Polymer vs. Metal

The price that SKF can offer their products and services to their customers for is a factor that needs to be satisfactory and attractive. This in order to please their customers as well as to compete strongly with other companies. Most companies are dependent on money in order to continue offering their products or services and to further develop. SKF is a company that works with business-to-business commerce and relations. In the case of SKF, this means that the customers of SKF often make large investments when buying products and services. By being able to offer high-quality products and services for an attractive and competitive price, SKF can satisfy their customers as well as gain market shares. This is where material choice can be a crucial factor. By using polymer cages instead of metal cages when manufacturing bearings, the manufacturing cost can decrease, and in turn lead to lower costs for customers of SKF. In addition to a more attractive price, polymer cages also offer more design freedom compared to metal cages. This design freedom can lead to implementing more traditionally challenging design features. This can be features such as lubrication channels in the bearing cages, which are not possible to obtain with traditional metal manufacturing techniques. By improving the control of lubricant distribution, it is possible to lower bearing temperature during use, reduce roller and raceway wear, as well as roller and raceway fatigue. This will increase the overall bearing service life. The manufacturing methods available for polymer parts have an advantage in terms of this, which makes polymer cages an interesting and appealing topic for SKF. An interview with D[redacted] F[redacted] who has experience with segmented polymer cages at SKF in Schweinfurt, was conducted (personal communication, 21/02/23). According to Fritz, the elasticity of PEEK materials in segmented cages offers big advantages over metal cages. The polymer material lets the segments bend a bit, which compared to metal segments leads to lower stresses under the same load. He also stated that the overall cost of a cage for a bearing with a diameter of three meters is around [redacted] lower for a segmented PEEK solution compared to a milled single-piece metal cage. This in turn leads to almost [redacted] lower total bearing manufacturing costs.

The main reasons for polymer usage over metal can be summarized as:

- Lower cost
- Lower weight
- Higher elasticity
- Design freedom
- High volume production by injection molding

6 Virtual Testing and Simulation

The computer-based simulation was implemented in the product development process as a method for testing and investigating certain phenomena digitally in an effective way. The purpose was to discover weaknesses in the designs in order to iterate the solid models as well as to find the best material fit. It was also a tool for analysing the concepts and comparing their strengths and weaknesses. After having benchmarked a number of materials including a selection of polymers approved by SKF and one metal for reference, it was crucial to test these and compare the polymer materials to the metal as this was one of the research questions. The following software were used for solid modelling and simulation of the concepts in the order shown in figure 25.

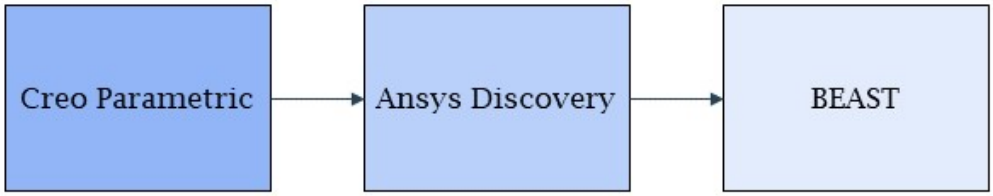

Figure 25: Softwares used for modelling and simulation

6.1 Purpose of Simulation

The two simulation software were used for different purposes. The finite element analysis in Ansys Discovery was a study for calculating the stresses and deformations in the segments which was also done to study material-related parameters. The simulations in BEAST were of a rigid dynamic kind and were used to give an insight into the kinematic behaviour of the segments in the bearing during operation.

The boundary conditions in the simulations were set up to resemble real situations and occurrences with some simplifications. The simulations in Ansys Discovery were completed on four different materials which provided a basis for comparison together with the material theory study and the economic assessment. When investigating the strength of a material, there are a few parameters which will be under investigation. The von Mises stress was measured in all three concepts in order to predict the yielding of the materials. All situations where the von Mises stress exceeded the limit for yield strength, σ_y, were to be avoided in this project. The initial part of the stress-strain curve seen in figure 26, leading up to σ_y, is elastic meaning that the material will return to its original shape once forces causing the stresses are removed. However, should the von Mises stress exceed σ_y, then the material will have a permanent deformation or fracture. Should the limit for tensile strength, $\sigma_t s$ be exceeded, then the material will start to break. The elastic regime which is the curve leading up to σ_y is the area desired to stay in (Ansys Granta, n.d.).

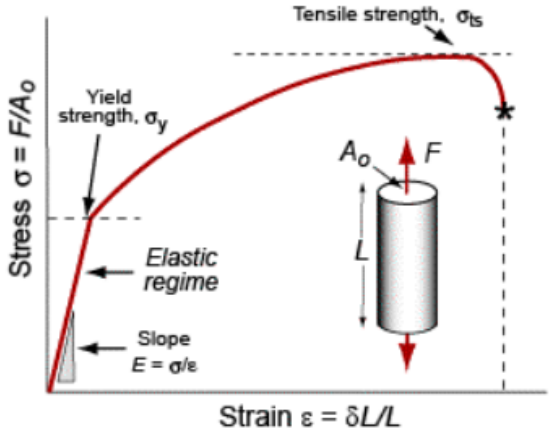

Figure 26: A tensile stress-strain curve, (*Ansys Granta*, *n.d.*)

6.2 Materials Tested

Listed below is the material data for the four materials tested during the simulation in Ansys Discovery. For the simulations in BEAST, only PEEK was used. The material data can be seen in table 8.

Table 8: Material Data for Ansys Discovery

Material	**PEEK**	**PA66**	**PA46**	**Steel**
Density $[\frac{kg}{m^3}]$				
Young's Modulus [MPa]				
Poisson's Ratio				
Shear Modulus [MPa]				
Bulk Modulus [MPa]				
Tensile Yield Strength [MPa]				
Tensile Ultimate Strength [MPa]				
Thermal Expansion Coefficient $[\frac{1}{°C}]$				
Thermal Conductivity $[\frac{W}{m*K}]$				
Specific Heat $[\frac{J}{kg*C}]$				

6.3 Simulation in Ansys Discovery

The simulations in Ansys Discovery consisted of simulations of different scenarios that can occur during the operation of the bearing or assembly of the cage segments. Ansys Discovery is a simplified simulation software which provides live physics simulations and answers design questions early in the design process. Ansys Discovery was used in connection with Creo which allowed an easy way to export solid models directly into the software (Ansys, 2021). The results from the simulations show how the different concepts are affected by

stress in the different loading conditions, as well as how they are deformed under certain circumstances. The results also consist of stress and displacement data from each test, where the performance of the different materials is compared. The results were also used to analyse the performance of the different concepts and to compare these.

6.3.1 Test Case 1 - Weight Induced Load on Segments

The first scenario studied was when a segment is induced by load from a certain amount of rollers and segments that rest on top of one segment. In order to simulate this, different forces were applied to the contact points on the segments, where the rollers would normally be in contact with the segments. The simulations were performed to test how the different concepts and materials handle the stress induced by the weight of 1, 4, 8, and 12 rollers and their respective segments. The amount of rollers and segments chosen for this purpose was derived from observation of the number of rollers in a certain area of the circumference of the bearing. The weight of the rollers and segments is assumed to load the studied segment from one direction, which is the same direction as the gravity. This is a simplification, since in reality, some of the force induced will be going towards the inner ring and the outer ring. The highest loads simulated are chosen to test the limits of the designs and materials and are assumed to be exaggerated extreme cases.

Individual Bar Segment

Figure 27 shows the *individual bar segment* in the first test case.

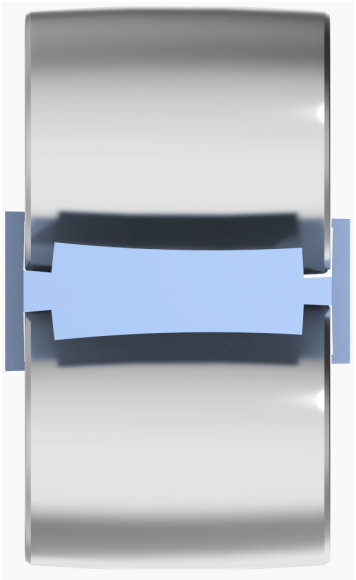

Figure 27: Individual Bar Segment - Test case 1

Boundary Conditions

In order to simulate these scenarios and to perform the various tests, different boundary conditions were chosen. The forces applied are shown as blue arrows, acting on the contact points. The forces are applied in the same direction as the gravity, which is shown as a green arrow. This can be seen in figure 28a. The part is fixed in the contact points on the other side of the geometry, to simulate the segment laying still on the roller below. These contact points can be seen in figure 28b.

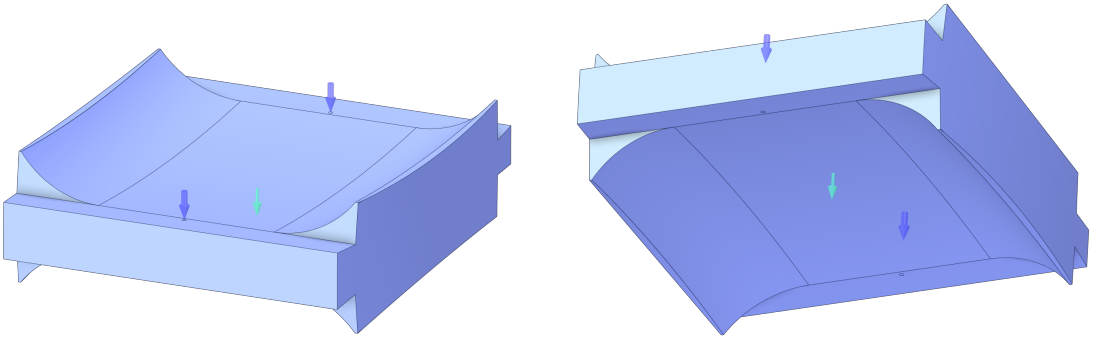

(a) Top view (b) Bottom view

Figure 28: Boundary conditions for test case 1 - Individual Bar Segment

Force Calculations

Firstly, a load representing the weight of one roller on the segment was tested. The load was induced by the weight of the roller and gravity. The force was distributed on two points on the segment. The material of the roller is steel with a density of [redacted] $\frac{kg}{m^3}$.

$$Roller \quad mass : m_{roller} = 4.7963181 \ kg$$

$$g = 9.81 \ \frac{m}{s^2}$$

$$F = m * a = 4.7963181 * 9.81 = 47.0518806 \ N \tag{5}$$

The next test was the set-up used to mimic the situation where several rollers and their segments are inducing load onto one segment. The following are the masses of the *individual bar segments*, using four different materials.

Table 9: Mass of the bar segment depending on material

BAR	**PA66**	**PA46**	**PEEK**	**Steel** [redacted]
Mass [kg]	0,1342	0,1446	0,1435	0,8106

The number of rollers used in each simulation have the variables N1, N2, and N3, where N1 means 4 rollers, N2 means 8 rollers, and N3 means 12 rollers.

The number of segments varied. In the case of the *individual bar segment*, the segments were just as many as the rollers. In *every other pocket*, then N was divided by 2 to get the

number of segments, and in the case of *every pocket*, the number of segments was the same as the number of rollers. In each case (N1, N2 or N3), the force applied to the segment being tested varied depending on the material and the number of rollers. The different forces, F1, F2, and F3 were calculated using the following equations. Similar equations were used for each of the concepts.

4 rollers - BAR

$$F_{1\ BAR\ PA66} = (N_1 * m_{roller} + N1 * m_{BAR\ PA66}) * g = 193,475\ N \tag{6}$$

$$F_{1\ BAR\ PA46} = (N_1 * m_{roller} + N1 * m_{BAR\ PA46}) * g = 193,8802\ N \tag{7}$$

$$F_{1\ BAR\ PEEK} = (N_1 * m_{roller} + N1 * m_{BAR\ PEEK}) * g = 193,8397\ N \tag{8}$$

$$F_{1\ BAR\ G90} = (N_1 * m_{roller} + N1 * m_{BAR\ G90}) * g = 220,0152\ N \tag{9}$$

8 rollers - BAR

$$F_{2\ BAR\ PA66} = (N_2 * m_{roller} + N2 * m_{BAR\ PA66}) * g = 386,9501\ N \tag{10}$$

$$F_{2\ BAR\ PA46} = (N_2 * m_{roller} + N2 * m_{BAR\ PA46}) * g = 387,7605\ N \tag{11}$$

$$F_{2\ BAR\ PEEK} = (N_2 * m_{roller} + N2 * m_{BAR\ PEEK}) * g = 387,6794\ N \tag{12}$$

$$F_{2\ BAR\ G90} = (N_2 * m_{roller} + N2 * m_{BAR\ G90}) * g = 440,0304\ N \tag{13}$$

12 rollers - BAR

$$F_{3\ BAR\ PA66} = (N_3 * m_{roller} + N3 * m_{BAR\ PA66}) * g = 580,4251\ N \tag{14}$$

$$F_{3\ BAR\ PA46} = (N_3 * m_{roller} + N3 * m_{BAR\ PA46}) * g = 581,6407\ N \tag{15}$$

$$F_{3\ BAR\ PEEK} = (N_3 * m_{roller} + N3 * m_{BAR\ PEEK}) * g = 581,5191\ N \tag{16}$$

$$F_{3\ BAR\ G90} = (N_3 * m_{roller} + N3 * m_{BAR\ G90}) * g = 660,0456\ N \tag{17}$$

Results

The simulation results studied are the stresses in the segments, as well as the deformation of the geometry. The stresses are visualized in figures 29a and 29b, where the red areas are where the highest stress occurs. The most affected areas were the same for every material and load case.

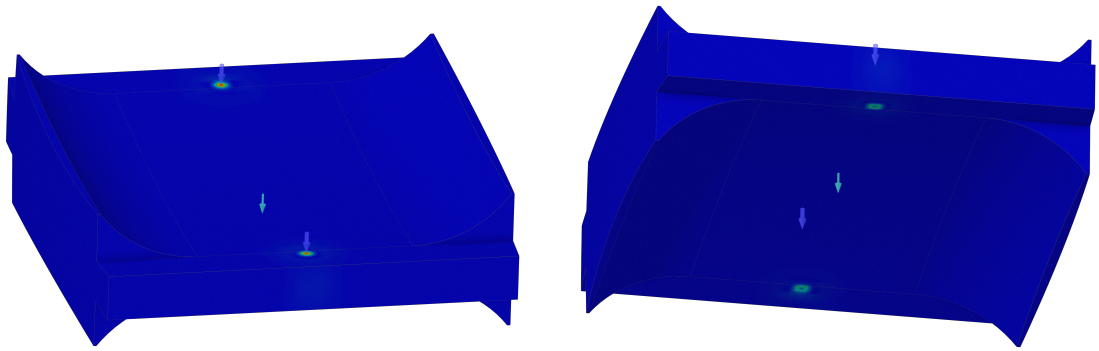

(a) Top view (b) Bottom view

Figure 29: von Mises stress from test case 1 - Individual Bar Segment

It is noticed that in this test case, most of the stress occurs at the contact points and in a small area around them.

Figures 30a and 30b show how the segments are deformed during the simulations.

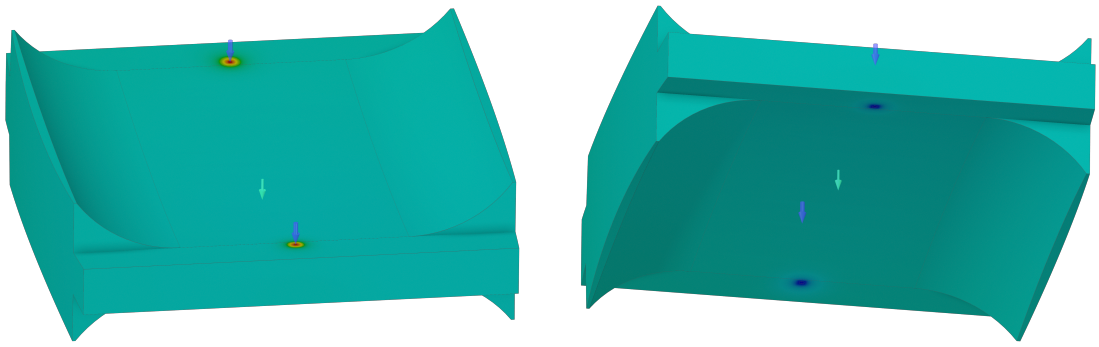

(a) Top view (b) Bottom view

Figure 30: Displacement from test case 1 - Individual Bar Segment

Here, most of the displacement occurs at the contact points where the forces are applied.

The maximum stress, as well as maximum displacement in the different simulations, are presented in the table below. The results marked with red are the tests where the maximum stress exceeds the yield strength of the material.

Table 10: Table of results for individual bar segment

Case	Total Force [N]	Model	Material	Yield Strength [MPa]	Max von Mises [MPa]	Max Displacement [mm]
1R	47,0519	Bar	PEEK	87	7,87	0,00406
4R	193,8397	Bar	PEEK	87	32,4	0,0166
8R	387,6794	Bar	PEEK	87	64,8	0,0331
12 R	581,5191	Bar	PEEK	87	97,2	0,0496
1R	47,0519	Bar	PA46	75	8,18	0,00485
4R	193,8802	Bar	PA46	75	33,7	0,0198
8R	387,7605	Bar	PA46	75	67,4	0,0395
12R	581,6407	Bar	PA46	75	101	0,0592
1R	47,0519	Bar	PA66	55	8,18	0,0044
4R	193,475	Bar	PA66	55	33,6	0,0179
8R	386,9501	Bar	PA66	55	67,2	0,0358
12R	580,4251	Bar	PA66	55	101	0,0537
1R	47,0519	Bar	Steel [redacted]	224	8,30	0,000135
4R	220,0152	Bar	Steel [redacted]	224	38,5	0,000555
8R	440,0304	Bar	Steel [redacted]	224	77	0,0011
12R	660,0456	Bar	Steel [redacted]	224	115	0,00165

As can be seen in the table, only the metal material managed to withstand the load from 12 rollers and segments without reaching its yield limit. The PA66 material reached its limit at the load case with 8 rollers and segments, which means that it performed worse than

the other materials, since all other materials managed to withstand the load from at least 8 rollers and segments.

Every Other Pocket
Figure 31 shows the *every other pocket* segment in the first test case.

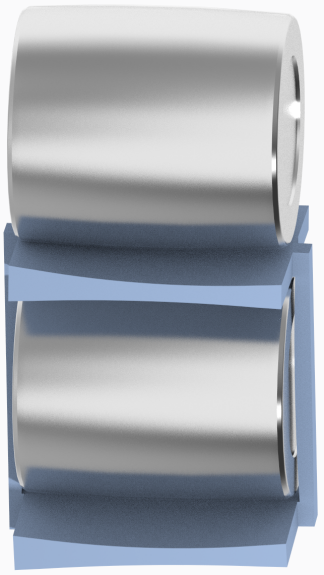

Figure 31: Every Other Pocket - Test case 1

Boundary Conditions
For the concept *every other pocket*, the loading conditions looked a little different compared to the test of the *individual bar segment*. Here, the force from one roller was applied to contact points resembling the contact between one roller inside of the pocket, and the segment. The additional loads were applied to the contact points at the top of the segment, as can be seen in figure 32a. All forces were directed in the same direction as the gravity. The segment was fixed in the contact points at the bottom of the segment, resembling a scenario where the segment is resting on an underlying roller. The fixed contact points can be seen in figure 32b.

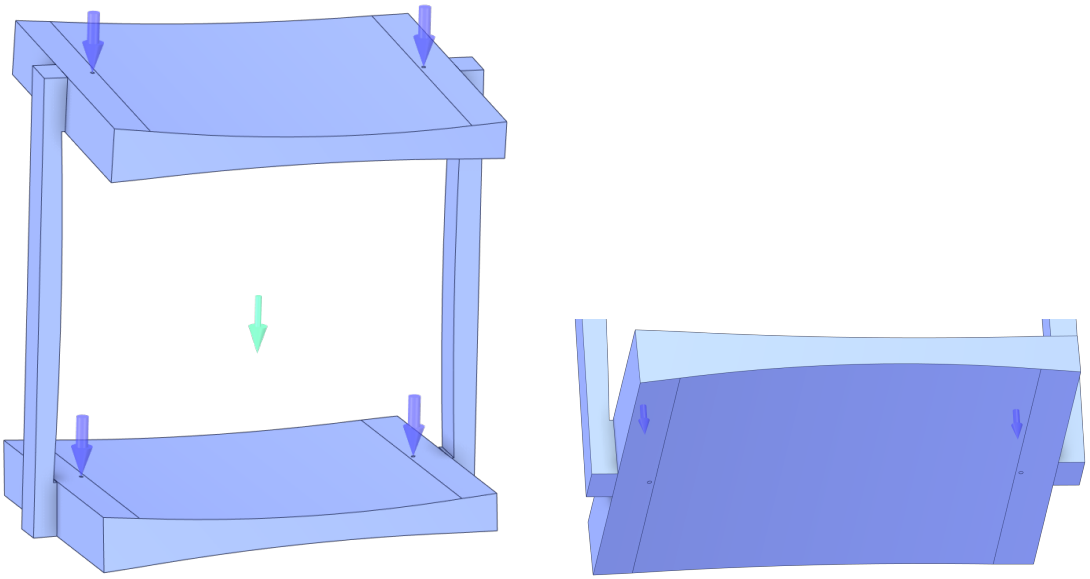

(a) Top view (b) Bottom view

Figure 32: Boundary conditions for test case 1 - Every Other Pocket

Force Calculations

The following are the masses of the *every other pocket* segments, using four different materials.

Table 11: Table of masses

EOP	**PA66**	**PA46**	**PEEK**	**Steel** [redacted]
Mass [kg]	0,2141	0,2306	0,2290	1,2931

The following calculations were done in order to obtain the different forces applied in the different load cases.

One roller:

$$m_{roller} = 4,7963181\ kg$$
$$g = 9,81\ \frac{m}{s^2}$$
$$F = m * g = 4,7963181 * 9,81 = 47,0518806\ N \tag{18}$$

4 rollers - EOP

$$F_{1\ EOP\ PA66} = (N_1 * m_{roller} + \frac{N1}{2} * m_{EOP\ PA66}) * g = 192,4091\ N \tag{19}$$

$$F_{1\ EOP\ PA46} = (N_1 * m_{roller} + \frac{N1}{2} * m_{EOP\ PA46}) * g = 192,7323\ N \tag{20}$$

$$F_{1\ EOP\ PEEK} = (N_1 * m_{roller} + \frac{N1}{2} * m_{EOP\ PEEK}) * g = 192,7\ N \tag{21}$$

$$F_{1\ EOP\ G90} = (N_1 * m_{roller} + \frac{N1}{2} * m_{EOP\ G90}) * g = 213,5787\ N \tag{22}$$

8 rollers - EOP

$$F_{2\ EOP\ PA66} = (N_2 * m_{roller} + \frac{N2}{2} * m_{EOP\ PA66}) * g = 384,8182\ N \tag{23}$$

$$F_{2\ EOP\ PA46} = (N_2 * m_{roller} + \frac{N2}{2} * m_{EOP\ PA46}) * g = 385,4646\ N \tag{24}$$

$$F_{2\ EOP\ PEEK} = (N_2 * m_{roller} + \frac{N2}{2} * m_{EOP\ PEEK}) * g = 385,4\ N \tag{25}$$

$$F_{2\ EOP\ G90} = (N_2 * m_{roller} + \frac{N2}{2} * m_{EOP\ G90}) * g = 427,1573\ N \tag{26}$$

12 rollers - EOP

$$F_{3\ EOP\ PA66} = (N_3 * m_{roller} + \frac{N3}{2} * m_{EOP\ PA66}) * g = 578,1969\ N \tag{27}$$

$$F_{3\ EOP\ PA46} = (N_3 * m_{roller} + \frac{N3}{2} * m_{EOP\ PA46}) * g = 578,1969\ N \tag{28}$$

$$F_{3\ EOP\ PEEK} = (N_3 * m_{roller} + \frac{N3}{2} * m_{EOP\ PEEK}) * g = 578,1\ N \tag{29}$$

$$F_{3\ EOP\ G90} = (N_3 * m_{roller} + \frac{N3}{2} * m_{EOP\ G90}) * g = 640,736\ N \tag{30}$$

Results

The stresses in the segments, as well as the deformation of the geometry, were studied. The stresses are visualized in figures 33a and 33b, where the red areas are where the highest stress occurs. The most affected areas were the same for every material and load case.

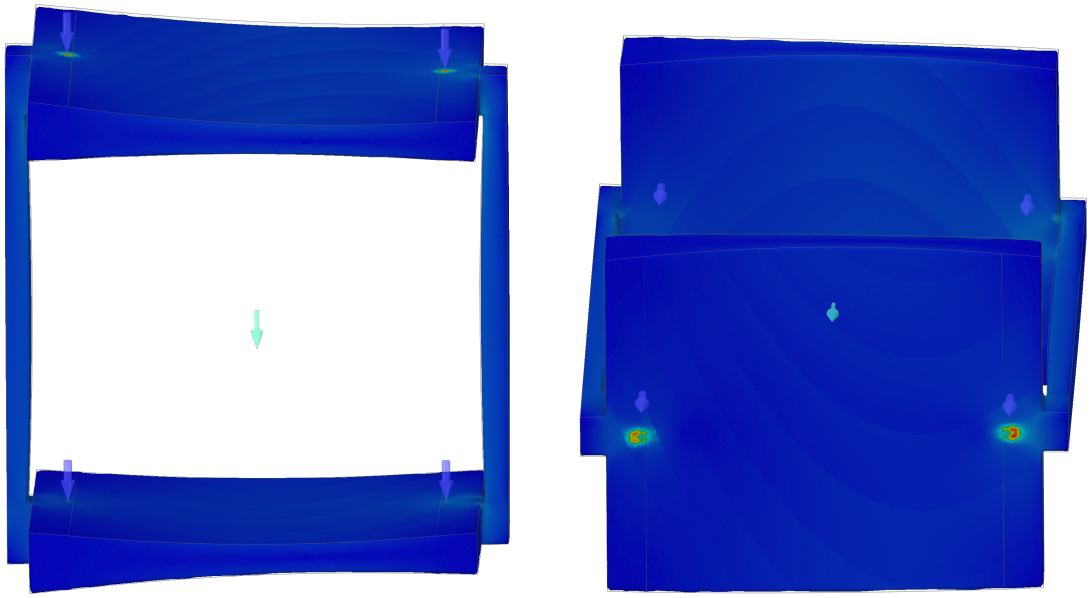

(a) Top view (b) Bottom view

Figure 33: von Mises stress from test case 1 - Every Other Pocket

As can be seen in the figures, the most affected areas are once again in the contact points, but it is also noted that some stress occurs in the stops as well, which are the beams on the sides of the geometry in the figures.

The figures 34a and 34b show how the segment looks before and after it is deformed during the simulations. The deformation is scaled and exaggerated, in order to see the deformation more clearly.

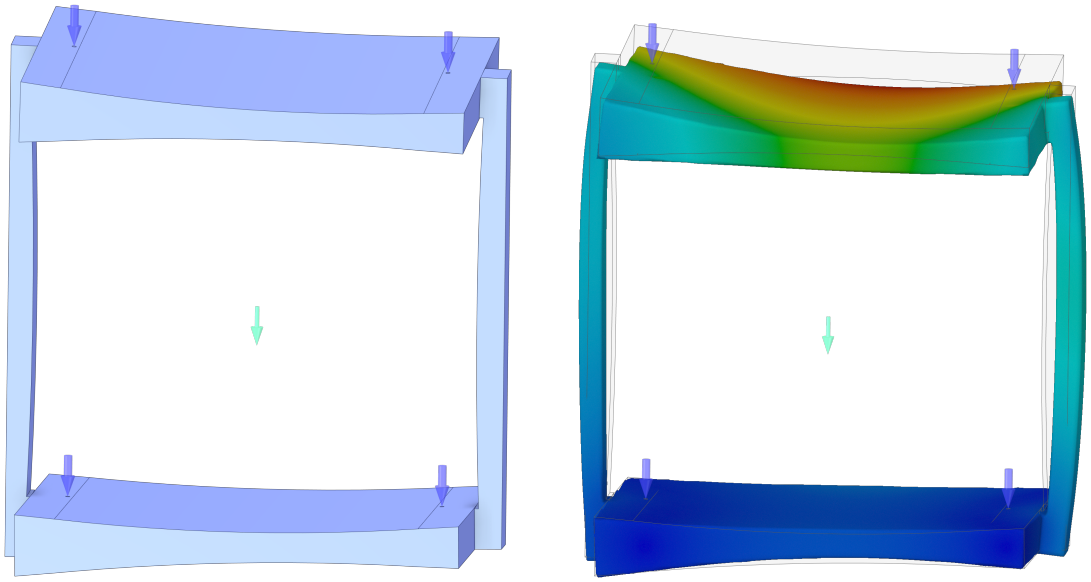

(a) Before deformation (b) After deformation

Figure 34: Displacement from test case 1 - Every Other Pocket

The figures show that bending occurs in both the stops on the sides, and in the upper part of the geometry where most of the load is applied. The most severe deformation can be seen in the red area on the farthest side of the top part.

The maximum stress, as well as maximum displacement in the different simulations, are presented in the table below. The results marked with red are the tests where the maximum stress exceeds the yield strength of the material.

Table 12: Table of results for every other pocket

Case	Total Force [N]	Model	Material	Yield Strength [MPa]	Max von Mises [MPa]	Max Displacement [mm]
1R	47,0519	EOP	PEEK	87	11,2	0,096
4R	192,7	EOP	PEEK	87	30,8	0,18
8R	385,4	EOP	PEEK	87	61,5	0,357
12 R	578,1	EOP	PEEK	87	92,3	0,55
1R	47,0519	EOP	PA46	75	11,4	0,11
4R	192,7323	EOP	PA46	75	31,7	0,204
8R	385,4646	EOP	PA46	75	63,4	0,406
12 R	578,1969	EOP	PA46	75	95	0,627
1R	47,0519	EOP	PA66	55	11,5	0,102
4R	192,4091	EOP	PA66	55	31,6	0,186
8R	384,8182	EOP	PA66	55	63,3	0,368
12 R	578,1969	EOP	PA66	55	95	0,569
1R	47,0519	EOP	Steel [redacted]	224	10,4	0,00206
4R	213,5787	EOP	Steel [redacted]	224	35,4	0,00673
8R	427,1573	EOP	Steel [redacted]	224	70,9	0,0127
12 R	640,736	EOP	Steel [redacted]	224	106	0,0187

As can be seen in the table, only the metal material managed to withstand the load from 12 rollers and segments without reaching its yield limit. The PA66 material reached its limit at the load case with 8 rollers and segments, which means that it performed worse than the other materials, since all other materials managed to withstand the load from at least 8 rollers and their respective segments.

Every Pocket

Figure 35 shows the *every pocket segment* in the first test case.

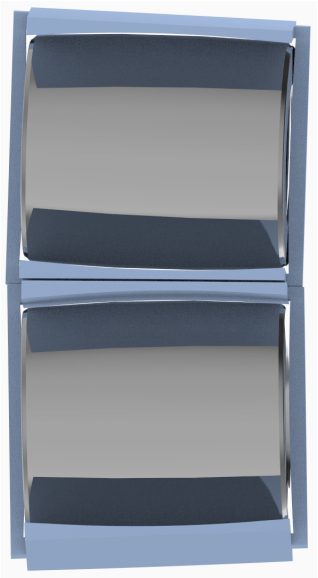

Figure 35: Every Pocket - Test case 1

Boundary Conditions

For the concept called *every pocket*, the boundary conditions were similar to the boundary conditions for the *every other pocket* concept. The difference is that the load was distributed on the whole top surface instead of being distributed on certain points. Similarly, the whole bottom surface was fixed. These boundary conditions are deemed to resemble the contacts between the segments. The boundary conditions are visualized in figures 36a and 36b.

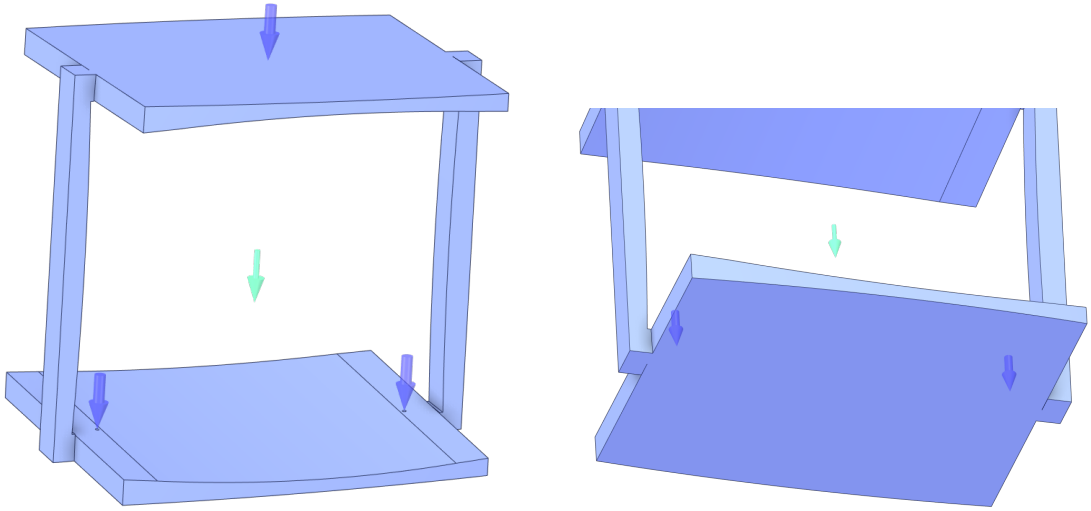

(a) Top view (b) Bottom view

Figure 36: Boundary conditions for test case 1 - Every Pocket

The following are the masses of the *every other pocket* segments, using four different materials.

Force Calculations

The following are the masses for *every pocket* with the four different materials.

Table 13: Table of masses

EP	**PA66**	**PA46**	**PEEK**	**Steel** [redacted]
Mass [kg]	0,1136	0,1224	0,1215	0,6862

The following calculations were done in order to obtain the different forces applied in the different load cases.

One roller:

$$m_{roller} = 4,7963181\ kg$$
$$g = 9,81\ \frac{m}{s^2}$$
$$F = m * g = 4,7963181 * 9.81 = 47,0518806\ N \tag{31}$$

4 rollers - EP

$$F_{1\ EP\ PA66} = (N_1 * m_{roller} + N1 * m_{EP\ PA66}) * g = 192,6668\ N \tag{32}$$
$$F_{1\ EP\ PA46} = (N_1 * m_{roller} + N1 * m_{EP\ PA46}) * g = 193,0098\ N \tag{33}$$
$$F_{1\ EP\ PEEK} = (N_1 * m_{roller} + N1 * m_{EP\ PEEK}) * g = 192,9755\ N \tag{34}$$
$$F_{1\ EP\ G90} = (N_1 * m_{roller} + N1 * m_{EP\ G90}) * g = 215,1347\ N \tag{35}$$

8 rollers - EP

$$F_{2\ EP\ PA66} = (N_2 * m_{roller} + N2 * m_{EP\ PA66}) * g = 385,3336\ N \tag{36}$$
$$F_{2\ EP\ PA46} = (N_2 * m_{roller} + N2 * m_{EP\ PA46}) * g = 386,0197\ N \tag{37}$$
$$F_{2\ EP\ PEEK} = (N_2 * m_{roller} + N2 * m_{EP\ PEEK}) * g = 385,9511\ N \tag{38}$$
$$F_{2\ EP\ G90} = (N_2 * m_{roller} + N2 * m_{EP\ G90}) * g = 430,2695\ N \tag{39}$$

12 rollers - EP

$$F_{3\ EP\ PA66} = (N_3 * m_{roller} + N3 * m_{EP\ PA66}) * g = 578,0004\ N \tag{40}$$
$$F_{3\ EP\ PA46} = (N_3 * m_{roller} + N3 * m_{EP\ PA46}) * g = 579,0295\ N \tag{41}$$
$$F_{3\ EP\ PEEK} = (N_3 * m_{roller} + N3 * m_{EP\ PEEK}) * g = 578,9266\ N \tag{42}$$
$$F_{3\ EP\ G90} = (N_3 * m_{roller} + N3 * m_{EP\ G90}) * g = 645,4042\ N \tag{43}$$

Results

The stresses in the segments, as well as the deformation of the geometry, were studied. The stresses are visualized in figures 37, 38, and 39, where the red areas are where the highest stress occurs. The most affected areas were the same for every material and load case.

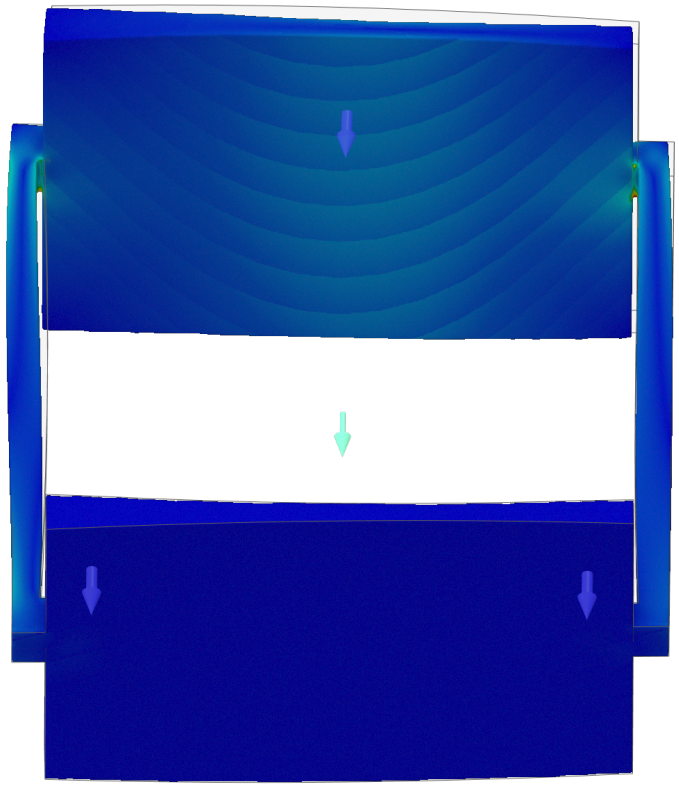

Figure 37: von Mises stress from test case 1 - Every Pocket

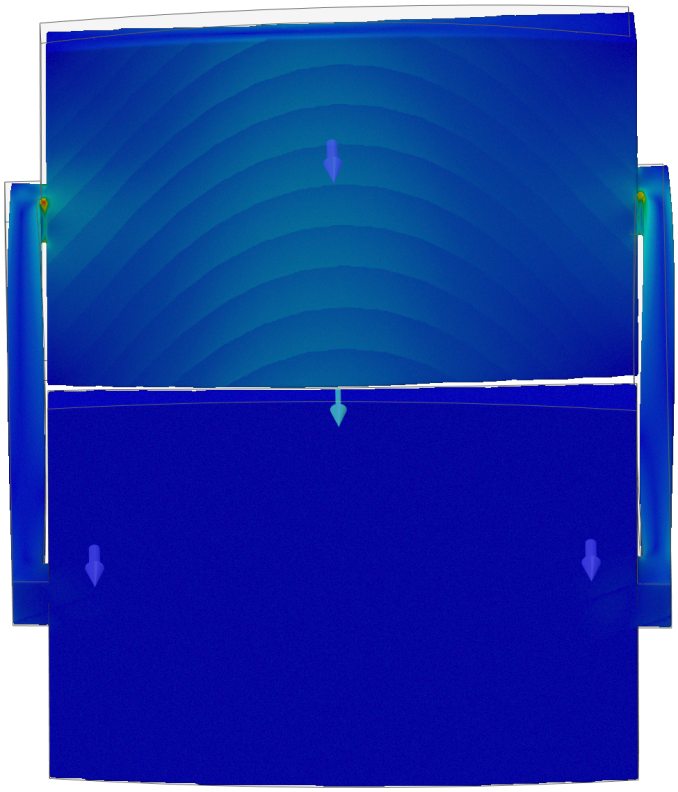

Figure 38: von Mises stress from test case 1 - Every Pocket, Other side

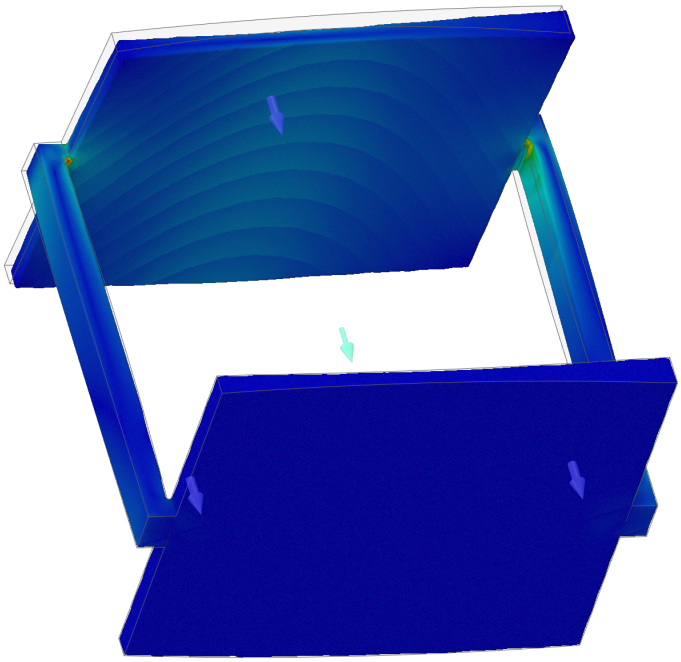

Figure 39: von Mises stress from test case 1 - Every Pocket, Overview

In the case of the *every pocket* concept, the most affected areas are in the axial stops, in the corners where they are connected with the loaded part of the geometry. Some stress can also be seen in the loaded top part itself and throughout the stops.

The figures 40a and 40b show how the segment looks before and after it had deformed during the simulations. The deformation is scaled and exaggerated, in order to see the deformation more clearly.

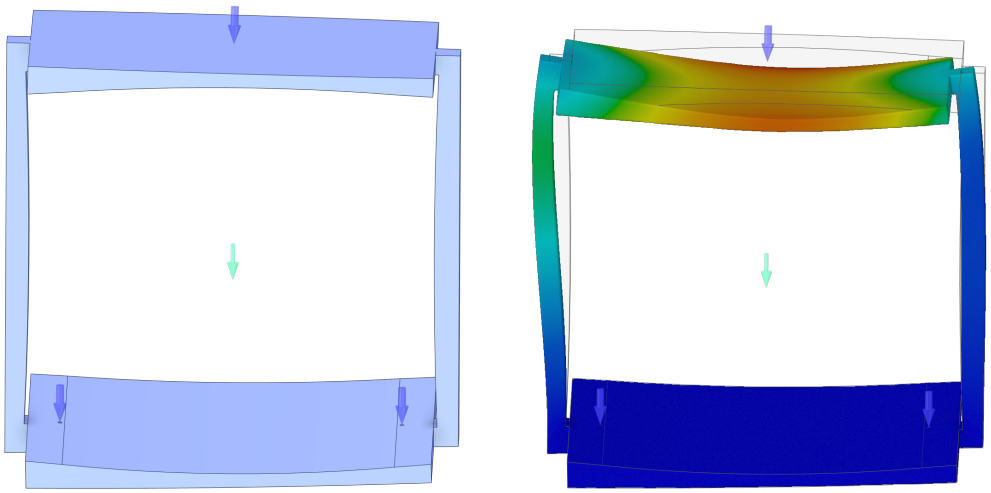

(a) Before deformation (b) After deformation

Figure 40: Displacement from test case 1 - Every Pocket

As can be seen in the figures, the highest amount of deformation can be seen on the edges of the loaded top part, and in the stop on the thicker part of the segment, located at the

left-hand side in the figures.

The maximum stress, as well as maximum displacement in the different simulations, are presented in the table below. The results marked with red are the tests where the maximum stress exceeds the yield strength of the material.

Table 14: Table of results for every pocket

Case	Total Force [N]	Model	Material	Yield Strength [MPa]	von Mises Stress [MPa]	Max Displacement [mm]
1R	48,2439	EP	PEEK	87	11,5	0,427
4R	192,9755	EP	PEEK	87	45,8	1,69
8R	385,9511	EP	PEEK	87	91,4	3,38
12 R	578,9266	EP	PEEK	87	137	5,07
1R	48,2525	EP	PA46	75	10,9	0,486
4R	193,0098	EP	PA46	75	43,4	1,93
8R	386,0197	EP	PA46	75	86,7	3,85
12 R	579,0295	EP	PA46	75	130	5,78
1R	48,1667	EP	PA66	55	10,9	0,441
4R	192,6668	EP	PA66	55	43,3	1,75
8R	385,3336	EP	PA66	55	86,5	3,49
12 R	578,0004	EP	PA66	55	130	5,24
1R	53,7837	EP	Steel [redacted]	224	12,6	0,0137
4R	215,1347	EP	Steel [redacted]	224	48,6	0,00526
8R	430,2695	EP	Steel [redacted]	224	96,5	0,105
12 R	645,4042	EP	Steel [redacted]	224	144	0,156

As can be seen in the table, the concept performed worse than the other two concepts. Only the metal material managed to withstand the load from 12 rollers and segments without reaching its yield limit. All other materials could only handle 4 rollers without yielding.

6.3.2 Analysis of Test Results - Test Case 1

The results from the simulations using this test case for the different concepts state that the *every other pocket* segment performed best, and the *individual bar* segment performed well. It was noticed that the *every pocket* segment did not perform as good as the other two concepts. For the materials, the PEEK and PA46 performed best in terms of how it handled the stress out of the polymer materials, but deformed more than the other materials. If the segment deforms too much, it might lose its optimal contact points, and this is something that needs to be taken into account when further developing the concepts. The PEEK material deformed the least out of the polymer materials, and performed better than the PA66 material in terms of how it handled the stress. The metal material performed better than the polymer materials in these simulations, due to it being able to handle heavier loads without reaching its yield limit, and not deforming as much as the other materials.

6.3.3 Test Case 2 - Simulation of Drag-Forces in Stops

The drag-force simulations were only performed on the bar segment due to it being the only concept which utilized the stops to connect with the rollers. As mentioned, the stops were designed to help during assembly by connecting to the dimples on the sides of the rollers with bulging geometry on the stops. This prevents rollers from falling out of the bearing during assembly but can cause stresses to the segments during operation. Stresses occur because of drag forces on the stops which occur when the weight of one roller and segment or several rollers and segments are ”hanging” on the stops which can be seen in figure 41. This can happen when the segments are situated in the bearing in a way that some rollers and segments are ”hanging” in the segment, due to them not resting on underlying rollers and segments. Figure 43 illustrates the position of the segment when the forces occur.

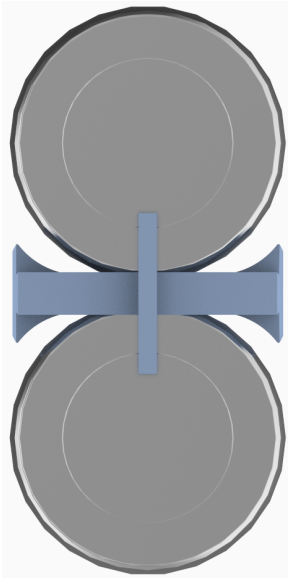

Figure 41: How the drag-forces can occur in the bar segment

Boundary Conditions

The following figures demonstrate how the boundary conditions were set up for this simulation. As can be seen in figure 42a and 42b, the forces were applied on the contact areas of the bulging geometry and were directed straight in the direction of the nearby roller. The segment was instead fixed in the contact areas on the opposite stops and a sliding support was added on the bottom surface of the geometry. Figure 44a and 44b provide a better view of how the bar segment is positioned between the rollers and how the drag-forces can occur.

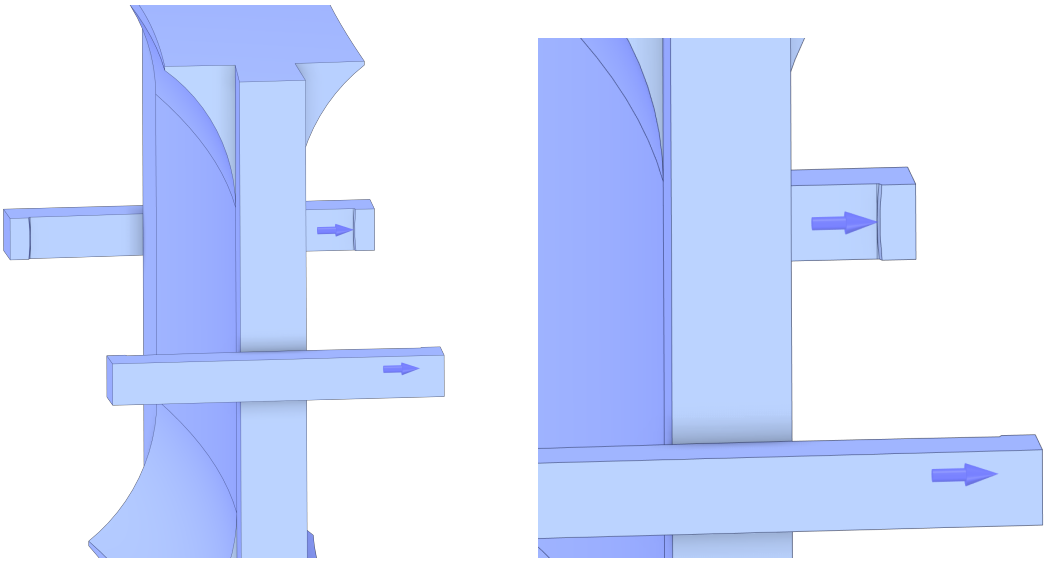

(a) Stops on the *individual bar segment* (b) Stops zoomed in

Figure 42: Stops

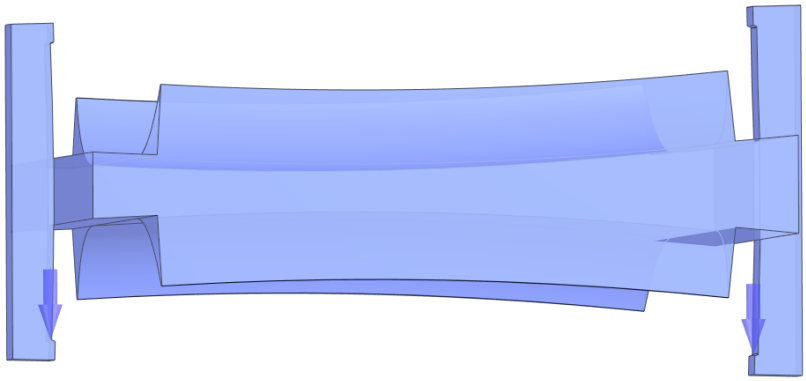

Figure 43: Position where forces can occur

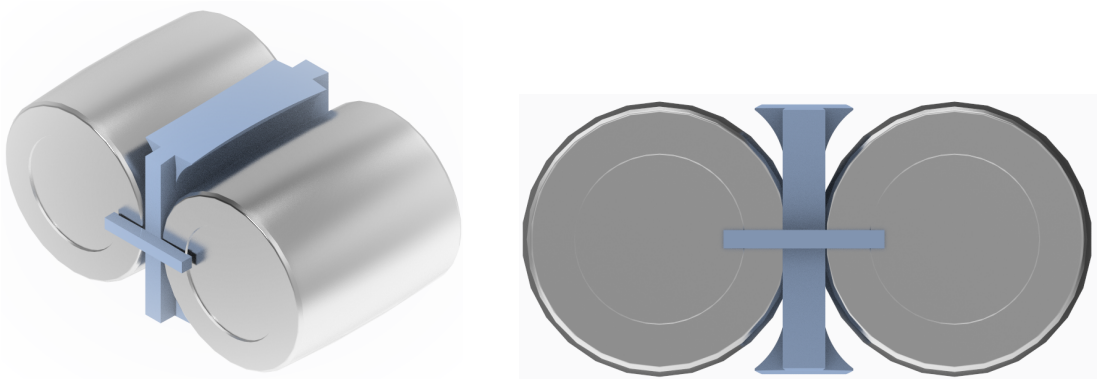

(a) Overview with rollers (b) Front view with rollers

Figure 44: *Individual bar segment* assembled with rollers

Force Calculations
The weight of the same amount of rollers and segments was used in these simulations as in the previous simulations. This was assumed to be a good estimation of the amount of rollers and segments that could "hang" on one segment. During operation, if the bearing is positioned vertically, the segments are resting on either the outer ring or the inner ring except for at the 9 o'clock or 3 o'clock positions. These are the positions where the situations occur which are simulated here.

One Roller:

$$m_{roller} = 4,7963181 \ \ kg$$
$$g = 9,81 \ \ \frac{m}{s^2}$$
$$F = m * g = 4,7963181 * 9.81 = 47,0518806 \ N \tag{44}$$

4 rollers - BAR

$$F_{1\ BAR\ PA66} = (N_1 * m_{roller} + N1 * m_{BAR\ PA66}) * g = 193.475 \ N \tag{45}$$
$$F_{1\ BAR\ PA46} = (N_1 * m_{roller} + N1 * m_{BAR\ PA46}) * g = 193.8802 \ N \tag{46}$$
$$F_{1\ BAR\ PEEK} = (N_1 * m_{roller} + N1 * m_{BAR\ PEEK}) * g = 193.8397 \ N \tag{47}$$
$$F_{1\ BAR\ G90} = (N_1 * m_{roller} + N1 * m_{BAR\ G90}) * g = 440.0304 \ N \tag{48}$$

8 rollers - BAR

$$F_{2\ BAR\ PA66} = (N_2 * m_{roller} + N2 * m_{BAR\ PA66}) * g = 386.9501 \ N \tag{49}$$
$$F_{2\ BAR\ PA46} = (N_2 * m_{roller} + N2 * m_{BAR\ PA46}) * g = 387.7605 \ N \tag{50}$$
$$F_{2\ BAR\ PEEK} = (N_2 * m_{roller} + N2 * m_{BAR\ PEEK}) * g = 387.6794 \ N \tag{51}$$
$$F_{2\ BAR\ G90} = (N_2 * m_{roller} + N2 * m_{BAR\ G90}) * g = 440.0304 \ N \tag{52}$$

12 rollers - BAR

$$F_{3\ BAR\ PA66} = (N_3 * m_{roller} + N3 * m_{BAR\ PA66}) * g = 580.4251 \ N \tag{53}$$
$$F_{3\ BAR\ PA46} = (N_3 * m_{roller} + N3 * m_{BAR\ PA46}) * g = 581.6407 \ N \tag{54}$$
$$F_{3\ BAR\ PEEK} = (N_3 * m_{roller} + N3 * m_{BAR\ PEEK}) * g = 581.5191 \ N \tag{55}$$
$$F_{3\ BAR\ G90} = (N_3 * m_{roller} + N3 * m_{BAR\ G90}) * g = 660.0456 \ N \tag{56}$$

Results

The stresses in the segments, as well as the deformation of the geometry, were studied. The stresses are visualized in figure 45, where the red areas are where the highest stress occurs. The most affected areas were the same for every material and load case.

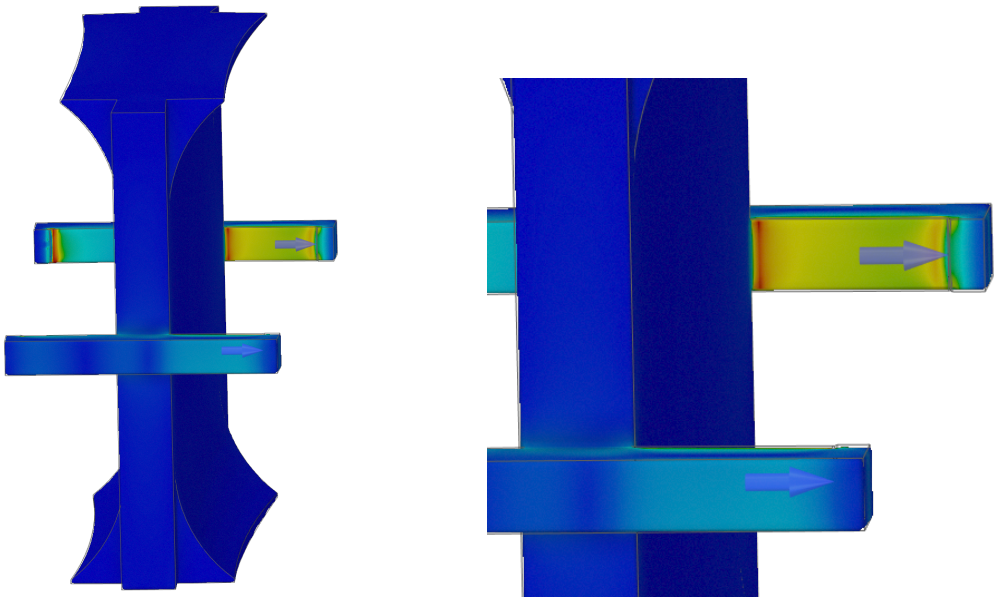

Figure 45: von Mises stress in the bar segment caused by drag forces

As can be seen in the figure, the highest stress occurs in the area by the corner of where the stops start. It can also be seen that there is high stress in the area where the stops are fixed. These stresses can be seen on both sides of the geometry. The rest of the geometry is fairly unaffected.

Displacement in the stops caused by the drag forces can be seen in figure 46. Here, the deformation is exaggerated and scaled to demonstrate the deformation more clearly. The true displacements and stresses can be seen in table 15.

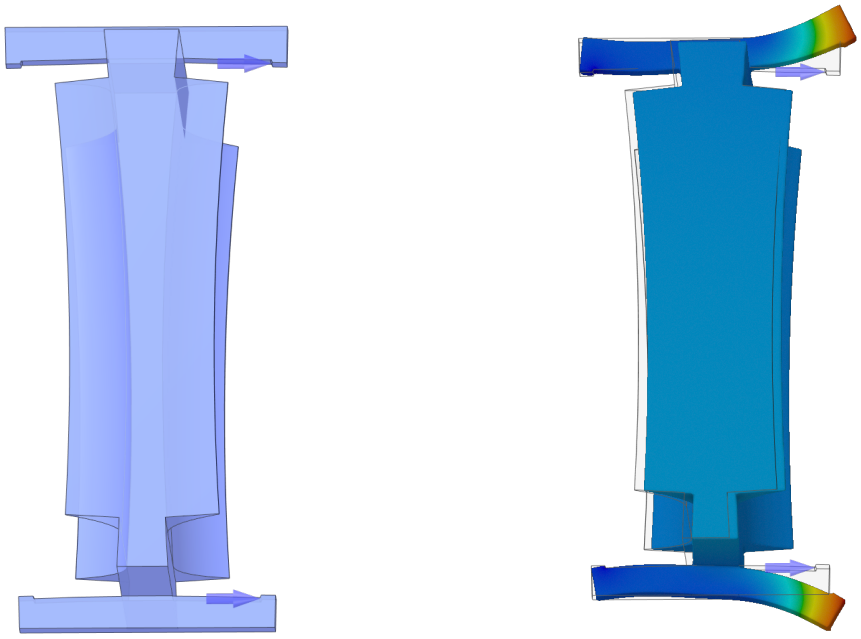

(a) Original shape (b) Shape after deformation

Figure 46: Displacement in the bar segment caused by drag forces

Table 15: Results from drag-force simulations

Cases	Drag Force on one stop [N]	Model	Material	Yield Strength [MPa]	Max von Mises [MPa]	Max Displacement [mm]
1R	23,52595	BAR	PEEK	87	4,53	0,0389
4R	96,91985	BAR	PEEK	87	18,6	0,16
8R	193,8397	BAR	PEEK	87	37,3	0,321
12 R	290,75955	BAR	PEEK	87	56	0,482
1R	23,52595	BAR	PA46	75	4,53	0,0451
4R	96,9401	BAR	PA46	75	18,6	0,186
8R	193,88025	BAR	PA46	75	37,3	0,373
12R	290,82035	BAR	PA46	75	55,9	0,559
1R	23,52595	BAR	PA66	55	4,53	0,041
4R	96,7375	BAR	PA66	55	18,6	0,169
8R	193,47505	BAR	PA66	55	37,1	0,338
12R	290,21255	BAR	PA66	55	55,7	0,507
1R	23,52595	BAR	Steel [redacted]	224	4,54	0,00109
4R	110,0076	BAR	Steel [redacted]	224	21,1	0,00512
8R	220,0152	BAR	Steel [redacted]	224	42,3	0,0103
12R	330,0228	BAR	Steel [redacted]	224	63,4	0,0154

6.3.4 Analysis of Test Results - Test Case 2

As can be seen in the table, the PA66 material was the only material which had a von Mises stress exceeding its yield strength during the simulation, which would cause the geometry to plasticize to the point of no return. A solution to this problem could be to create a stronger design with more robust stops in both height and thickness. However, since the stress exceeded the yield strength at the number of twelve rollers and segments, which is an extreme case, this might not be necessary.

6.3.5 Test Case 3 - Simulation of Displacement of Stops

During assembly of the *individual bar segment*, the rollers are inserted between the stops, securing the roller by locking the stops in the dimples. How the rollers are assembled between the stops can be seen in figure 47. This is done manually with manpower and as the rollers are inserted between the stops, there has to be a displacement of one of the stops so that the roller can fit. For this simulation, the displacement chosen for the stops was the same as the depth of the dimple on the roller which was 0.5 millimetres. The stops were displaced on both sides, in different simulations, in order to find out if it was beneficial to choose one side over the other during assembly.

(a) Top view with rollers (b) View from the side with rollers

Figure 47: How the bar segment is assembled between two rollers

Boundary Conditions

As can be seen in figures 48a - 49b, the stops were displaced 0,5 millimetres in order to simulate the stresses occurring during assembly. The bottom surface of the segment was fixed.

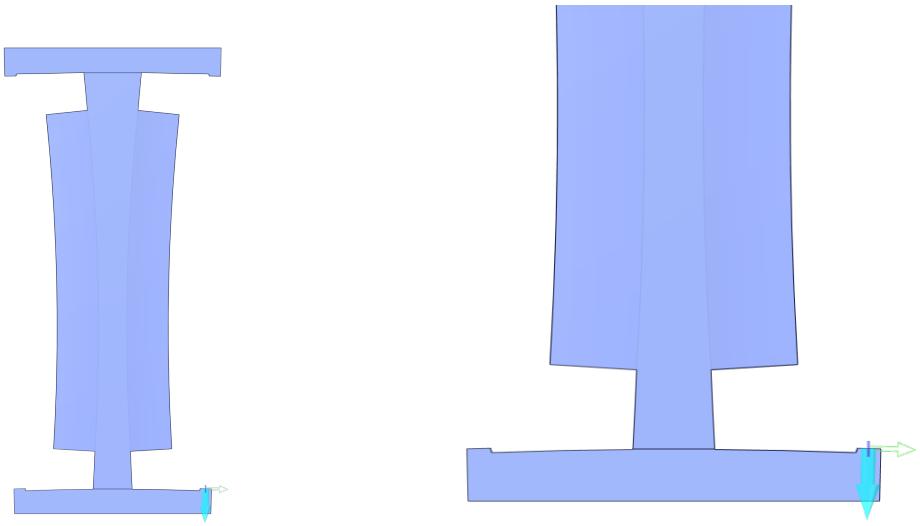

(a) Displacement of stops (b) Zoomed in

Figure 48: Displacement of stops closest to the center of the bearing - Side A

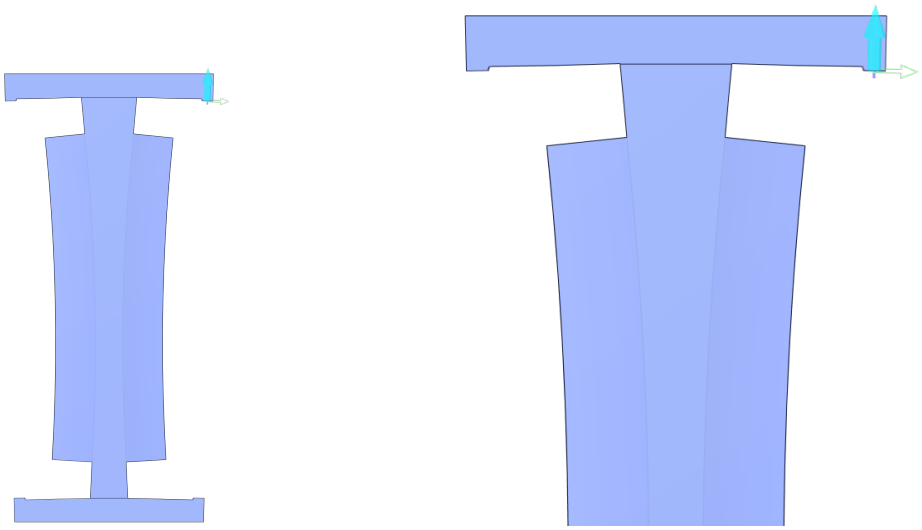

(a) Displacement of stops (b) Zoomed in

Figure 49: Displacement of stops closest to outer radius of the bearing - Side B

Results

The stresses in the segments were analysed and can be seen in figure 50 The stresses are visualized in the figures below, where the red areas are where the highest stress occurs. The most affected areas were the same for every material.

von Mises stress

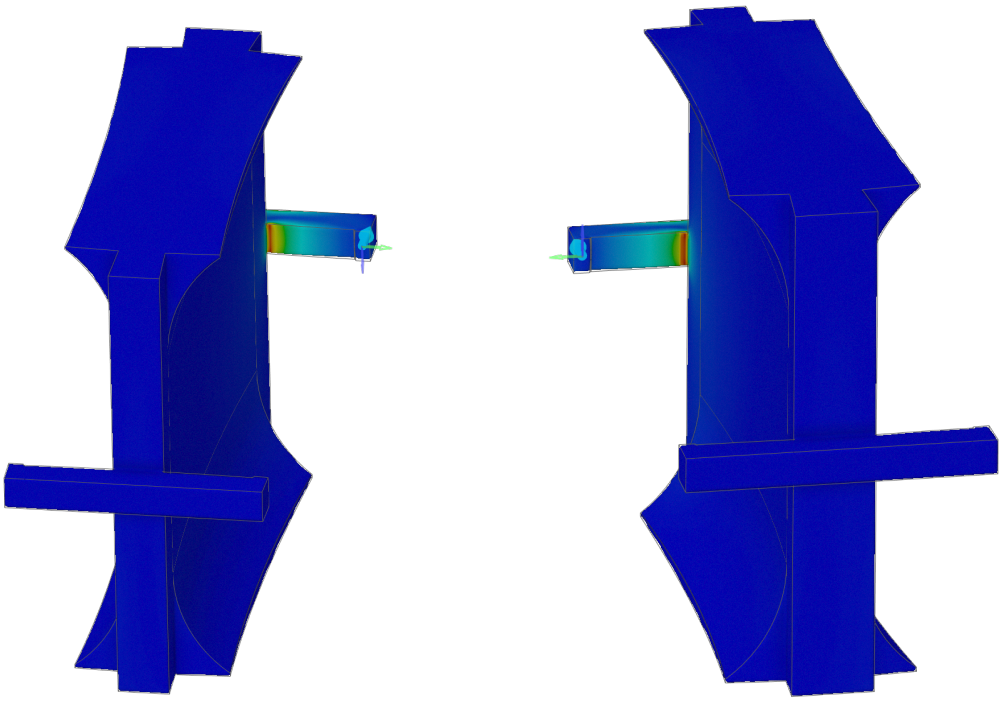

(a) von Mises stress in side A (b) von Mises stress in side B

Figure 50: von Mises stress in *individual bar segment*

The highest stress occurs in the area by the corner of where the stops start. This is the case for both sides of the segment.

Deformation

Figure 58 illustrates the displacements of the stops. The displacement is scaled to exaggerate the deformations when displaced 0,5 millimetres, in order to visualise it more clearly. As can be seen, the rest of the geometry will not be very affected by this way of assembly.

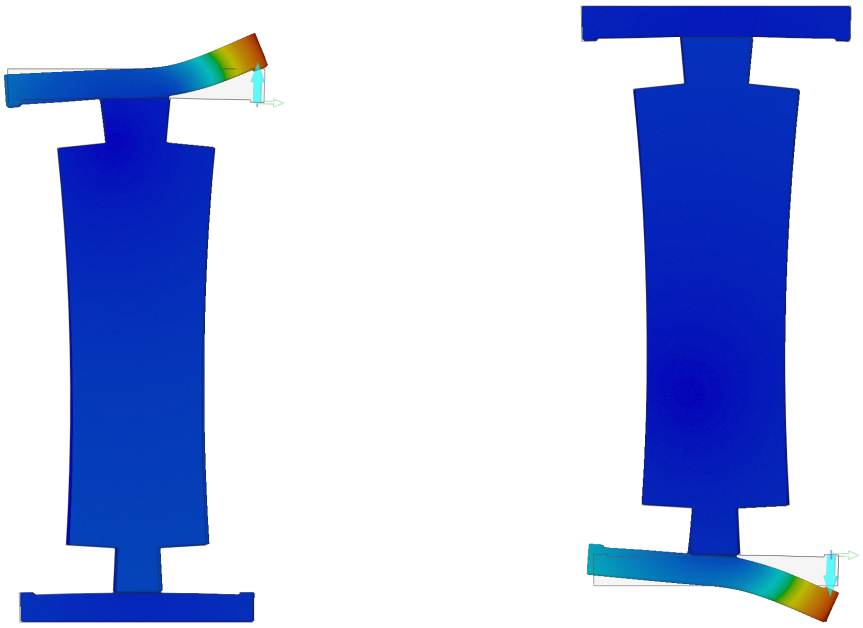

(a) Deformations in side A (b) Deformations in side B

Figure 51: Deformations in *individual bar segment*

The following is the maximum stresses in the stops after the displacement.

Table 16: Results of displacement simulations

Displacement in stop (Side A) [mm]	Model	Material	Yield Strength [MPa]	Max von Mises [MPa]
0,5	BAR	PEEK	87	50,1
0,5	BAR	PA46	75	43,2
0,5	BAR	PA66	55	47,6
0,5	BAR	Steel [redacted]	224	1780
Displacement in stop (Side B) [mm]	Model	Material	Yield Strength [MPa]	Max von Mises [MPa]
0,5	BAR	PEEK	87	60,2
0,5	BAR	PA46	75	51,9
0,5	BAR	PA66	55	57,1
0,5	BAR	Steel [redacted]	224	2130

6.3.6 Analysis of Test Results - Test Case 3

There are in total, four stops on the individual bar segment. This simulation was done to test the stops and find out which two were the strongest and therefore most appropriate for displacement during assembly. There are two stops closer to the outer radius of the circumference called side A, and there are two stops close to the centre of the circumference which are called side B. It turned out after the simulations, that the highest stresses occurred in the stops closest to the centre of the circumference, side B. Therefore it would be wise to displace side A with 0,5 millimetres during assembly. To avoid higher stress, one can also choose to displace both sides at smaller distances instead of 0,5 on one side to even out the stresses.

6.4 Simulation in BEAST

BEAST is an advanced internal bearing simulation toolbox used by SKF for bearing simulations, specialized in detailed contact calculations (Linköping University, n.d.). The simulations in BEAST were of a rigid dynamic kind and were used with the help of the supervisor Luke Dickens at SKF to give an insight into the kinematic behaviour of the segments in the bearing during operation. Ten different simulations were run with different load cases, resembling different scenarios during operation. Different segments and rollers around the circumference were studied. It was decided to include the *every other pocket* segment in the BEAST simulations, due to it being the most developed concept and having shown good results during the previous simulations in Ansys Discovery. It was also deemed to be a good choice since this concept also included the geometry of the *individual bar* segment to a large extent. It included connecting beams as well, which was of interest to study further since stress had been noticed there during the finite element analysis. The other concepts were not studied in BEAST due to the time constraints of the project, and one concept had to be prioritised in this study. The simulations were performed using the prototype size bearing with a roller diameter of 24 millimetres, which has a smaller size compared with the wind turbine bearing. This was to shorten the lengthy set-up and calculation times. Since every contact needed to be manually defined, having fewer rollers such as in the prototype bearing required less manual work to set up. During the simulation, more contacts mean longer calculation times, and these were shortened by using the bearing with fewer rollers.

Figure 52 shows an exploded view of the SAT bearing including the inner ring, outer ring and rollers with the segments assembled in it. Figure 53 illustrates what the simulation results could look like. The blue arrows are roller to ring force vectors which demonstrate the load direction and size, and the red arrow is the load applied to the inner ring displayed as a force vector.

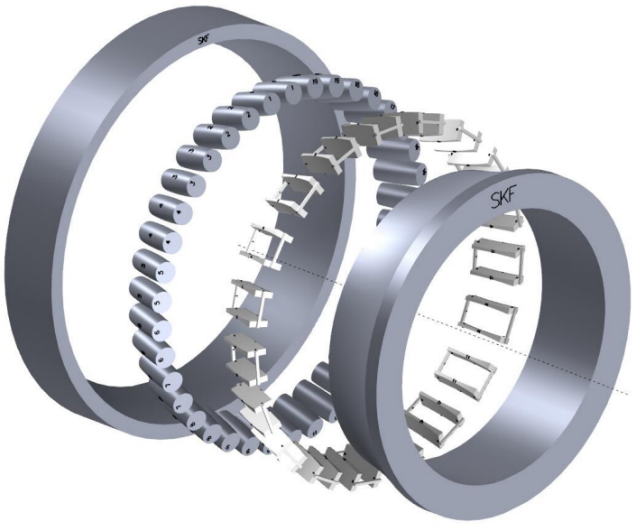

Figure 52: Exploded view of the SAT bearing with *every other pocket* segments assembled

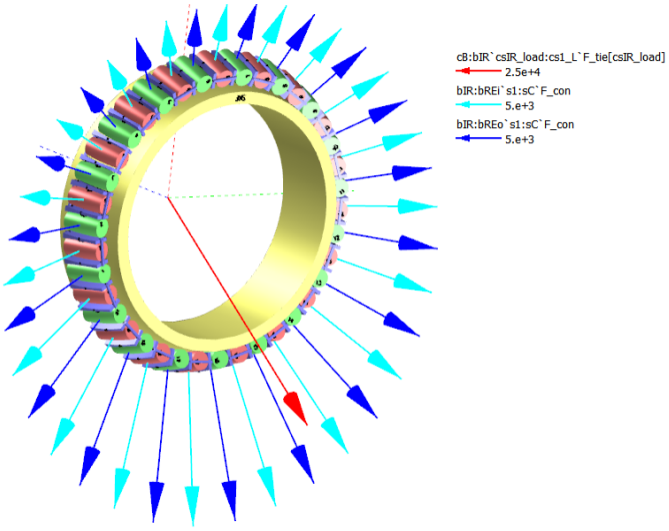

Figure 53: Load case and force vectors

6.4.1 General Overview

By studying the results on one segment and its surrounding rollers, the contact forces of the surrounding rollers to the cage segment, the contact gaps between the segment and surrounding rollers, the skew levels of the rollers, and the surrounding roller loads could be studied. Figure 54 details the dynamics of one segment and showcases the results of the tests of the mentioned parameters.

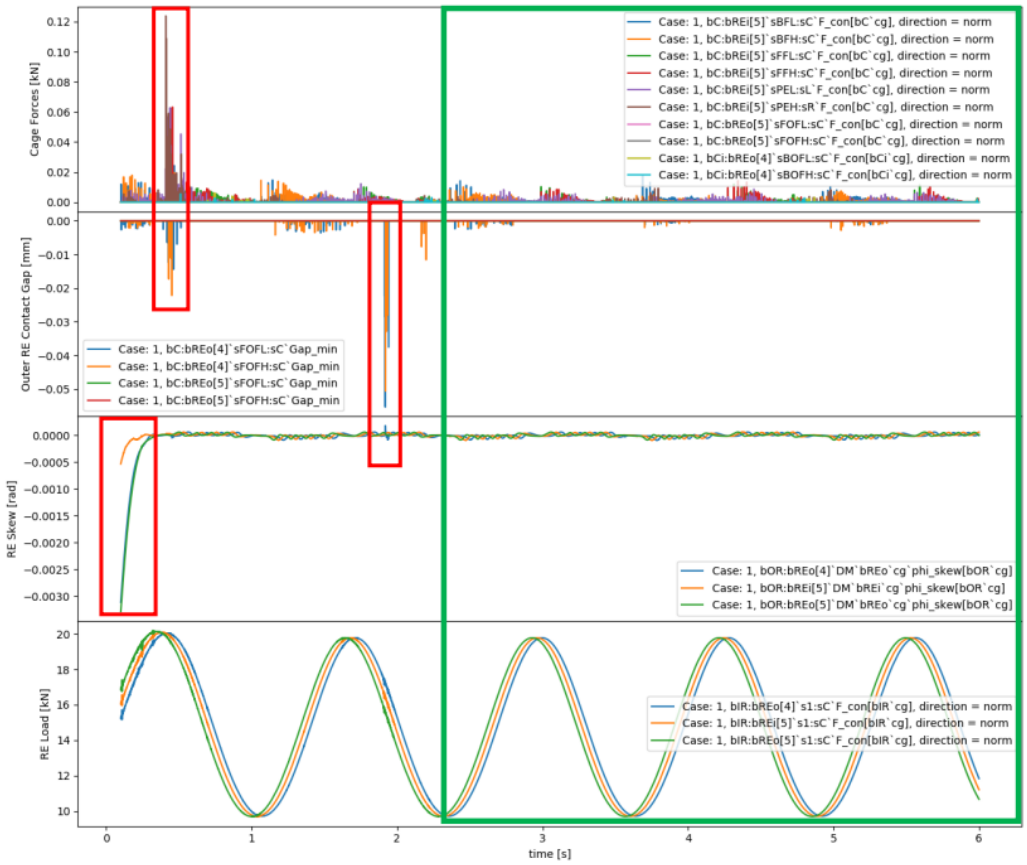

Figure 54: Overview of the dynamics of segment 5 and surrounding rollers

The red boxes in the figure indicate some of the symptoms of the start-up instability of the tested segment before it reaches a steady and repetitive running condition, which is highlighted by the green box. It can be seen that apart from some start-up instability, the current design does in fact find a good running state in all of the ten cases run. This shows that the geometry tested under the prescribed loading conditions, whilst acknowledging the simulations' assumptions and limitations, shows that the core of the design could be feasible, and even work well with some enhancements and tweaks. The contact forces are quite low on all of the assessed segments in the steady state condition. The gaps between the contact points of the rollers in between segments seem to find a repetitive and stable rhythm of increasing small amounts in the same location around the circumference of the bearing, and the skew of all rollers is extremely controlled, repetitive and low.

6.4.2 Segment Stability

The stability of the segments was studied by looking at the position and alignment of one segment. The results can be seen in figure 55.

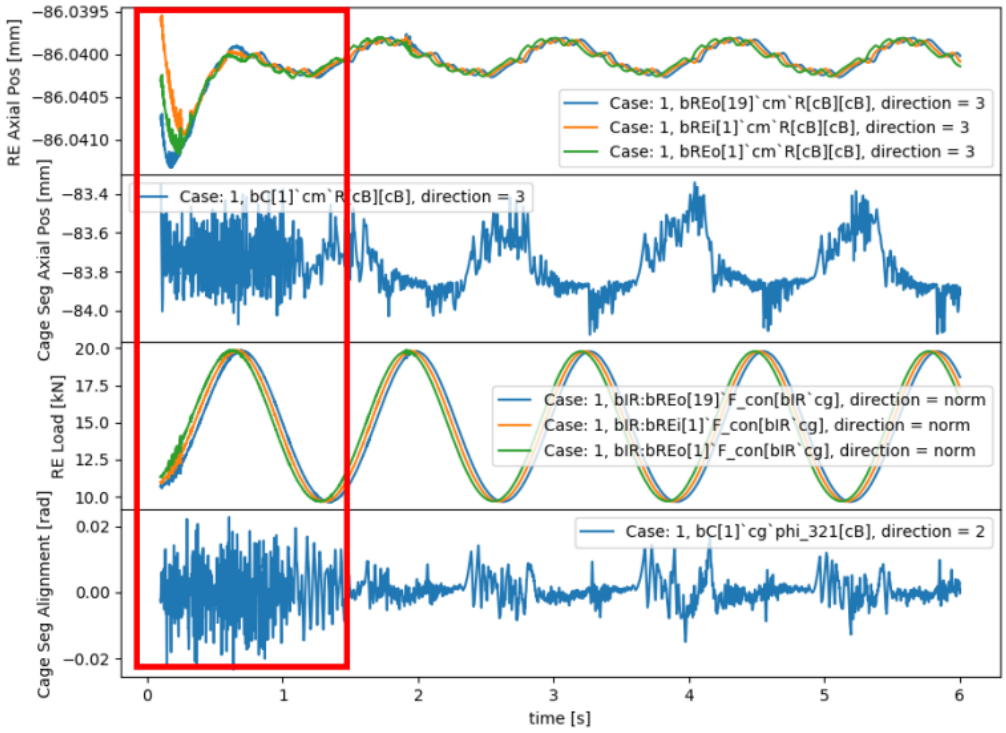

Figure 55: Position and alignment of Segment 1

The figure details from top to bottom: the axial position of the rollers surrounding the studied segment, the axial position of the studied segment, the roller load of the rollers around the studied segment, and the radial alignment (yaw) of the studied segment. The red box highlights that there is around 1,5 seconds of erratic cage movement before it reaches a steady and repetitive running condition. It is normally accepted that there is a small degree of noise or shake at the start-up of dynamic simulations, as the components in the simulation are released from their nominal start positions and establish contact with the surrounding bodies. However, in regular simulations with a solid one-piece cage, this start-up condition is normally overcome in some fractions of a second. So the question is posed as to why the segments across all the 10 simulations run have a much lengthier start-up instability period before steady state running condition is achieved. This could be in part due to or exacerbated by any of the following points:

- As segment cages are many individual pieces, they have less guidance from numerous contacts compared to a one-piece cage.

- As the segments are much smaller than a traditional one-piece cage and are simulated with a PEEK material applied, their individual mass is very low which could aggravate the ability to find stability.

- The simulation was set up to use the solve time advantage of ”dry” contacts. A lubricated coefficient of friction was employed in replacement of actual lubricant in the contacts to speed up the solve process. This could exacerbate the ability to overcome the start-up instability due to the removal of part of the contact-dampening properties that comes from the lubricant.

6.4.3 Start-up Skew

The start-up skew was also observed in relation to the roller loads. This was done in order to investigate how the different skews can affect the roller loads. The graphs can be seen in figure 56.

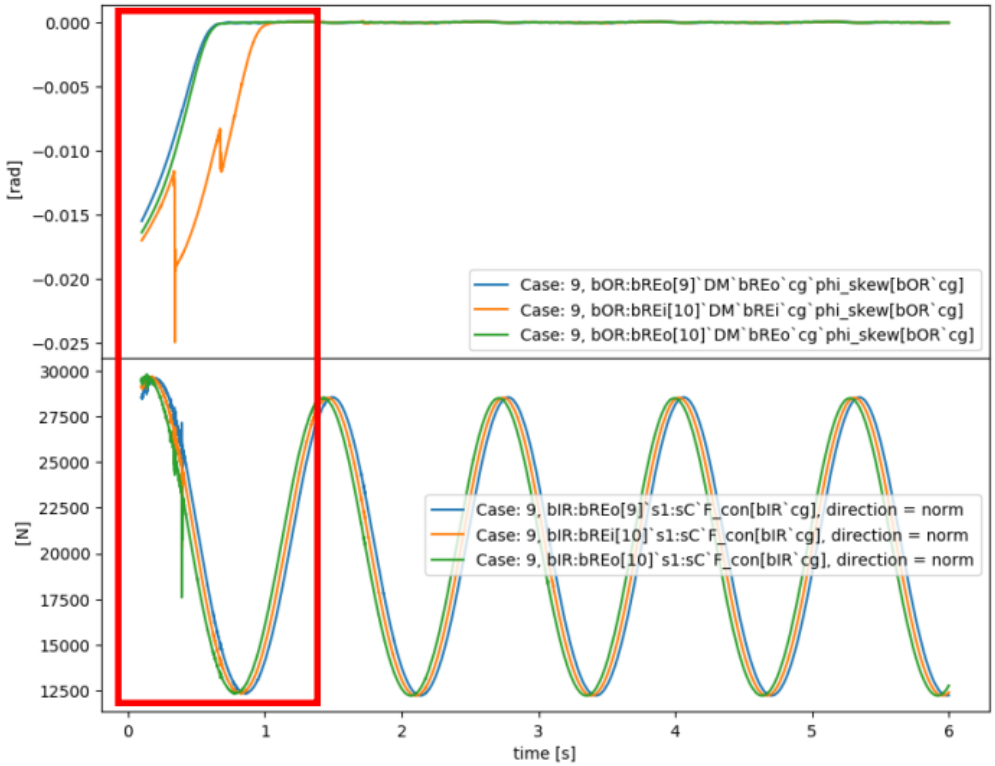

Figure 56: Skew plot over roller load plot for segment 10

In most of the simulations, it was possible to see some of the rollers skew excessively at the very beginning of the simulations. The skew is always corrected in every simulation run but is done so at varying rates, which can be seen in the figure. However, this phenomenon poses the question as to why this occurs in the first place. Furthermore, the figure also shows that the levels of skewness can be so severe that it causes the roller loads to spike. The leading thought as to why this phenomenon occurs is that the ”gap stack up” is too large. The ”gap stack up” is the gap remaining/formed after all the clearance was closed between segments and rollers moving around the bearing. So, it may be prudent to check the segments' wall thickness calculation in BEAST. Does the wall thickness calculation look at the gap formed at the designed contact points or in the center of the roller? Maybe the calculation just needs to be slightly adjusted in order to reduce the nominal clearance to the outside segment rollers.

7 Physical Prototyping and Testing

After having seen that the *every other pocket* segment performed well during the simulations is Ansys Discovery and BEAST, a physical prototype was 3D printed in a size which would fit the prototype of the SAT bearing which can be seen in figures 57a and 57b. This is also the same size which was used in the BEAST simulations.

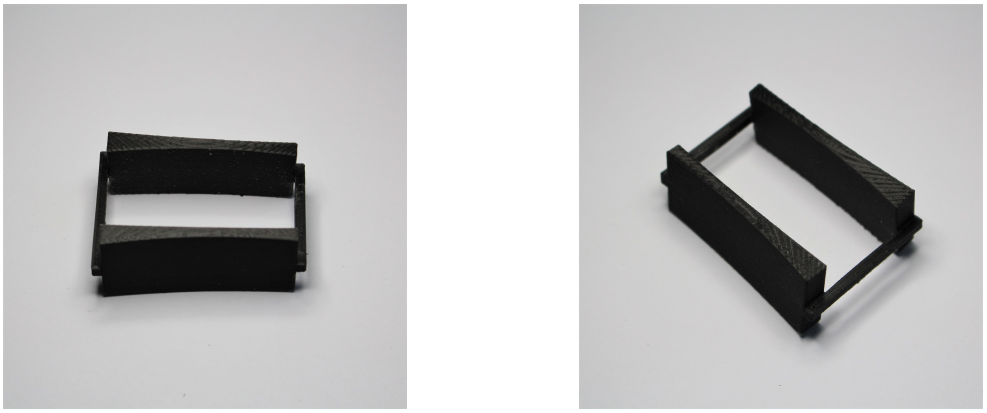

(a) Side view (b) Top view

Figure 57: First 3D-print of the *every other pocket* segment

Firstly, a prototype was printed using the same design as in BEAST. The results looked good and the contact with the rollers and the clearances gave an indication of good feasibility of the design. However, it was noticed that the beams of the pocket, acting as axial stops, were very thin in relation to the rest of the geometry. It was therefore decided to iterate the design with a more robust design for these, by increasing their size.

After the iteration, 19 segments were printed in order to be able to assemble them in the prototype bearing. The iterated design and second 3D-prints can be seen in figure 58a and 58.

(a) Close-up of beam with increased size (b) Top view

Figure 58: Second 3D-print of the *every other pocket* segment

The segments were assembled with good results, the full SAT prototype bearing with segments in place can be seen in figure 59a. When in place, it was possible to rotate the inner ring. The inner ring could be misaligned slightly and the rollers seemed to be able to self-align together with the segments. The physical testing showed that the segments fit and work. A close-up of the assembly is provided in figure 59b. It was also noted that an assembly procedure and appropriate tools for this need to be studied and developed further in order for the assembly process to be easier, safer, and more straightforward if these segments are to be produced and assembled in larger quantities.

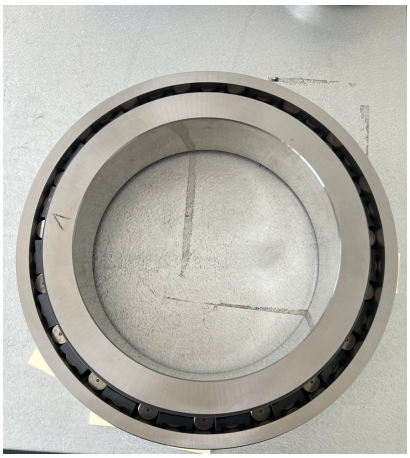

(a) The SAT prototype bearing with the segments assembled in it

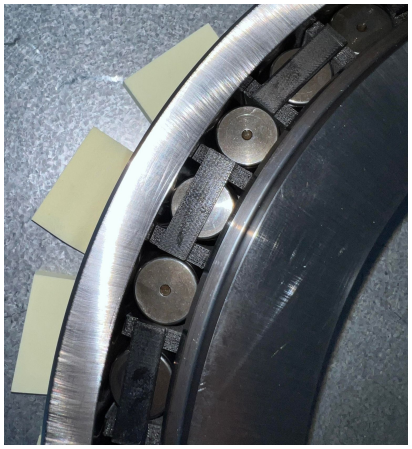

(b) Close-up of segments and rollers in the SAT prototype bearing

Figure 59: SAT prototype bearing assembly with *every other pocket* cage segments

8 Economic Assessment

An economic assessment was conducted in order to provide an overview of what aspects of the manufacturing were the most critical cost-wise and to compare the price of different materials. For the assessment, two experts on the subject matter were interviewed.

M[redacted] B[redacted] is a product development engineer and works at SKF in Schweinfurt, he was able to answer many questions about the manufacturing of cages and batch sizes.

M[redacted] [redacted]. K[redacted] also works in Schweinfurt with business development and was able to answer questions about the manufacturing but also about the commercial strategy of the company as a whole.

The SAT bearing can be produced in an array of sizes, however, the wind turbine bearing was chosen as a reference for the requirement specification, material study and manufacturing method study. The wind turbine bearings are made to last for approximately 20-30 years in operation. This indicates that there will be no commercial plan similar to products made for mass production and sold to the greater masses on a daily basis. The quality and longevity of the material and product are of great importance and influence the choice of material and production processes heavily. To execute this assessment, inspiration was drawn from the facility in Schweinfurt which produces the polymer pocket segments for the TRB-bearing, which proved to be an adequate inspiration for design as well.

8.1 Commercial Strategy

For the size of the wind turbine bearing, there are in this case, 60 rollers. This indicates that for each respective wind turbine bearing, there needs to be a production of 60 segments for *individual bar segment* and *every pocket* or 30 segments for *every other pocket*.

The biggest customers of SKF's wind turbine bearings in Europe are for the time being Vestas, SiemensGamesa, Enercon and GE Wind. The sales teams are in charge of reaching out to customers and when introducing them to SKF, the factories can provide tours of the production facilities where customers can view machining lines and heat treatment areas to be reassured about the competence of the company. According to Michael Kirchner, it is communicated by customers that SKF does not provide the cheapest alternative in the area of wind turbine bearings, but it is by far the alternative with the highest quality and longevity (personal communication, 2023-05-30).

8.1.1 Priorities

As stated by SKF, the company creates value by developing new technologies and by constructing value-adding solutions which gives them a competitive advantage to customers. A big focus is on contributing to the sustainability of the global society (SKF, 2020).

The conditions in which wind turbines operate are often tough. Remote locations, extreme temperatures and both offshore and onshore wind parks are all various factors which can affect the performance and reliability of the bearings and cages. High repair costs and long replacement lead times are all aspects during operation which must be avoided and taken into account during the design and development process. This implies that the focus while developing these segments was not time to market but quality and longevity. Preventing service trips leads to a boost in return on investment and therefore, many years have been

spent by SKF on developing lubrication systems and condition monitoring systems which have helped enable cost-effective wind energy generation (SKF, n.d.).

This means that the benefits of spending more time on iterating concepts and perfecting systems are far greater than the ones gained by prioritising a short time to market. By spending time evolving the geometry and details of the segment and choosing materials wisely, more time is won during the lifespan of the bearing and costs can thereby be reduced.

As stated by Asfoor et al., the project management triangle also known as the *iron triangle*, illustrates this balance between the three corners of the triangle, namely quality, cost and time. Depending on the project and product, this choice will vary. The emphasis was during this project, on quality and cost but the quality was prioritized above all which can be seen in the position of the star in figure 60.

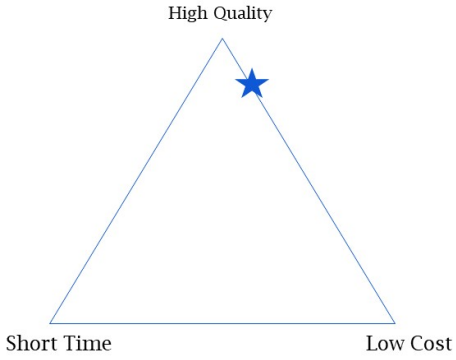

Figure 60: The iron triangle

The cages need to last and operate for a long time with as little maintenance as possible, as well as provide a competitive advantage for the SAT bearing and therefore, time should not be a constraining factor during the development (Asfoor, AL-Jandeel, Igorevich, & Ivanovna, 2022).

8.2 Production of Product

Each individual concept is created using only one material and consists of one individual part which simplifies the cost comparisons. The production process differs depending on if polymer or metal is chosen for the cage segments. For this comparison, steel was chosen which was the same steel simulations were performed on.

8.2.1 Polymer Cage - Injection Moulding

When investigating polymers for producing the segments, injection moulding is the process used for manufacturing. Injection moulding is traditionally used to create fittings, containers, housings, and automotive and aerospace components to name a few. With injection moulding, very complex shapes can be achieved with intricate detail, and the tooling cost for polymers only varies from 1-2% and seldom above 5% if the geometry is more complex. Should cavities or details on the foundations be added to the concept in further iterations, this would not add too much to the costs. Tooling costs and equipment costs are very high for injection moulding and the dies are mostly made from hardened tool steel. Labour costs are usually low as well as the finishing costs necessary for trimming to remove runners and gates.

The tooling cost for the polymer segment is not heavily influenced by the size of the cage segment. It is almost independent of the size and the cost is 40 000 - 50 000 euros which is 467 017,60 - 583 772,00 SEK. The lead times can be many weeks since the manufacturing of complex dies can be time-consuming. The material utilization is good for injection moulding and many of the tools can be reused.

8.2.2 Steel Cage - Stamping

The smaller steel cages are generally made from sheet metal by forming and stamping (Tadic, 1998). This process is traditionally used for applications such as machine frames, automotive body panels, light structural sections and electrical fittings (Ansys Granta, n.d.).

In the size of the wind turbine bearing which is approximately 2 meters in diameter, the steel cages which are used by SKF in Schweinfurt are [redacted]. Should there be delays in the delivery of machine parts, then one has lost a whole day of work in the assembly areas since complete shifts are lost if the cages do not arrive on time.

When ordering a new design of a one-piece steel cage from an external company, there will be a one-time tooling cost of [redacted].

8.2.3 Assembly

Another aspect of the cost is how the cages are assembled in the bearing. For a bearing the size of the wind turbine bearing, this is done by one blue-collar employee in the assembly area. It takes approximately three hours to assemble it and the Schweinfurt factory is used for reference. The labour cost for three hours is [redacted]. Some are assembled in-house and the customer receives a unit with the cage already in the bearing and some are assembled and mounted by the customers themselves.

8.2.4 Lubrication

The bearings are either lubricated in the factory before delivery to customers, or the customers will have to lubricate the bearing themselves. This depends on the type of bearing and currently, SKF has both options. The lubrication is produced in-house and the cost is approximately [redacted] per bearing when it is lubrication in-house which translates to [redacted] for both polymer and metal.

8.2.5 Summary

The costs depending on the material are summarized in the tables below. For a wind turbine bearing with a diameter of around 2 meters, approximately 60-70 rollers fit which is the case for the SAT bearing. The break-even for polymer segments happens at around 70-80 pieces and for steel cages, 30-40 pieces. The break-even is the point when the investment for the tools starts to be profitable. [redacted]. The tooling costs and the cost of the material are the biggest differences depending on what material is chosen. Based on the material data from Granta, steel is cheaper than all of the polymers with PA66 being the cheapest polymer

alternative. However, based on personal communication, it seems that polymer segments will be cheaper over time because of it being more lightweight and could be manufactured in-house. What is not included in the tables is that the transportation of a lighter material will also be cheaper due to lower weight with the same volume.

Material	PEEK
Material Cost $[\frac{SEK}{kg}]$	[redacted]
Lubrication Cost $[\frac{SEK}{bearing}]$	[redacted]
Tooling Cost [SEK]	[redacted]
Assembly Cost $[\frac{SEK}{bearing}]$	[redacted]

Material	PA66
Material Cost $[\frac{SEK}{kg}]$	[redacted]
Lubrication Cost $[\frac{SEK}{bearing}]$	[redacted]
Tooling Cost [SEK]	[redacted]
Assembly Cost $[\frac{SEK}{bearing}]$	[redacted]

Material	PA46
Material Cost $[\frac{SEK}{kg}]$	[redacted]
Lubrication Cost $[\frac{SEK}{bearing}]$	[redacted]
Tooling Cost [SEK]	[redacted]
Assembly Cost $[\frac{SEK}{bearing}]$	[redacted]

Material	Steel [redacted]
Material Cost $[\frac{SEK}{kg}]$	[redacted]
Lubrication Cost $[\frac{SEK}{bearing}]$	[redacted]
Tooling Cost [SEK]	[redacted]
Assembly Cost $[\frac{SEK}{bearing}]$	[redacted]

9 Further Development

The scope of the project was adjusted to the timespan. This chapter summarizes what can be done in the future regarding both the design and the testing of the concepts.

9.1 Further Development of Design

The following are suggestions of design changes for further iterations.

9.1.1 Weaknesses in the *every other pocket* Design

The simulations in Ansys Discovery demonstrated how the maximum stresses occurred in the cage beams which connected the two bar segments in the concept *every other pocket*. The end beams will transmit load and bend as a function of the load. Such thin beams can cause plasticizing which was the result of simulations with a weight of eight or twelve rollers and their respective segments for several polymers tested. This plasticization is undesirable and should be avoided at all costs. The result of the beams having a stiffness which is too low could be an increase in friction and power loss. When the cage segment is pressed down because of weakness in the beams, the roller might lose its point contacts and have contact with a larger area on the segment which will result in an increase in friction which leads to power losses. This will also lead to a reduction in the cage segments' longevity. This could also lead to a change in the gap between the roller end and the *every other pocket* segment beams. To fix this problem, future work on an iteration of the *every other pocket* would have to include further considerations of the loading conditions and states in order to optimise the geometry of the beams.

9.1.2 Diminish Clearances

All three concepts were designs with centering alternating between inner ring centering and outer ring centering and will never be centered on the rollers in the bearing. When designing the total height of the segments, there was a clearance set to [redacted] millimetres to make sure the segments would not get stuck- between the rings during BEAST simulations. This caused the segments to have too much radial play and wobbly behaviour. The optimal clearance would be in the range of [redacted] of the roller diameter. One could also redesign the concepts completely by designing the cages so that they allow for roller centering.

9.1.3 Design for Transportation

Another aspect to consider is the transportation conditions the segments will withstand before being delivered to the customers. When designing the cage segments, three technical attributes were considered; geometry, centering and pitch. Another further development is designing the segments so that they can be stacked and packed easily into more compact containers for ease of transportation. Infrastructure in developing countries might not be as established and therefore the roads might be uneven, causing the containers with segments to wobble due to instability. Should the material chosen be slightly brittle, then a solution would have to be added to distance the segments from each other to reduce the risk of damaging them.

9.1.4 Design for Lubrication

All three concepts have foundations with a curvature that matches the radius of the inner ring and outer ring to an extent. Osculation was utilised when designing the surfaces facing the inner ring raceway and the outer ring raceway. This led to the surfaces having point contact with the raceways. However, even though there is point contact, all three segments will not allow for perfect lubrication flow and the segments will scrape off the lubrication from the inner and outer rings and hinder it from spreading evenly. This leads to some rollers being starved of lubricant and poor lubrication is a leading cause of bearing failures. A solution to this would be to modify the foundations with cavities to create ”feet” which has been done in Creo and can be seen in figure 61. The length of the feet would be optimised to retain stability, minimise the length and not impede lubricant flow. Should the design be changed to roller centered instead of inner and outer ring centered, then the same issues would not occur since there would be space on the inner and outer rings for the lubricant. On the other hand, many other aspects of the lubrication would have to be taken into account with this type of design.

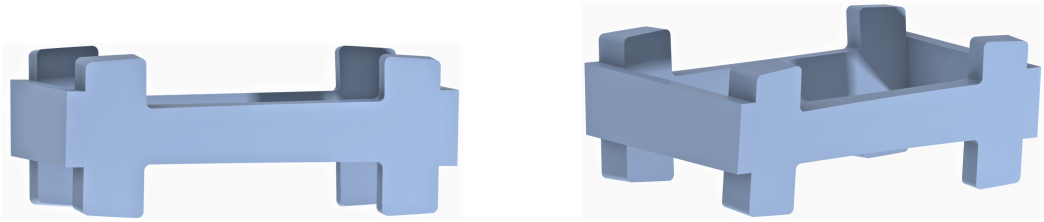

Figure 61: Every other pocket with cavities and increased beam size

By detailing the surfaces of the segments with features such as slots and tracks, cavities are created which are helpful to collect and retain lubricant within the cage segment and this will help enhance lubrication inside the bearing.

9.2 Further Simulations

Computational fluid dynamic simulations are necessary to simulate the lubrication flow based on the design of the cavities. The results would also help suggest new designs for the cavities.

In the scope of the project, a dynamic simulation of a drop-down test was not performed but can be a future activity. On some occasions, when clearances stack up and maximum clearance occurs between a roller or a segment, and a segment below it, there will be a free fall and the two objects will collide. The impact could be studied to investigate stresses and eventual design changes.

Fatigue over time could also be simulated in future studies. The life span of the wind turbine bearings is expected to be 20-30 years and therefore a simulation of the fatigue which occurs over time would also be beneficial for justification of the concepts.

9.3 Further Development of Assembly Procedures

For the *individual bar segment*, an assembly procedure is proposed in chapter 4.4.2. For the other concepts, this is something that needs to be studied further and developed. It is likely that certain tools need to be used during the procedure, and that some of these tools might have to be designed for the specific cage segments.

10 Environmental Assessment

The action of switching from steel to polymer will decrease the carbon footprint vastly. CO2 emissions are directly linked to the mass of the material and therefore, switching to a light-weight material will help lower these. The potential use of bio-polymers in the future has also been investigated.

For this phase of the project, a final interview was conducted with **V[redacted] F[redacted]** who is a program manager at *growth development* at SKF in France. He was able to answer many questions about the potential use of bio-polymers in the future which proved to be very helpful.

10.1 Carbon Emissions from Polymer Materials

The various materials compared, all differ when it comes to carbon emissions. These are listed in tables 17 and 18. The material carbon footprint is directly related to the process steps of transforming petrol to polymer. The process carbon footprint is directly related to the injection moulding process and is both applicable to full cages and individual segments.

Table 17: Material Carbon Footprint

Material	Carbon Emission $\frac{kg\ CO2}{kg}$
PEEK	14-15
PA66	5-5,6
PA46	5-5,6

Table 18: Process Carbon Footprint

Material	Carbon Emission $\frac{kg\ CO2}{kg}$
PEEK	1,02-1,45
PA66	0,26-2,60
PA46	0,26-2,60

PA66 and PA46 have the lowest amounts of C02 per kilogram, both for the material and the processing. PEEK, being a premium choice in the polymer segments, also has higher emissions.

10.2 Contribution to Renewable Energy

The wind energy market has developed greatly over the last few decades. SKF contributes many different machine parts to wind turbines, not only with bearings but also with sealing solutions, housings et cetera (Budinszki, 2012).

Wind generation capacity has globally increased by a factor of 98 in the two latest decades and this includes both on-shore and off-shore wind parks. There is still great potential

for further improvement and deployment globally, due to the constant technology improvements (International Renewable Energy Agency, n.d.) and the political narrative regarding sustainable energy solutions (International Energy Agency, 2022).

The growing demand for wind power machine parts will increase the demand for wind power bearings which means that the bearings and their cages make a contribution to the industry of renewable energy.

10.3 Potential Use of Bio-Polymers

As the environmental debate progresses, so does the topic of the use of renewable materials for machine design. The subject of bio-based polymers has developed increasingly during the past decades and there is an increasing demand for industries to shift to bio-based polymers. Bio-polymers also offer competitive advantages regarding price and physical properties (Özeren, 2021).

In an article about the use of bio-polymers in gear transmissions, Zorko et al., write about the advantages such as bio-polymers being biodegradable (Zorko, Demšar, & Tavčar, 2021).

However, there are also some disadvantages to using bio-polymers. The material can be more brittle, but this can be resolved using plasticizers and to find the right one, one needs to better understand the mechanisms of plasticizers, and a methodology to do so is necessary (Özeren, 2021). The properties of bio-polymers can also be improved using additives like cellulose fibre and nanoclay. This was the case for Battegazzore et al. who enhanced the properties of bio-polyamides by adding nanoclay and rice husk ash (Zorko et al., 2021).

There is also a concern that bio-polymers lose a lot of their functional properties when subjected to moisture which could be a problem in certain applications. There is therefore a need to make bio-polymers more adapted to certain industrial applications where this is the case (Muneer, 2014).

11 Ethics

The goal is that the SAT bearing should be used in wind turbine applications which in turn aids the extraction of renewable energy. This is positive from an environmental standpoint. What the SAT-bearing will contribute to is operation with less friction, less wear, and a longer lifespan.

The progress made in research and design can very well be used for applications other than wind power. This could be applications that are considered unethical for various reasons, but this is something that is hard to avoid when working with research and development.

The working conditions for the people working with the manufacturing of the products have to be taken into account, and the products were designed with respect to how these are gonna be assembled. The assembly procedure should be safe, ergonomic, and straightforward.

12 Analysis and Discussion of Project

The following chapter provides an analysis of the project methodology, the software used as well as the final concepts.

12.1 Analysis of Methodology

At the beginning of the project, it was planned in a more waterfall-like fashion, where the development process would flow like a waterfall through all phases of the project, where each phase completely wrapping up before the next phase begins. Due to the nature of the product that was to be developed, it was noted early in the project that a more agile approach was needed to be adopted. Since this is a completely new product that should fit and offer the right features in a completely new bearing, not much was known about all the technical aspects that needed to be considered at the beginning of the project. A lot of new information was retrieved throughout the whole project, which meant that it was deemed more suitable to use a more iterative approach for the development process. The complexity of the product that was to be developed was an additional reason why a more agile approach would benefit the project. The product which is a cage for a roller bearing, is a part of a very complex and dynamic system and is dependent on and affected by many other parts of the system and many different factors. This means that there is no clear path in the development process and it was needed to be extremely adaptable from beginning to end. The concepts and solid models were iterated multiple times as more information and knowledge were obtained.

At the start of the project, it was planned to use a Kesselring matrix in order to compare the remaining concepts after the first eliminations. It was noticed that this was not a viable method in the earlier stage of the project, due to difficulties in weighing certain parameters about which not enough was known. These parameters were later in the project assessed using other methods such as simulations, material studies, and economic assessments, and the results for the different concepts were compared.

The material study where the different material data and properties were studied gave a good first insight into how the materials differ from each other in terms of cost, density, and maximum service temperature. Due to the limited time frame of the project, it was not prioritized to look more deeply into the theory behind the materials. With more time, it would be interesting to study the materials more deeply and take more parameters into account, such as how they react to humidity, their aging effects, how they react to different lubricants, and how the materials could be reinforced further in order to obtain certain properties for certain applications, for example. The data studied was obtained from Ansys Granta, which is a widely used material database. The data is therefore trustworthy, but since the materials studied were not the exact same materials approved by SKF, the data might not be completely representative of the materials. The reason why similar, publicly available material data was chosen instead of the data for the SKF-approved materials is that the latter is confidential information.

The simulations in Ansys Discovery gave a good first insight into how the different concepts and materials react and behave under certain loading conditions. The loading conditions were simplified and designed using engineering assumptions. With more time, it could be possible to calculate the forces affecting the segments more precisely. It could also be possible to include the rollers in the simulation and establish contacts between the rollers and the segments. This would be beneficial in order to investigate how the contacts change

when the segments deform but would require another software.

The simulations in BEAST gave a good insight into the dynamic behaviours of the cage and showed that the concept tested should work in operation. With more time, it could be possible to perform tests using the larger bearing size, suited for wind turbine applications. Since more contact points need to be defined, more preparational work needs to be done in order to set up the simulations. The calculation times would also be longer. In order to perform full flexible analysis, and simulations of lubrication flow, more time would be required, both for preparation and in terms of calculation times. These simulations were disregarded due to the time limitations of the project.

Having said that, the different methods used throughout the project led to sufficient and valuable information and results.

12.2 Analysis of Software Used

The use of the software Creo Parametric was new to the product developers of this project, however, previous knowledge in other software such as Catia proved to be very helpful in learning a new one. There was no issue searching for how to complete a task or achieve a certain design feature.

The use of Ansys Discovery was also new to the product developers, but with previous experience in Ansys Mechanical and Comsol, it was simple to learn and use. Ansys Discovery is a simplified FE software and worked well for the purpose of the simulations, however, for heavier FE simulations, then Ansys Mechanical would have worked better and given more extensive results. One of the perks of Ansys Discovery was that it had an extension in Creo Parametric which allowed the students to export a solid model directly to the FE software.

The results from the BEAST software were satisfactory. Still, simplifications were made in the software due to the time span of the project and as mentioned before, it was performed with the individual parts of the bearing being in a rigid state. The simulations were also done on a digital prototype of a smaller size than the wind turbine bearing to save time. More detailed simulations would have been time-consuming but are necessary for a complete verification of the concepts.

12.3 Further Analysis of Concepts

The three concepts developed are similar since they are all individual segments and all of them are ring-guided. One of the reasons for keeping all three instead of moving forward with only one was that there are far many more applications where the SAT-bearing could be used and not just for wind turbines, therefore more alternatives were provided so that the choice could be made later depending on the application and need.

13 Conclusions

During the project, three bearing cage concepts were developed, tested and compared. With bearing theory being studied throughout the project, and with knowledge about customer needs, requirements, applications, and materials, it was possible to develop feasible products for the use case. The design choices derived from bearing theory, and the various test results gave good insight into what needed to be done in the iterations of the design and development.

Further development is needed in order to have a final product which is ready for use, but the results of the study suggest that it is of great interest to continue on the route of the segments developed during this project and to use a polymer material.

The benefit of developing three concepts is that every concept has its own strengths, and it can be possible for all designs to be the most suitable choice for a certain application.

Based on the results of the material study, there are many advantages of choosing a polymer material over a metal material. The biggest advantages are the lower weight, higher elasticity and design freedom. For the *every other pocket* segment, it is exceptionally beneficial with a polymer material, since the elasticity of the material allows the segment to bend slightly in order to absorb load. This is also the concept that performed best during the various simulations, and proved to be a feasible concept in the BEAST study. The *individual bar segment* performed second best during simulations and is also a promising concept.

After the environmental assessment, it was clear that it would be beneficial to produce the cage segments in polymer instead of steel. The carbon footprint of a polymer material is much lower than steel, which is an important factor. Based on the material study, the simulation results and the economic assessment, PA46 can be recommended out of the three polymers. PA46 performed very well in the simulations, together with PEEK, but was an inexpensive option compared to PEEK. The maximum service temperature is lower than for PA66 and PEEK, but still adequate for the wind turbine application.

The *individual bar segment* has a proposed assembly method which would utilize its design in order to aid the assembly procedure.

References

Ansys. (2021). *Ansys Discovery Reveals Critical Insights Early in the Design Process.* Retrieved from https://www.ansys.com/products/3d-design/ansys-discovery

Ansys Granta. (n.d.). *Granta selector.*

Asfoor, H., AL-Jandeel, A., Igorevich, K., & Ivanovna, L. (2022, 1). Control of time, cost and quality of construction project management. *E3S Web of Conferences*, *336*, 00072. doi: 10.1051/e3sconf/202233600072

Axelson, M., Berglund, M. M., Cederburg, S. R., Dahlqvist, J., Fischer, R., Franza, F., ... Wising, K. (2022, 10). *Decarbonizing in progress - the skf path to net zero emissions in operations and supply chain by 2050.*

Budinszki, J. (2012). *SKF in Wind Energy.* Retrieved from http://www.ewea.org/fileadmin/files/events/event-proceedings/fourth-hungary-workshop/EWEA_Hungary_Policy_Workshop_3-4_Jozsef_Budinszki_SKF.pdf

Clarivate. (2021). *The software solution for ip experts.* Retrieved from https://clarivate.com/products/ip-lifecycle-management/patent-and-trademark-management-software/unycom/?lid=c

Espacenet. (2022, 10). *Services & organisational structure (organigram) of the European Patent Office.* Retrieved from https://www.epo.org/about-us/services-and-activities/services.html

Forbes. (2022). *The Global 2000.* Retrieved from https://www.forbes.com/lists/global2000/?sh=2efd6ea45ac0

Gómez, G., & Lopez-Leon, R. (2019, 7). *Impossible design: fostering creativity by quick and dirty prototyping.* doi: 10.21606/learnxdesign.2019.14026

International Energy Agency. (2022). *Wind Electricity.* Retrieved from https://www.iea.org/reports/wind-electricity

International Renewable Energy Agency. (n.d.). *Wind Energy.* Retrieved from https://www.irena.org/Energy-Transition/Technology/Wind-energy

Karl T. Ulrich, S. D. E. (2011). *Product Design and Development* (5th ed.). McGraw-Hill/Irwin.

Linköping University. (n.d.). *Beast.*

Muneer, F. (2014). Bioplastics from natural polymers.

ProductPlan. (2021). *Product Requirements Document.* Retrieved from https://www.productplan.com/glossary/product-requirements-document/

PTC. (n.d.). *Download The Creo Trial.* Retrieved from https://www.ptc.com/en/products/creo/trial-ppc?utm_source=Google_Search&utm_medium=cpc&utm_campaign=Creo_Trial_Google_Search_CLC&utm_content=Creo_Trial_Google_Search_CLC-cpc-Creo_Trial_Pixalione_Nordics-46969&cl1=Creo_Trial_Google_Search_CLC-cpc-Creo_Trial_Pixalione_Nordics-46969&cmsrc=Google_Search&cid=7015A000002HGZjQAO&elqCampaignId=16869&gad=1&gclid=EAIaIQobChMI8bn58bGz_wIV2IbVCh2sRQ3sEAAYASAAEgKbAPD_BwE

Robotham, A. (2002, 9). The use of function/means trees for modelling technical, semantic and business functions. *Journal of Engineering Design*, *13*(3), 243–251. doi: 10.1080/09544820110108944

SKF. (n.d.). *Wind energy.* Retrieved from https://www.skf.com/sg/industries/wind-energy

SKF. (2016). *SKF Annual Report 2016.* Retrieved from https://investors.skf.com/sites/default/files/pr/201703078224-1.pdf

SKF. (2018). *Rolling bearings product catalogue.* Retrieved from https://www.skf.com/binaries/pub12/Images/0901d196802809de-Rolling-bearings---17000_1-EN

_tcm_12-121486.pdf

SKF. (2020). *How SKF creates value.* Retrieved from https://investors.skf.com/en/how-skf-creates-value

Tadic, V. (1998, 2). Engineering polymers for designer cages. *Evolution.*

Zorko, D., Demšar, I., & Tavčar, J. (2021, 1). An investigation on the potential of bio-based polymers for use in polymer gear transmissions. *Polymer Testing*, *93*, 106994. doi: 10.1016/j.polymertesting.2020.106994

Özeren, D. H. (2021). *Plasticization of biobased polymers: A combined experimental and simulation approach* .

Appendices

A Appendix

US 20160138648A1

(19) **United States**

(12) **Patent Application Publication**

KELLSTROM et al.

(10) **Pub. No.: US 2016/0138648 A1**

(43) **Pub. Date: May 19, 2016**

(54) **ANGULAR CONTACT SELF-ALIGNING TOROIDAL ROLLING ELEMENT BEARING**

(71) Applicants: **Magnus KELLSTROM**, Partille (SE); **Arne Lars Jonas KULLIN**, Landvetter (SE); **Andreas LOFQVIST**, Goteborg (SE)

(72) Inventors: **Magnus KELLSTROM**, Partille (SE); **Arne Lars Jonas KULLIN**, Landvetter (SE); **Andreas LOFQVIST**, Goteborg (SE)

(73) Assignee: **AKTIEBOLAGET SKF**, Goteborg (SE)

(21) Appl. No.: **14/932,257**

(22) Filed: **Nov. 4, 2015**

(30) **Foreign Application Priority Data**

Nov. 13, 2014 (SE) 1451353-5

Publication Classification

(51) **Int. Cl.**

F16C 23/08 (2006.01)

F16C 19/36 (2006.01)

(52) **U.S. Cl.**

CPC ***F16C 23/084*** (2013.01); ***F16C 19/36*** (2013.01)

(57) **ABSTRACT**

An angular contact self-aligning toroidal roller bearing comprising an inner ring, an outer ring, and a set of rolling elements formed of rollers arranged in an intermediate configuration between the inner and outer rings. Each roller is arranged to self orient in its axial direction in relation to the inner and outer rings in a loaded zone during operation. Furthermore, a method for determining dimensional parameters of structural members of an angular contact self-aligning toroidal rolling element bearing and a method for manufacturing an angular contact self-aligning toroidal rolling element bearing are described herein.

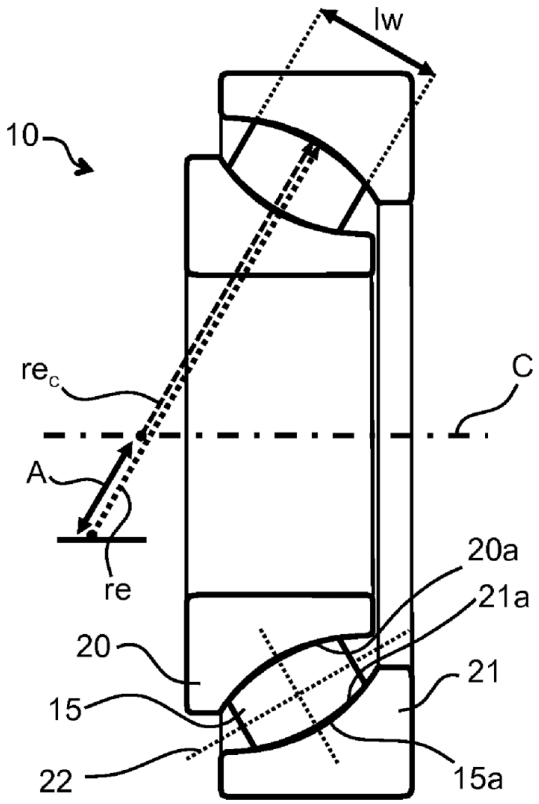

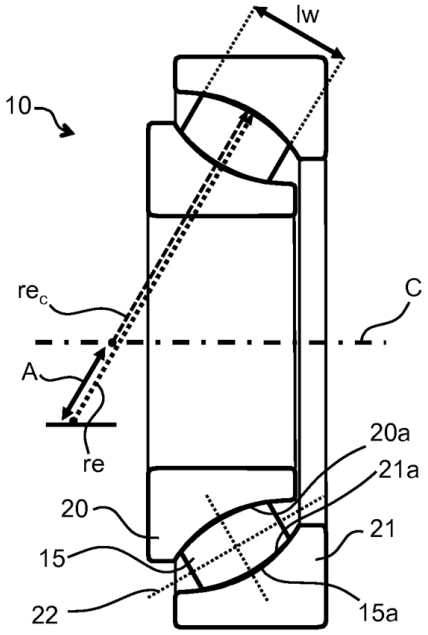
lw
10
re_c
C
A
re
20a
21a
20
21
15
22
15a

Fig. 1

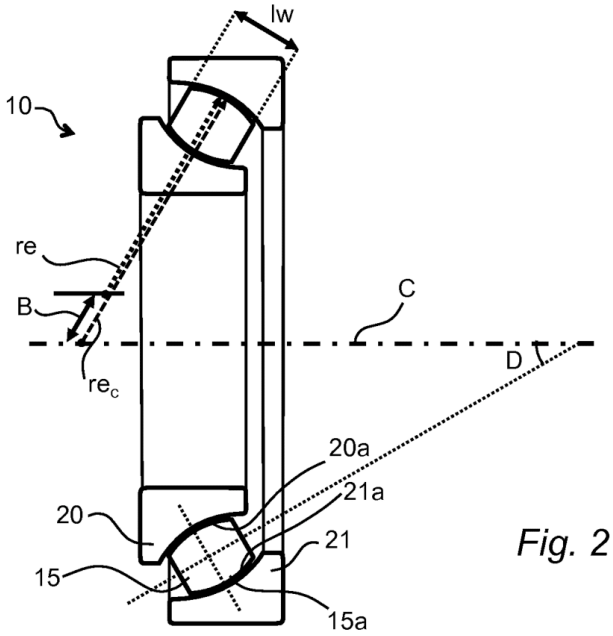
lw
10
re
C
B
re_c
D
20a
21a
20
21
15
15a

Fig. 2

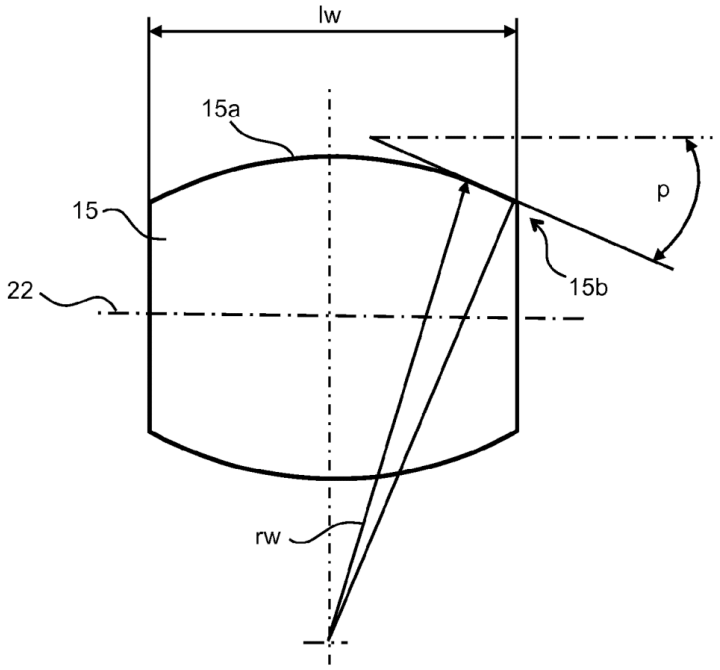

Fig. 3

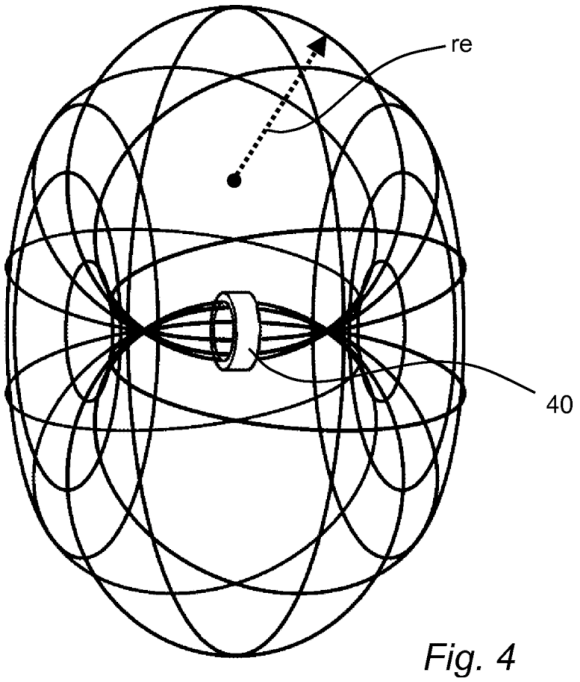
re
40

Fig. 4

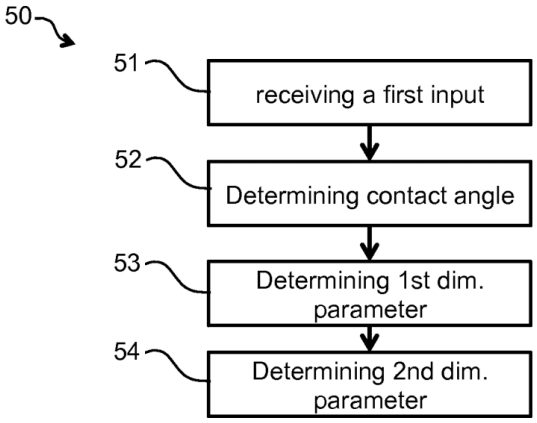
50
51
receiving a first input
52
Determining contact angle
53
Determining 1st dim. parameter
54
Determining 2nd dim. parameter

Fig. 5

ANGULAR CONTACT SELF-ALIGNING TOROIDAL ROLLING ELEMENT BEARING

CROSS REFERENCE TO RELATED APPLICATION

[0001] This is a Non-Provisional Patent Application, filed under the Paris Convention, claiming the benefit of Sweden (SE) Patent Application Number 1451353-5, filed on 13 Nov. 2014 (13.11.2014), which is incorporated herein by reference in its entirety.

FIELD OF THE INVENTION

[0002] The present invention relates to rolling element bearings.

[0003] More specifically, the present invention relates to an angular contact self-aligning toroidal roller bearing comprising an inner ring, an outer ring, and a set of rolling elements formed of rollers arranged in an intermediate configuration between the inner and outer rings. The present invention also relates to a method for determining dimensional parameters of structural members of an angular contact self-aligning toroidal rolling element bearing and to a method for manufacturing an angular contact self-aligning toroidal rolling element bearing.

BACKGROUND ART

[0004] In a typical application, a rolling bearing arrangement may be arranged to accommodate misalignment, shaft deflections and thermal expansion of the shaft. To cope with misalignment and shaft deflections, design engineers conventionally use a self-aligning bearing arrangement consisting of two self-aligning ball bearings or two spherical roller bearings. However, thermal expansion of the shaft is a complex issue and one of the bearings is often arranged as a "locating" bearing and the other as a "non-locating" bearing. For example, the locating bearing may be secured in the housing and on the shaft and the non-locating bearing may be arranged to be able to move axially on its seat in the housing. However, the movement in relation to the housing of the non-locating bearing moves typically generates a considerable amount of friction, which then induces vibration, axial forces in the bearing system, and heat—all of which can significantly reduce bearing service life.

[0005] For various applications, a known solution involves utilizing a toroidal rolling element bearing, which is a self-aligning radial bearing having an inner ring that moves independently of the outer ring, enabling e.g. thermal elongation and contraction of the shaft or structure due to temperature variations without inducing internal axial loads. Furthermore, since the inner and outer rings of a toroidal roller bearing can be mounted with an interference fit, problems associated with a loose outer ring, such as fretting corrosion and distortion of the ring may be avoided.

[0006] However, for applications involving thrust loads, design engineers are required to coop with high axial loads, misalignment and shaft deflections. Known solutions and design rules suffer from resulting bearing arrangements having low design freedom, are expensive and over dimensioned.

SUMMARY OF THE INVENTION

[0007] In view of the above-mentioned and other drawbacks of the prior art, a general object of the present invention is to provide an angular contact self-aligning toroidal rolling element bearing, improved method for determining dimensional parameters of structural members of an angular contact self-aligning toroidal rolling element bearing, and an improved method for manufacturing an angular contact self-aligning toroidal rolling element bearing.

[0008] These and other objects are met by the subject matters provided in the independent claims. Preferred embodiments of the invention are presented in the dependent claims.

[0009] According to a first aspect thereof, the present invention relates to an angular contact self-aligning toroidal rolling element bearing, comprising an inner ring, an outer ring, and a set of rolling elements formed of rollers arranged in an intermediate configuration between the inner and outer rings, wherein each roller has a curved raceway-contacting surface arranged for being in load carrying contact with a curved inner raceway of the inner ring and in load carrying contact with a curved outer raceway of the outer ring, a contact angle between each roller and the inner and/or outer raceway is inclined in relation to a bearing axis, and wherein each roller is arranged to self orient in its axial direction in relation to the inner and outer rings in a loaded zone during operation.

[0010] The invention is based on the realization by the inventors that bearing system in applications involving high axial loads, misalignment and shaft deflections may be considerably improved by providing an angular contact self-aligning toroidal roller bearing being designed which focus on allowing for self orientation of the rollers, also referred to as a soap effect. This allows for more compact and efficient bearing solutions. In more detail, this approach allows for more compacts bearings, which in turn allow for reductions of load capacity over-dimensioning and dimensional over-dimensioning of the bearing system. Thereby, more compact bearing solutions, requiring less material and manufacturing resources, such as time, material, transport, etc., may be used for achieving similar or better performing bearings for a particular application involving e.g. high axial loads, misalignment and shaft deflections.

[0011] According to an embodiment, conventional design rules relating to non-angled toroidal rolling element bearings may be omitted when designing the angular contact self-aligning toroidal roller bearing. In other words, only the axial self-orientation criteria, also known as the soap effect criteria, is used for determining the optimum bearing design.

[0012] Furthermore, for various applications, an angular contact self-aligning toroidal roller bearing according embodiments of the present invention, allows for e.g. safer, more optimized designs, extended bearing service life, extended maintenance intervals, lower running temperature, lower vibration and noise levels, greater throughput of the machine, same throughput with a lighter or simpler machine, improved product quality/less scrap, etc.

[0013] According to an exemplifying embodiment, the angular contact self-aligning toroidal bearing is a large bearing. A large rolling bearing is for example a bearing having an external diameter of 500 mm or more.

[0014] According to an exemplifying embodiment, each roller is arranged to orient itself in its axial direction in relation to the inner and outer ring based on changing running conditions of the bearing. For example, during the changing running conditions involving misalignment of the structural members of the bearing, load changes, for example entering and leaving the loaded/unloaded zone, or ring deformations, displacements or twistings, etc. By axial self-orientation of

the rollers, self-balancing is achieved leading to symmetric stress distributions and the avoiding of unfavorable roller edge loading under typical running conditions.

[0015] According to an exemplifying embodiment, the curvature of the curved raceway-contacting surface of each roller and the curvature of the inner and outer raceways are adapted to allow for self-orientation of the rollers in the axial direction of the rollers.

[0016] According to various exemplifying embodiments, each roller has a roller transverse radius 'rw' and a roller length 'lw', and a ratio between the roller transverse radius and roller length, for each roller, is less than 12, or is less than 10, or less than 8.5, or less than 6, or less than 4. The ratio between the roller transverse radius and roller length is characteristic for soap effect capability, i.e. the self-orientation capability of the rollers in their axial direction during changing running conditions. It may be determined based on the roller-raceway friction. In more detail, the roller transverse radius 'rw' to roller length 'lw' ratio is characteristic for the slope angle of the raceway-contacting surface of the roller and the slope of the raceway close to the axial ends of the roller. The relationship between the slope and a friction based angle influences the self orientation via axial sliding of the rollers such that unfavorable roller edge loads and stress may be avoided.

[0017] According to an exemplifying embodiment, the outer raceway comprises a transverse raceway radius and a circumferential raceway radius. In more detail, the transverse raceway radius may be defined as the radius of the outer raceway in the direction transverse rolling direction of the rollers. Furthermore, the circumferential raceway radius may be defined as the radius of the outer raceway in the rolling direction of the rollers in the contact point between a roller and the outer raceway.

[0018] Furthermore, according to an exemplifying embodiment, the transverse raceway radius is between 1.65 and 1.0 times the circumferential raceway radius, or between 1.62 and 1.02 times the circumferential raceway radius. Thereby, ratios providing design rules allowing for more compact and efficient bearings, with reduced over-dimensioning, both in terms of load capacity and external dimension of the bearing, is achieved.

[0019] Also, this ratio regime between the transverse and circumferential raceway radius is advantageous in that is allows for a positive offset transverse radius design of the bearing, wherein the transverse raceway radius is more than the circumferential raceway radius. In other words, the toroidal geometry of the curvature of the bearing raceways is arranged such that the outer ring transverse raceway radius center point extends beyond the center axis line of the bearing.

[0020] According to yet an exemplifying embodiment, the transverse raceway radius is less than 1.0 times the circumferential raceway radius, or less than 1.02 times the circumferential raceway radius. This ratio regime between the transverse and circumferential raceway radius allows for a negative offset transverse radius design of the bearing, wherein the transverse raceway radius is less than the circumferential raceway radius. In other words, the toroidal geometry of the curvature of the bearing raceways is arranged such that the outer ring transverse raceway radius center point does not reach the center axis line of the bearing. According to a further embodiment, the transverse raceway radius is less than 1.0 times the circumferential raceway radius, but not less or equal to 50% of the roller length 'lw', or not less or equal to 60% of the roller length 'lw'.

[0021] According to an exemplifying embodiment, the contact angle is between 10 and 45 degrees, or between 15 and 35 degrees. The contact angle may be defined as the angle of the line along which the resulting load is transmitted via a roller element from one raceway to another, typically along an axial center portion of the roller, in relation to the normal direction of the bearing center axis. The contact angle is key for providing sufficiently high axial load carrying capacity of the bearing.

[0022] According to various arrangement comprising embodiments of the bearing, the bearing may be arranged with a positive internal operational clearance, negative internal operational clearance, or no internal operational clearance. For example, depending on the preferred design of the application, the rolling elements may have no axial play in relation to the raceways of the inner and outer rings, or the rolling elements may be arranged with a suitable play in the radial and axial direction in relation to the raceways of the inner and outer rings. The bearings may alternatively be arranged with a negative operational clearance, i.e. a preload, in order to e.g. enhance the stiffness of the bearing arrangement or to increase running accuracy. For example, the application of a preload may be provided by springs, or by solution involving hydraulic pressure devices.

[0023] According to a further aspect thereof, the present invention relates to a method for determining dimensional parameters of structural members of an angular contact self-aligning toroidal rolling element bearing for an application, the bearing having rolling elements formed of rollers arranged between an inner ring and an outer ring. The method comprises receiving a first input representative of required load carrying characteristics associated with the application. Furthermore, the method comprises, determining, based on the first input:

[0024] a contact angle for the angular contact self-aligning toroidal rolling element bearing,

[0025] a first dimensional parameter representative of a transverse radius 'rw' for the rollers, and

[0026] a second dimensional parameter representative of a roller length 'lw', wherein the first and second dimensional parameter are determined based on a ratio between the roller transverse radius and roller length.

[0027] The method for determining the dimensional parameters, and embodiments thereof, advantageously allow for determination of bearings having the same advantageous effects and benefits as described in relation to the first aspect of the invention. In more detail, improved bearings for applications involving high axial loads, misalignment and shaft deflections may be provided by determining improved dimensional parameters of structural members of the angular contact self-aligning toroidal roller bearing. In particular, by focusing the design on allowing for self-orientation of the rollers based on the ratio between the roller transverse radius and roller length, more compact and efficient bearing solutions may be achieved. By focusing on the ratio between the roller transverse radius and roller length, the bearing design may be optimized in relation to axial self-orientation of the rollers, and previous design rules for toroidal bearings may be alleviated. This allows for reductions of over-dimensioning in terms of load capacity and external dimensions of the bearing and its structural members. The method may for example be used by design engineer for determining suitable bearing

dimension for a given application having predetermined properties, such bearing outer ring diameter, or inner ring bore diameter, etc.

[0028] According to an exemplifying embodiment, the method comprises determining a contact angle between 10 and 45 degrees, or between 15 and 35 degrees.

[0029] According to an exemplifying embodiment, the method further comprises determining the ratio between the roller transverse radius and roller length, such that each roller is arranged to self orient in its axial direction in relation to the inner and outer rings in a loaded zone during operation. According to an exemplifying embodiment, the ratio, for each roller in the bearing, is less than 12, or is less than 10, or less than 8.5, or less than 6, or less than 4.

[0030] According to an exemplifying embodiment, the method further comprises specifying, a transverse raceway radius of the outer raceway, and a circumferential raceway radius of the outer raceway. For example, according to an exemplifying embodiment, the method comprises specifying that the transverse raceway radius is between 1.65 and 1.0 times the circumferential raceway radius, or between 1.62 and 1.02. According to an alternative exemplifying embodiment, the method comprises specifying that the transverse raceway radius is less than 1.0 times the circumferential raceway radius, or less than 1.02. Thereby, a positive or a negative transverse bearing design of the bearing may be provided, respectively.

[0031] According to an exemplifying embodiment, the method is a computer-implemented method, which method is performed by one or more processors of a computing device. Also, the present invention relates to a computer-readable medium containing instructions that, when executed by a computing device, cause the computing device to perform the computer-implemented method of any one of the embodiments described herein. Furthermore, according to an exemplifying embodiment, the computer-implemented method comprises outputting a representation of the first and/or second dimensional parameter. It may e.g. be outputted on a display our outputted to a bearing manufacturing control unit.

[0032] According to a further aspect thereof, the present invention relates to a method for manufacturing an angular contact self-aligning toroidal rolling element bearing, comprising an inner ring, an outer ring, and a set of rolling elements formed of rollers arranged in an intermediate configuration between the inner and outer rings, the method comprises providing each roller with a curved raceway-contacting surface for being in load carrying contact with a curved inner raceway of the inner ring and in load carrying contact with a curved outer raceway of the outer ring, wherein the curvature of the raceway-contacting surface of each roller and the curvature of the inner and outer raceway is adapted such that each roller self orient in its axial direction in relation to the inner and outer rings. The method for manufacturing the bearing is advantageous in similar manner as described in relation to the first and second aspects of the invention. According to various embodiments, the method may further comprises manufacturing a bearing according to any one of the embodiments described in relation to the first and second aspects of the invention.

[0033] The angular contact toroidal roller bearing is advantageous in that it can accommodate both radial loads and axial loads. This is due to the optimized design of the rings combined with the design and number of rollers. For example, it may be used in a face-to-face or back-to-back arrangement with another bearing taking up the axial load in the other direction. Due to their robust design, toroidal bearings can cope with small deformations and machining errors of the bearing seat. The rings accommodate these small imperfections without the danger of roller edge stresses. The high load carrying capacity plus the ability to compensate for small manufacturing or installation errors provide opportunities to increase machine productivity and uptime. Together with high axial load carrying capacity of the angular contact toroidal rolling element bearing, this means that for the same bearing size in an application arrangement, performance can be increased and/or or service life extended. Also, new machine designs can be made more compact to provide the same, or even better performance.

[0034] Generally, other objectives, features, and advantages of the present invention will appear from the following detailed disclosure, from the attached dependent claims as well as from the drawings are equally possible within the scope of the invention.

BRIEF DESCRIPTION OF DRAWINGS

[0035] Embodiments of the invention will now be described, by way of example, with reference to the accompanying drawings, wherein:

[0036] FIG. **1** is a schematic cross-sectional view of an exemplifying embodiment of the angular contact self-aligning toroidal roller bearing according to the present invention.

[0037] FIG. **2** is a schematic cross-sectional view of an exemplifying embodiment of the angular contact self-aligning toroidal roller bearing according to the present invention.

[0038] FIG. **3** is a schematic partial cross-sectional view of an exemplifying embodiment of the angular contact self-aligning toroidal roller bearing according to the present invention

[0039] FIG. **4** is a schematic view of a torus shape in combination with a rolling element bearing.

[0040] FIG. **5** is a schematic flow chart of an embodiment of a method according to the present invention.

[0041] It should be understood that the drawings are not true to scale and, as is readily appreciated by a person skilled in the art, dimensions other than those illustrated in the drawings are equally possible within the scope of the invention.

DETAILED DESCRIPTION OF EMBODIMENTS OF THE INVENTION

[0042] In the drawings, similar, or equal elements are referred to by equal reference numerals.

[0043] In FIG. **1**, a schematic cross-sectional view of an exemplifying embodiment of the angular contact self-aligning toroidal roller bearing **10** according to the present invention is shown.

[0044] In FIG. **2**, a schematic cross-sectional view of an exemplifying embodiment of the angular contact self-aligning toroidal roller bearing **10** according to the present invention is shown.

[0045] Each one of the bearing **10** illustrated in FIG. **1** and FIG. **2** comprises an inner ring **20**, an outer ring **21**, and a set of rolling elements formed of symmetric rollers **15** arranged in an intermediate configuration between the inner and outer rings **20** and **21**. Each roller **15** of the angular contact self-aligning rolling element bearing is an axially symmetrical bearing roller. As shown, the bearing **10** is a single row rolling element bearing.

[0046] Furthermore, each roller **15** has a curved raceway-contacting surface **15***a* arranged in contact with a curved inner raceway **20***a* of the inner ring **20**, and in contact with a curved outer raceway **21***a* of the outer ring **21**. As shown, the contact angle between each roller **15** and the inner raceway **20***a* and the outer raceway **21***a* is inclined in relation to a bearing axis C, as indicated by D in FIG. **2**. The toroidal curvature of the curved raceway-contacting surface **15***a* of each roller **15** and the toroidal curvature of the inner and outer raceways **20***a* and **21***a* are adapted to allow for self-orientation of the rollers in the axial direction **22** of the rollers. The toroidal curvature of the curved raceway-contacting surface **15***a* of each roller **15** corresponds to the toroidal curvature of the inner and outer raceways **20***a* and **21***a*. The transverse raceway radius, characteristics for the toroidal geometry, of the outer raceway **21***a* is indicated by re. As illustrated, the transverse raceway radius re is offset in relation to the bearing axis C and the radius of the outer ring raceway **21***a*, as indicated by A and B, respectively. Roller axial length is indicated by lw.

[0047] Each one the illustrated bearings **10** in FIG. **1** and FIG. **2** is a single row roller bearing **10** with relatively long, slightly crowned rollers. The inner and outer ring raceways **20***a* and **21***a* are correspondingly concave and symmetrical. The outer ring raceway geometry is based on a torus, as schematically illustrated in FIG. **4**, hence the term toroidal roller bearing. The angular contact toroidal roller bearing is designed as a locating bearing that allows for self-aligning ability, similar to the ability of a spherical roller bearing, and ability to allow for twisting displacements, such as twisting of any one or both of the rings and/or housing structure. Self-aligning capability and ability to allow for twisting displacement is for example particularly important in applications where there is misalignment as a result of inaccurate manufacturing, mounting errors or shaft deflections. To compensate for these conditions, the bearing **10** may for example be arranged to accommodate misalignment up to 0.5 degrees between the bearing rings **20** and **21** without any detrimental effects on the bearing or bearing service life. Further advantages are that the bearing run cooler, the lubricant lasts longer and maintenance intervals can be appreciably extended.

[0048] With reference to FIG. **1**, the transverse raceway radius re of the outer raceway is between 1.62 and 1.0 times the outer ring circumferential raceway radius re_c. This ratio allows for a positive offset transverse radius design toroidal bearing, wherein the transverse raceway radius re is greater than the outer ring circumferential raceway radius re_c, within a limited interval. In other words, the toroidal geometry of the curvature of the bearing raceways **20***a* and **21***a* as well as the rollers **15***a*, are arranged such that the transverse raceway radius re center point reaches over the center axis line C of the bearing **10**. As shown, the transverse raceway radius re center point is located beyond the bearing axis line C by distance A.

[0049] With reference to FIG. **2**, the transverse raceway radius re of the outer raceway **21***a* is less than 1.0 times the outer ring circumferential raceway radius re_c. This ratio allows for a negative offset transverse radius design toroidal bearing, wherein the transverse raceway radius re is less than the outer ring circumferential raceway radius re_c. In other words, the toroidal geometry of the curvature of the bearing raceways **20***a* and **21***a* as well as the rollers **15***a* are arranged such that the transverse raceway radius re center point does not reach the center axis line C of the bearing **10**. As shown, the transverse raceway radius re center point is located before the bearing axis line C by distance B.

[0050] In FIG. **3**, a schematic partial cross-sectional view of an exemplifying embodiment of the angular contact self-aligning toroidal roller bearing according to the present invention is shown. More specifically, an axially symmetric roller **15** of an angular contact self-aligning toroidal roller bearing is shown, having raceway contacting surface **15***a*, roller end **15***b*, roller axis **22**, transverse radius rw, roller length lw, and friction based angle p at the roller end **15***b*.

[0051] The axial self-orientation is dependent on the curvature geometries of the bearing, and a self-locking limit, wherein the axial self-orientation of the rollers is prevented, may be determined based on the existing friction characteristics and geometries at the roller axial end **15***b*.

[0052] The following relationships are valid, wherein mu is representative of a coefficient of friction between the raceway contacting surface of the roller **15** and the raceway of the bearing:

$$mu(limit)<\tan(p)$$

[0053] Wherein the friction based angle p at the roller end may be defined as:

$$p=\arcsin((lw/2)/rw)$$

EXAMPLE

[0054] According to an exemplifying example (approx.):

[0055] if mu(limit) is 0.05 (depending on e.g. material properties, bearing operation parameters, etc.), and roller length lw=195 mm, then the roller transverse radius should be less than approx. 1950 mm for ensuring axial self-orientation of the roller during operation. The approximated transverse radius limit rw<1950 mm corresponds to a ratio between the roller transverse radius rw and roller length lw of 10. This ratio is bearing pitch diameter independent. Lower ratio provides increased self-orientation ability of the rollers, such as less than 8.5, or less than 6, or less than 4.

[0056] In FIG. **4**, a schematic view of a torus shape in combination with a rolling element bearing **40** is shown. As shown, the curvature of the bearing raceways forms a torus geometry. The illustrated bearing **40** is a toroidal bearing with zero contact angle.

[0057] In FIG. **5**, a schematic flow chart of an embodiment of the method **50** according to the present invention is shown. As illustrated, the method **50** comprises a step **51** comprises receiving a first input representative of required load carrying characteristics associated with the application. Furthermore, the method comprises the step **52**, **53**, and **54**, which steps comprise determining different features of the bearing based on the first input. In more detail, step **52** comprises determining a contact angle for the angular contact self-aligning toroidal rolling element bearing, step **53** comprises determining a first dimensional parameter representative of a transverse radius rw for the rollers, and step **54** comprises determining a second dimensional parameter representative of a roller length lw, wherein the first and second dimensional parameter are determined based on a ratio between the roller transverse radius and roller length.

[0058] According to an exemplifying implementation of the method depicted in FIG. **5**, the dimensional parameters of the structural members of an angular contact self-aligning toroidal rolling element bearing for a specific application may be determined based on various input parameters representa-

tive of required load carrying characteristics associated with the specific application. For example, the first input may comprise any one or more of the following input parameters:

[0059] D, outer diameter of the bearing, or the diameter of the bearing housing,

[0060] d, diameter of the axle, or the bore of the bearing,

[0061] P, the load.

[0062] The method may further comprise determination of any one or more of the following additional parameters:

[0063] Dw, height roller element,

[0064] z, number of rolling elements in the bearing,

[0065] dm, pitch diameter of the bearing,

[0066] According to various embodiments, any one or all of the above input parameters D, d, and P and the determined parameters Dw, z, and dm may advantageously be used as a base for determining the first and second dimensional parameters representative of the transverse radius rw and the roller length lw, respectively.

[0067] It is noted that the transvers radius of the raceways, such as the transverse raceway radius of the outer raceway re, typically corresponds to the transverse radius of the roller rw based on a suitable ratio, also known as osculation. The level of correspondence, i.e. the osculation ration rw/re, between the roller and raceway transvers radius may for example be about 0.98, or between 0.965 and 0.995.

[0068] It should be noted that the invention has mainly been described above with reference to a few embodiments. However, as is readily appreciated by a person skilled in the art, other embodiments than the ones disclosed above are equally possible within the scope of the invention, as defined by the appended patent claims.

[0069] For example, even though the angular contact self-aligning toroidal rolling element bearing has been mainly been described in relation to a stand alone configuration, it may be utilized in a wide range of applications, including but not limited to turbines, mills, and other machines including rotating shafts with axial and radial support requirements.

[0070] In the claims, the word "comprising" does not exclude other elements or steps, and the indefinite article "a" or "an" does not exclude a plurality. A single apparatus or other unit may fulfill the functions of several items recited in the claims. The mere fact that certain features or method steps are recited in mutually different dependent claims does not indicate that a combination of these features or steps cannot be used to advantage.

What is claimed is:

1. An angular contact self-aligning toroidal rolling element bearing, comprising:

an inner ring;

an outer ring; and

a set of rolling elements formed of rollers arranged in an intermediate configuration between the inner ring and the outer ring,

wherein each roller has a curved raceway-contacting surface arranged for being in load carrying contact with a curved inner raceway of the inner ring and in load carrying contact with a curved outer raceway of the outer ring, wherein a contact angle between each roller and at least one of the inner raceway and outer raceway is inclined in relation to a bearing axis, wherein each roller is arranged to self orient in its axial direction in relation to the inner ring and the outer in a loaded zone during operation.

2. The rolling element bearing according to claim **1**, wherein each roller is arranged to orient itself in its axial direction in relation to the inner and outer ring based upon changing running conditions of the bearing.

3. The rolling element bearing according to claim **1**, wherein the curvature of the curved raceway-contacting surface of each roller and the curvature of the inner raceway and the outer raceway are adapted to allow for self orientation of the rollers in the axial direction of the rollers.

4. The rolling element bearing according to claim **1**, wherein

each roller having a roller transverse radius and a roller length, and

a ratio between the roller transverse radius and roller length, for each roller, is less than 12.

5. The rolling element bearing according to claim **1**, wherein

each roller having a roller transverse radius and a roller length, and

a ratio between the roller transverse radius and roller length, for each roller, is less than 10.

6. The rolling element bearing according to claim **1**, wherein

each roller having a roller transverse radius and a roller length, and

a ratio between the roller transverse radius and roller length, for each roller, is less than 8.5.

7. The rolling element bearing according to claim **1**, wherein

each roller having a roller transverse radius and a roller length, and

a ratio between the roller transverse radius and roller length, for each roller, is less than **6**.

8. The rolling element bearing according to claim **1**, wherein

each roller having a roller transverse radius and a roller length, and

a ratio between the roller transverse radius and roller length, for each roller, is less than **4**.

9. The rolling element bearing according to claim **1**, the outer raceway further comprising a transverse raceway radius and a circumferential raceway radius.

10. The rolling element bearing according to claim **9**, wherein the transverse raceway radius is between 1.65 and 1.0 times the circumferential raceway radius.

11. The rolling element bearing according to claim **9**, wherein the transverse raceway radius is between 1.62 and 1.02 times the circumferential raceway radius.

12. The rolling element bearing according to claim **9**, wherein the transverse raceway radius is less than 1.0 times the circumferential raceway radius.

13. The rolling element bearing according to claim **9**, wherein the transverse raceway radius is less than 1.02 times the circumferential raceway radius.

14. The rolling element bearing according to claim **1**, wherein the contact angle is between 10 and 45 degrees.

15. The rolling element bearing according to claim **1**, wherein the contact angle is between 15 and 35 degrees.

16. A method for determining dimensional parameters of structural members of an angular contact self-aligning toroidal rolling element bearing for an application, the bearing having rolling elements formed of rollers arranged between an inner ring and an outer ring, the method comprising steps of:

receiving a first input representative of required load carrying characteristics associated with the application, and

determining, based on the first input:

a contact angle for the angular contact self-aligning toroidal rolling element bearing,

a first dimensional parameter representative of a transverse radius for the rollers, and

a second dimensional parameter representative of a roller length,

wherein the first and second dimensional parameter are determined based on a ratio between the roller transverse radius and roller length.

17. The method according to claim **16**, further comprising a step of:

determining the ratio between the roller transverse radius and roller length, such that each roller is arranged to self orient in its axial direction in relation to the inner ring and the outer ring in a loaded zone during operation.

18. The method according to claim **17**, wherein the ratio, for each roller in the bearing, is less than 12.

19. The method according to claim **17**, wherein the ratio, for each roller in the bearing, is less than 10.

20. The method according to claim **17**, wherein the ratio, for each roller in the bearing, is less than 8.5.

21. The method according to claim **17**, wherein the ratio, for each roller in the bearing, is less than 6.

22. The method according to claim **17**, wherein the ratio, for each roller in the bearing, is less than 4.

23. The method according to any one of claim **16**, further comprising a step of:

specifying:

a transverse raceway radius of the outer raceway, and

a circumferential raceway radius of the outer raceway.

24. The method according to claim **23**, further comprising specifying that the transverse raceway radius is between 1.65 and 1.0 times the circumferential raceway radius.

25. The method according to claim **23**, further comprising specifying that the transverse raceway radius is between 1.62 and 1.02 times the circumferential raceway radius.

26. The method according to claim **23**, further comprising specifying that the transverse raceway radius is less than 1.0 times the circumferential raceway radius.

27. The method according to claim **23**, further comprising specifying that the transverse raceway radius is less than 1.2 times the circumferential raceway radius.

28. A method for manufacturing an angular contact self-aligning toroidal rolling element bearing, comprising an inner ring, an outer ring, and a set of rolling elements formed of rollers arranged in an intermediate configuration between the inner and outer rings, the method comprising a step of:

providing each roller with a curved raceway-contacting surface for being in load carrying contact with a curved inner raceway of the inner ring and in load carrying contact with a curved outer raceway of the outer ring,

wherein the curvature of the raceway-contacting surface of each roller and the curvature of the inner and outer raceway is adapted such that each roller self orient in its axial direction in relation to the inner and outer rings.

* * * * *

B Appendix

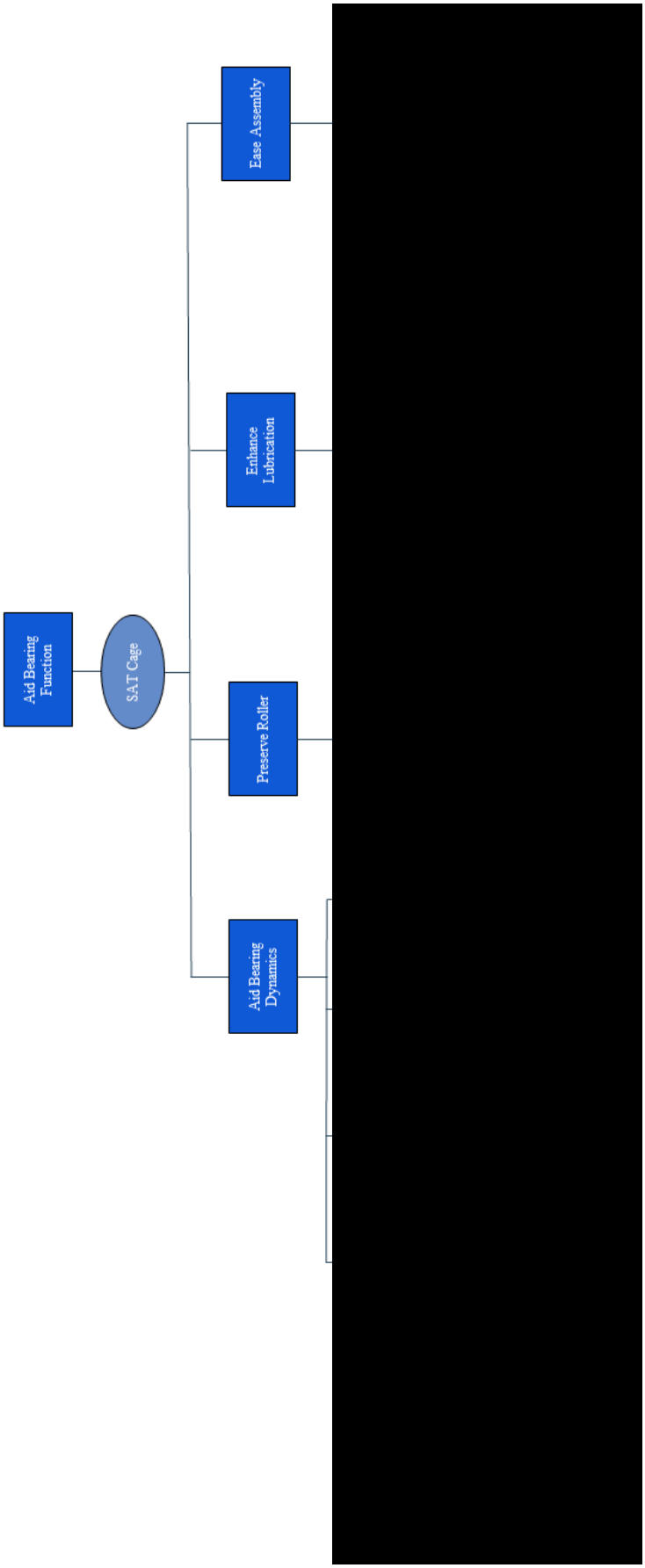
Ease Assembly
Enhance Lubrication
Aid Bearing Function
SAT Cage
Preserve Roller
Aid Bearing Dynamics

DEPARTMENT OF INDUSTRIAL AND MATERIALS SCIENCE
CHALMERS UNIVERSITY OF TECHNOLOGY
Gothenburg, Sweden
www.chalmers.se

CHALMERS
UNIVERSITY OF TECHNOLOGY